Carl von Ossietzky
Universität
Oldenburg

Dissertation

A computational neuroscience approach to studying the mechanisms of magnetic orientation and navigation in birds

Von der Fakultät für Mathematik und Naturwissenschaften Carl von Ossietzky Universität Oldenburg zur Erlangung des Grades und Titels eines

Doktors der Naturwissenschaften (Dr. rer. nat.)

vorgelegt von

Karim Habashy

geboren am 07. Februar 1986 in Kairo, Ägypten

April 26, 2024

Erstbetreuer:	**Prof. Dr. Michael Winklhofer** Carl von Ossietzky Universität Oldenburg
Zweitgutachter:	**Prof. Dr. Heiko Schmaljohann** Carl von Ossietzky Universität Oldenburg

Defence date: 16/09/2024

Abstract

Migratory birds rely on a keen sense of orientation to maintain their course towards the destination during their long-distance flights. It is widely accepted that birds possess two systems for this purpose: a compass and a map. Map information is needed to determine the current location relative to the destination, while the correct heading towards this destination can be determined based on compass information.

Numerous experiments suggest that birds can gain not only compass but also map information from the Earth's magnetic field. The sensory and cognitive mechanisms responsible for this remarkable ability are the subject of intensive research. While the magnetic compass of migratory birds is an inclination compass and likely based on the radical pair mechanism of magnetoreception, it is not known how they perceive and process magnetic map information. In this regard, extensive experiments have been conducted to test this elusive magnetic map system, including the physical and virtual magnetic displacement of birds across the migration route to test whether they adjust their migration direction accordingly.

In addition, based on the hypothesis that magnetic map information is detected by tiny magnets (magnetite particles) in sensory nerve cells, another experimental paradigm involves exposing birds to a strong and brief magnetic pulse aimed at remagnetizing their internal magnets before testing. This pulse distorts their perception of the magnetic field at the test site and potentially causes them to perceive themselves at a different location where they must adjust their migration direction accordingly. Although such pulse experiments have led to reorientation, it is by no means clear whether they are equivalent to virtual magnetic displacement, especially since the possible displacement location after pulse treatment is uncertain. Furthermore, all pulse experiments so far have been designed like a compass experiment, which investigates birds at a stopover along the migration route without knowing whether the birds actually use magnetic map information there. Without an obvious anatomical candidate for the magnetosensory structure, it is also unclear how precisely a pulse affects a magnetoreception mechanism based on magnetic particles.

To better understand the effects of pulses, we have developed a neural fields model in which we varied the preferred direction of magnetic excitability from one receptor unit to the next, then simulated the output of the system under the influence of a pulse. From these simulations, we were able to reproduce some results from literature and make some predictions for future experiments. A key result of these simulations is that the neural system can encode both magnetic field direction and intensity, and that a pulse effect at the level of receptors then manifests as a changed magnetic field percept in both

intensity and direction, which can be interpreted as magnetic displacement. Since the magnetite-based system apparently automatically generates compass information, this result suggests some functional redundancy to the radical pair-based inclination compass. Conversely, the question arises whether the radical pair mechanism can provide more than just compass information.

The previous question leads to the second major series of simulations in this work, which aims to test navigational ability using the inclination compass. For this purpose, we developed a simulated navigational environment with a spatial gradient in both inclination and declination, and tested an artificial learning agent representing the migratory bird in it. This artificial bird uses an inclination compass coupled with a star compass, which in turn detects the geographical north direction. With the help of these sensory cues, the learning agent was able to successfully navigate from any randomly selected location in the environment to a target destination. Furthermore, we have demonstrated other experimentally discovered properties of navigation, such as extrapolation. Summing up these two simulations, there may be some ambiguity regarding the exact role of the magnetite-based system and the visual compass. All of this discussion and work questions the following prevailing notion that both systems are isolated from each other, each with a singular function. Finally, it should be noted that birds are opportunistic (and have to be so to survive!) so they use every cue they can, with all senses wide open. Provided they have the neuronal wiring, they will integrate it all and then weigh the different pieces of evidence in the process of decision-making before resuming their journey.

Abstrakt

Zugvögel sind auf einen zuverlässigen Orientierungssinn angewiesen, um auf ihren Langstreckenflügen den Kurs zum Zielort einhalten zu können. Es ist allgemein anerkannt, dass Vögel hierzu über zwei Systeme verfügen: einen Kompass und eine Karte. Karteninformationen werden benötigt, um den aktuellen Standort relativ zum Ziel zu bestimmen, während die korrekte Peilung zu diesem Ziel auf der Grundlage von Kompassinformationen ermittelt werden kann. Zahlreiche Experimente deuten darauf hin, dass Vögel aus dem Erdmagnetfeld nicht nur Kompass-, sondern auch Karteninformationen gewinnen können. Welche sensorischen und kognitiven Mechanismen für diese bemerkenswerte Fähigkeit verantwortlich sind, ist Gegenstand intensiver Forschung. Während der magnetische Kompass von Zugvögeln ein Inklinationskompass ist und sehr wahrscheinlich auf dem Radikalpaarmechanismus der Magnetorezeption basiert, ist es nicht bekannt, wie magnetische Karteninformation aufgenommen und verarbeitet werden. Um das schwer fassbare System "magnetische Karte" zu testen, wurden umfangreiche Experimente durchgeführt. Dazu gehören die physische und virtuelle magnetische Versetzung von Vögeln quer zur Zugrichtung, um zu prüfen, ob sie ihre Zugrichtung entsprechend korrigieren. Basierend auf der Hypothese, dass magnetische Karteninformationen mittels winziger Magnete (Magnetitpartikel) in sensorischen Nervenzellen erfasst werden, besteht ein weiteres experimentelles Paradigma darin, Vögel vor dem Testen einem starken Magnetimpuls auszusetzen, um ihre inneren Magnete umzumagnetisieren, so dass sie in Folge das Magnetfeld am Testort verfälscht wahrnehmen und möglicherweise sich an einem anderen Ort wähnen, an dem sie ihre Zugrichtung entsprechend korrigieren müssen. Obwohl solche Pulsexperimente zu Reorientierung geführt haben, ist keineswegs klar, ob sie äquivalent zu einer virtuellen magnetischen Versetzung sind, zumal der mögliche Versetzungsort nach Pulsbehandlung unbestimmt ist. Zudem wurden alle Pulsexperimente bislang wie ein Kompassexperiment konzipiert, derart dass Vögel an einem Zwischenstop entlang der Zugroute untersucht wurden, ohne zu wissen, ob die Vögel dort überhaupt magnetische Karteninformationen nutzen. Ohne einen offensichtlichen anatomischen Kandidaten für die magnetosensorische Struktur zu kennen, ist es außerdem unklar, wie genau ein Magnetpuls einen auf Magnetpartikeln basierenden Magnetorezeptions¬mechanismus beeinflusst. Um die Pulseffekte besser zu verstehen, haben wir ein neural fields Model entwickelt, bei denen wir die bevorzugte Richtung der magnetischen Stimulierbarkeit von einem Rezeptorfeld zum nächsten variiert haben, um dann den Netzwerk-Output des Systems in Abhängigkeit von der Pulsfeld-Richtung zu simulieren. Aus diesen Simulationen konnten wir einige Ergebnisse in der Literatur reproduzieren und einige Vorhersagen für zukünftige Experimente treffen. Ein wesentliches Ergebnis dieser Simulationen

besteht darin, dass das neuronale System sowohl Magnetfeldrichtung als auch Magnetfeldintensität kodieren kann, und dass ein Pulseffekt auf der Ebene der Rezeptoren sich über den geänderten Netzwerkoutput dann als ein in Intensität und Richtung verändertes Magnetfeld-Perzept ausdrückt, was als magnetische Versetzung interpretiert werden kann. Da das Magnetit-basierte System Kompassinformationen offenbar automatisch mitgeneriert, suggeriert dieses Ergebnis eine gewisse funktionelle Redundanz zum Radikalpaar-basierten Inklinationskompass. Anders herum stellt sich die Frage, ob der Radikalpaar-Mechanismus mehr also nur Kompassinformationen liefern kann. Dies führt zur zweiten großen Simulationsreihe dieser Arbeit, deren Ziel es ist, die Navigationsfähigkeit anhand des Inklinationskompass zu testen. Hierzu haben wir eine simulierte Navigationsumgebung mit einem räumlichen Gradienten in Inklination und Deklination entwickelt und darin einen künstlichen Lernagenten getestet, der den Zugvogel symbolisiert. Dieser künstliche Vogel nutzt einen Inklinationskompass gekoppelt mit einem Sternenkompass, der wiederum die geographische Nordrichtung detektiert. Mithilfe dieser sensorischen Hinweise war der Lernagent in der Lage, von jedem zufällig ausgewählten Ort in der Umgebung aus erfolgreich zu einem Zielort zu navigieren. Darüber hinaus haben wir andere experimentell entdeckte Eigenschaften der Navigation gezeigt, wie z. B. die Extrapolation. Fasst man diese beiden Simulationen zusammen, besteht möglicherweise Unklarheit hinsichtlich der genauen Rolle des Magnetit-basierten Systems und des visuellen Kompasses. All diese Diskussionen und Arbeiten stellen die vorherrschende Vorstellung in Frage, dass beide Systeme voneinander isoliert sind und jeweils eine einzige Funktion haben. Abschließend sollte beachtet werden, dass Vögel opportunistisch sind (und dies auch sein müssen, um zu überleben!), sodass sie jeden verfügbaren Hinweis nutzen und dazu alle Sinne offen halten. Vorausgesetzt, sie verfügen über die neuronalen Schaltkreise, werden sie alle Informationen integrieren und dann die Qualität der verschiedenen Informationen im Entscheidungsprozess abwägen, bevor sie ihre Reise fortsetzen.

Danksagungen

From all my heart, I want to thank everyone who supported me and stood by me during my PhD times. I am truly lucky, as despite all the circumstances, I was able to make it this far. First of all, I want to thank my supervisor Prof. Dr. Michael Winklhofer, who I had the pleasure of being one of his students. He understood my situation and supported me in various ways. I enjoyed our discussions and because of him I have a clear understandings of what I need to do next. I want to thank Prof. Dr. Heiko Schmaljohann for his warm acceptance of being my second reviewer.

I want to thank all members of the MSB RTG managing and coordinating teams. Being in the MSB was truly a memorable experience. Thanks Prof. Dr. Karl-Wilhelm Koch for accepting me into the group. Thanks Petra and Kristin for the wonderful coordination, I always found help in my time of need. Thanks Prof. Dr. Henrik Mouritsen and Prof. Dr. Martin Greschner for the helpful insights and feedback. Thanks to Apl. Prof. Dr. Karin Dedek, I was truly lucky to have known you and also thanks for your support during my team of need and your understanding. Thanks Prof. Dr. Christopher Lienau for your aid and support. Thanks to all my team members, especially Franziska Curdt and Laura Ziegenbalg for there support and understanding. Thanks to all my colleges in the MSB RTG, especially Charlotte Beelen, Constanze Krohs, Jannes Vagts and Anne Depping, because of them I did not feel alone and as a foreigner.

Thanks to the managing and coordinating team of the PPRE program and community, especially Dr. Hans Holtorf. He was like a grandfather to many students including me. He gave me advice and counseled me during my time of need. Thanks to all current and past members at the Department of Urban and Building Technologies at DLR, especially Dr. Martin Vehse and Volker Steenhoff for their support and guidance over the years. Thanks Renate Pfaffenberger, just mentioning her, makes me feel warm. She helped and guided many foreign students during their stay at Oldenburg. She offered us wonderful Christmas dinners, presents and showed us the local church performances. Her dedication and passion towards helping others was truly inspiring. I would like to give thank to my house mate Luqman Alimi for the amazing discussions we had during our stay together. From him, I learned a lot about the culture of Nigeria.

I would like to thank my best friends in Germany, Raul Granados, Ela Romero-Lopez,

Amr Khaled and Saleem Barkeel for the wonderful times we spent together, the cultural exchanges we had, the places we visited together and the support we provided each other. With them, I always knew my back was covered. I would like to thank the Coptic Orthodox community at the church of Wilhelmshaven. Specially, Roushdy Tadros, Nabil Yassa, Ibram Wasfy, Basem Saman and Yosab Wagdy for their support over the years. I would like to thank Dr. Adel Sobhy, whom recently provided invaluable counseling to elevate my mental status.

Finally, I would like to thank my family: my father, mother and my brothers, Remoun and Peter. They were my lighthouse. They understood me very well and understood the pains of living with an annoying life-altering chronic disease for the rest of your life. They supported and encouraged me through every step of the way. I wouldn't have asked for a better family. Without their support and guidance I wouldn't have overcame many hurdles in life. Without them, I wouldn't have reached anywhere and I would be nothing.

Contents

List of Figures

Chapter 1

Motivation and brief outline

The problem of how birds perform reliable long distance migration is not solved yet. It is widely accepted that birds have two systems to achieve this feat: a compass and a map. Map information is needed to determine the current location relative to the goal, while the correct bearing towards that goal can be obtained on the basis of compass information. A wealth of literature suggests that birds can extract both map and compass information from the Earth's magnetic field, but how they do so is a matter of intensive research. There is good evidence that the magnetic compass of birds is based on the radical pair mechanism of magnetoreception [Hore and Mouritsen, 2016], which can readily explain the three hallmarks of the so-called inclination compass of songbirds, which i) is insensitive to magnetic polarity, ii) depends on light of short wavelength, and iii) can be perturbed by low-intensity radio-frequency magnetic fields in the lower MHz range. Experimentally, the inclination compass is studied on caged birds deprived of celestial cues, but at a test site known to the bird, typically at a stop-over site along the migratory route. In contrast, for experiments on map navigation, birds are transferred from a stop-over site to a location off the normal migratory route, either by physical displacement or by virtual magnetic displacement, where the magnetic field at the stopover site is altered such that it mimics the field parameters that the bird would experience at a location off its route [Kishkinev et al., 2021]. Indeed, either type of displacement under provision of celestial cues, has been shown to result in orientation tendencies which would lead the displaced birds back onto their normal migratory route [Chernetsov et al., 2008; Chernetsov et al., 2017]. Such corrective behaviour was observed only in adult birds with prior experience in migration, but not in juveniles, suggesting that navigation by a magnetic map in combination with celestial cues is a learned behaviour. When it comes to sensing magnetic map factors, a popular, yet not generally accepted hypothesis assumes magnetic particles in specialized sensory cells, innervated by the ophthalmic branch (V1) of the trigeminal nerve. The involvement of V1 is supported by a study in which an intact V1

was found necessary for corrective orientation behaviour of physically displaced songbirds [Kishkinev et al., 2013], along with other studies from the same lab where sensory nuclei in the trigeminal brainstem were found to have higher activity under magnetic stimulation. However, there is no anatomical evidence thus far for magnetic particles in the sensory periphery of V1 [Curdt et al., 2022], the only indication toward an involvement of magnetic particles comes from orientation experiments on birds pretreated with a strong magnetic pulse [Beason et al., 1995; Wiltschko et al., 2009; Karwinkel et al., 2022a], designed to remagnetize magnetic particles with the aim to alter the perceived magnetic map factors. Although the pulse pre-treatment often resulted in deflected orientations, it remains unclear whether the pulsed birds perceived an altered magnetic field and related it to a meaningful location on the magnetic landscape, or if they rather ignored magnetic map percepts and performed some default orientation.

A major source of ambiguity comes from the very design of these experiments, which do no study pulse effects on displaced birds that actively use the map, but instead are conducted at a stop-over site in a lab setting similar to magnetic compass orientation experiments, without knowing if control birds rely on magnetic map information to begin with. Further, without an obvious anatomical candidate for the magnetosensory structure at hand, it is unclear how exactly a pulse affects a magnetic-particle based magnetoreception mechanism.

While answers to the questions above can be given only by carefully designed experiments and neuroanatomical work, such approaches would benefit from theory inspired guidance on experimental design and interpretation of findings. Therefore, a major aim of this thesis is to develop a theoretical framework for predicting pulse effects on orientation behaviour. In the approach taken here, established computational neuroscience tools are used to model pulse experiments at the level of a neuronal population with each cell in the population receiving input from the sensory periphery according to a biophysical model for magnetic field transduction. We will study how the results will depend on the physical and biological assumptions underlying the models. For example, it is not known if the pulse just remagnetize particles or even damages the transduction machinery of the cell, while in the model we can conveniently alter the output of cells according to the assumptions. Should the model not crucially depend on the assumptions, then we can arrive at general conclusions. On the basis of the simulation results, we will then give guidelines for future pulse experiments with more diagnostic power.

Another major problem concerns the nature of the cognitive magnetic map itself: How and where is it mentally represented and how does it interact with other internal presentations of directional and spatial information? In the mammalian hippocampus, space is explicitly encoded by place cells, so it is conceivable that birds could also have

cells in higher brain areas that fire only when a specific magnetic field is present. But to be useful for navigation, this magnetic information, which still resides in the egocentric frame, needs to be tied to allocentric information about the body orientation/head direction in space. As mentioned above, night-migratory birds in virtual displacements experiments have access to the starry sky, which suggests that they derive information about true North (geographic North) from the star compass. With true North given, the local geomagnetic field vector can now be expressed in a geocentric coordinate system, in terms of the three components intensity, inclination (dip angle), and declination, the latter defining the angle between local magnetic North and true North. Because of the predominantly dipolar nature of the geomagnetic field, it varies systematically on larger scales, but with high covariance between parameters intensity and inclination, making one of them redundant. This prompts the question if reliable magnetic map navigation is possible on the basis of declination and inclination only and if so, is the inclination compass in the visual system sufficient for this purpose.

To address these questions, the second study of the thesis presents a machine learning approach, where a neural network is trained in a reinforcement learning setting to navigate in a magnetic landscape fixed on a geographic grid. The network, which can be regarded as higher brain areas where sensory integration and decision-making takes place, constantly receives noisy magnetic field information from the sensory periphery as it is moving across the grid. To model the magnetic sensory input, we adopt, with no loss of generality, the model by [Ritz et al., 2000], according to which the magnetic field is perceived as a visual modulation pattern, such that the projection point of the magnetic field axis onto the retina appears as a dark disk against the visual background (starry sky). When the network moves into a new direction, the azimuthal position of the disk shifts accordingly in the egocentric frame. The perceived elevation of the disk corresponds to the inclination angle, which allows for inclination sensing, too. After all, there is evidence that birds can measure the inclination angle; for example, European songbirds use the inclination angle as a stop sign [Wynn et al., 2022]. Given that birds have high visual acuity, visual modulation pattern would allow them to determine the inclination angle with sufficient precision for navigational purposes. The same argument can be applied to the declination angle, provided true north is known from the star compass. Again, there is evidence that the declination angle is part of the map system and birds can correct for new declination angles after displacement [Chernetsov et al., 2017]. Taken together, it would be computationally 'easy' for the bird to navigate using the visual system. All the information is packed into one system, so no need for extra computational overhead to integrate information of another sensory system (i.e. trigeminal). Even if the retinal magnetopercept is not projected along the tectofugal pathway onto the perceived opti-

cal image, but along the thalamofugal visual pathway into another brain region such as Cluster N [Heyers et al., 2007], as long as the magnetic information arriving in Cluster N encodes the azimuth and elevation of the projection point of the field axis on the retina, it can be uniquely related to the optical information at a higher level. Based on this intuition, the second study aims at a detailed analysis of this hypothesised navigational system. In addition, the emergent properties of this system are compared to experimental findings in literature. We finalize this study by few predictions that can prove useful in designing future map-related experiments.

Both simulation studies presented here thus address important aspects of neuronal processing of magnetic information, received by plausible biophysical mechanisms for the sensory detection process. The results of the studies challenge the widely accepted functional division between visual and trigeminal magnetosensory system for compass and map, respectively. Instead, the results support the hypothesis each system has more than one function or that at least both systems work together to solve the navigational problem. Both studies are two faces of the same coin, and depending on the assumptions, a magnetic particle based system can provide both compass and map information, while the established inclination compass can supply also a map information. This can be experimentally tested by exposing virtually displaced birds not only to a pulse, but also to a broadband radio-frequency magnetic field.

Finally, a secondary motivation of this work is to demonstrate the power of modeling. It is faster and incurs less cost compared to the physical experiments. Both of the studies provided here are not only explanatory, but they also provide testable predictions to aid the experimental paradigm. Modeling can also motivate further aspect of a theory. For example, in the first study we hypothesize that a reference frame upon which the magnetic field angle is measured is necessary for orientation. We hypothesize that this reference frame is the head direction. There is emerging evidence that birds might possess head direction cells. A consequence of this analysis is the question: do other spatial cells exist. For the second study, using a biologically plausible training/learning algorithms can provide powerful insights into the relationship between the navigational environment and the learned behavior. Learning agents(birds) can demonstrate unexpected behavior in various artificial environments which stimulates deeper though regarding the nature of the problem. So, we hope that the modeling tools used here would prove useful in enriching the animal behavioral research.

Chapter 2

General introduction

In this chapter, we present a literature review of the various topics encountered in this work. In section one, we discuss the dominate cue in this study, the Earth's magnetic field, its physical origin and properties. In sections two and three, we review the compass and map mechanisms in birds. These include the widely accepted views regarding how they operate and the utilized environmental cues. In section four, we discuss the pulse experiments. We discuss the motivation behind them, the methodologies and the various results. In section five, we discuss modeling in biology; especially modeling of cortical neural circuits using computational neuroscience tools, modeling of animal navigation and machine learning in biology. In the last part, we discuss how machine learning is gaining traction in biology. Specifically, how reinforcement learning is utilized to further our understanding of animal behavior.

2.1 The Earth's magnetic field

The Earth's magnetic field for the largest part originates from convective motion in the electrically conducting Earth's liquid outer core, which according to dynamo theory is transformed into magnetic energy. Mathematically speaking, the Earth's magnetic field is a three-dimensional vector field, which on the Earth's surface can be approximated by a dipole located at the Earth's center, with the dipole axis tilted relative to the rotational axis by 11.5° (Müller and Stieglitz, 2000). Somewhat counterintuitively, the magnetic poles are flipped relative to the geomagnetic poles; the magnetic South pole is near the geographic North and the magnetic North pole is near the geographic South. Thus, the magnetic vector field lines leave the Earth in the southern hemisphere and re-enter in the northern hemisphere, see Fig. 2.1a for a graphical representation. The dipolar approximation accounts for 90% of the magnetic field observed on the globe on average, but there are some regions where the contribution of nondipolar components to the field

considerably exceeds 10%, up to 30% in the Southern Atlantic Ocean. Thus far, we have been concerned with the so-called main field, whose sources in the deep Earth are so far away from the Earth's surface that they produce relatively smooth, predictable spatial field variations on the globe. In contrast, magnetized rocks in the Earth's crust are responsible for irregular spatially variations, so called magnetic anomalies. Last, there are also temporal variations of the Earth's magnetic field, mainly due to magnetic fields carried by the solar wind. In addition, the core field itself is highly dynamic and varies on a secular time scale, producing a slow drift of the magnetic field.

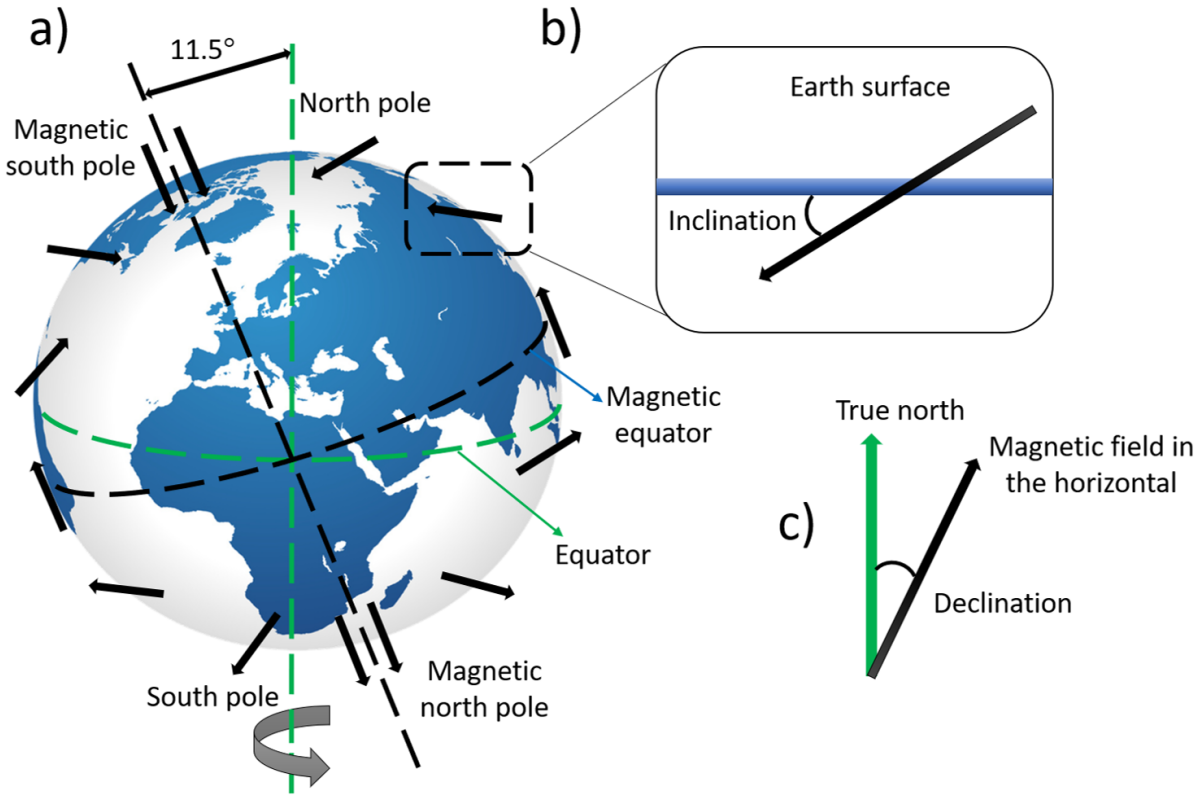

Fig. 2.1: The Earth's magnetic field. a) the magnetic globe with the magnetic field vectors. The shown angle is the difference between the rotational axis and dipole axis. b) the inclination angle as the angle between the horizon/horizontal and the magnetic field vector in the vertical. c) the declination angle as the angle between the true north and the magnetic field in the horizontal. Earth globe source: https://pixabay.com/vectors/globe-world-Earth-black-white-308065/.

For migratory birds, several magnetic field parameters are relevant for orientation and navigation; these are the inclination (Wiltschko et al., 1993), intensity (Wiltschko and Wiltschko, 2013) and declination angle (Chernetsov et al., 2017). The inclination angle is the angle between the magnetic field and the horizontal (Fig. 2.1b). It runs from 90° (magnetic north) to 0° (magnetic equator) to -90° (magnetic south). The inclination angle and the magnetic field intensity (which runs from 60 µT at the poles to 30 µT at the equator) vary along the latitude. The declination angle is the angle between the

magnetic field in the horizontal and the true north (Fig. 2.1c). The declination angle varies mostly along the longitude.

2.2 The biological compass

A compass in the broadest sense allows one to determine the direction of a target relative to a reference direction (e.g., local magnetic North). A compass sense enables migratory birds to find their appropriate migratory direction towards their goal and maintain it during the journey. Migratory birds have proven to possess multiple compass senses (reviews: Muheim et al., 2006; Chernetsov, 2016), relying on cues such as the sun position ("sun compass"), the celestial pole about which the night sky rotates ("star compass"), magnetic field, and perhaps skylight polarization patterns, although birds – unlike insects – are not known to have anatomical structures suitable for detecting the polarization axis of light. Regardless, the three established compass senses in migratory birds form a system and have a certain degree of redundancy, due to the magnetic field being always present, at daytime and at night. This redundancy is evolutionary advantageous, because the two mentioned visual cues can be obscured under overcast conditions. In this regard, intense studies have been conducted to understand the cue priority in the compass system. In these so-called cue-conflict experiments, one compass/orientation cue is varied while the other is held constant; and it is tested if directional tendencies of migratory birds shift in accordance with the shifted cue. Generally speaking, celestial cues seem to have higher salience than magnetic ones. It was shown that migratory birds, in the pre-migratory period, recalibrated their magnetic compass in accordance to a shift in the celestial cues (Bingman, 1983; Prinz and Wiltschko, 1992; Able and Able, 1993). This was observed when birds are tested during the migratory period but had access only to the magnetic cues. However, during the migratory period, the opposite trend was observed. Rotating the magnetic field led to a related shift in the migratory direction (Wiltschko et al., 1998b ; Wiltschko et al., 1999; Sandberg et al., 2000). Also during the migratory period, birds seem to recalibrate their magnetic compass like in the pre-migratory period; for a review see Muheim et al., 2006. Thus, it seems that celestial cues dominate magnetic cues when there is a clear view of the sky, while the opposite is true when birds are tested indoors or with an incomplete view of the sky.

It was realized more than 50 years ago that magnetic compass orientation in songbirds had to be studied in absence of visual cues. Studying caged European robins in the migratory season, Wiltschko and Wiltschko, 1972 observed that an inversion of the horizontal component of the ambient magnetic field vector caused birds to reorient by ca. 180° relative to controls, i.e., the expected behaviour for a magnetic compass. Surpris-

ingly, reorientation by 180° also happened when only the vertical component was inverted (reversing inclination angle), while inverting both components simultaneously had no effect. Thus, the magnetic compass of songbirds depends on the sign of the inclination angle of the fieldlines but not on their polarity, i.e., it does not point north or south, like the traditional human compass, but instead indicates poleward or the equatorward (Wiltschko and Wiltschko, 1972). This so-called inclination compass is narrowly tuned to a certain magnetic field intensity band. When taken outside the working range, robins were not oriented. However, after three days in the new field, they regained orientation and realigned towards their natural migratory path (Wiltschko and Wiltschko, 1996). This might be an indication of an intensity-based adaption for the functional range of the magnetic compass. Unlike the stellar compass which needs learning (Foster et al., 2017), the magnetic compass is thought to be inherited.

Several hypotheses exist about the biophysical process underlying magnetic field detection for the inclination compass. These being, electromagnetic induction, a chemical transduction mechanism mediated by radical pairs, and a mechanical transduction mediated by magnetite particles. The support for the electromagnetic induction hypothesis comes from studies on the Elasmobranch fish. Sharks and rays have an electric sense and with it they can sense the prey-generated electrical fields (Johnsen and Lohmann, 2005). This electric sensory organs, the ampullae of Lorenzini, are considered sensitive enough to detect a small voltage difference generated by the Lorentz force when an elasmobranch fish moves across magnetic field lines. Although there is evidence that Elasmobranch fish do sense the magnetic field (Klimley, 1993; Meyer et al., 2005), there is no concrete evidence that the detection method utilized is electromagnetic induction. For example, rays conditioned to react to magnetic anomalies have their conditioning disappear when small magnets were inserted into their nasal cavities. Conversely, inserting non-magnetic brass bars had no effect. This is in conflict with the electromagnetic induction because a static field should have no effect. The analogues of this theory in birds(pigeons) is the presence of sensitive voltage-gated ion channels in the hair cells of the semicircular canal of the inner ear (Nimpf et al., 2019). This voltage-gated channels is thought to be sensitive to the electromotive force induced by the change in the magnetic fields.

According to the radical pair mechanism of magnetoreception, the magnetic field affects light-dependent biochemical reactions of short lived radical-pair intermediates (Schulten et al., 1978; Steiner and Ulrich, 1989; Ritz et al., 2000), which ultimately requires a chemical transduction cascade to convert a magnetic field into a change in membrane potential of the magnetoreceptor cell. Importantly, the chemical composition of the reaction output depends on the strength and axial orientation of the magnetic field, but not on its polarity (Schulten et al., 1978), in perfect accord with the inclination

compass. A convenient way of generating radical pairs is through excitation with short wavelength light (Ritz et al., 2000), which was found necessary for the magnetic compass to work (e.g., Phillips and Borland, 1992; Wiltschko and Wiltschko, 2005). Further evidence for light-dependent magnetoreception comes from brain activity studies using immediate early gene expression (Mouritsen et al., 2005; Zapka et al., 2009; Hein et al., 2010). Once generated, a radical pair becomes sensitive to the external magnetic field, modulating hyperfine-field driven singlet-to-triplet interconversion, which occurs in the MHz frequency range. Therefore, the most effective method of perturbing the radical pair mechanism is by application of a radiofrequency magnetic field, which interferes with the natural hyperfine interactions between nuclear spins and unpaired electrons spins of the radical pair (Ritz et al., 2004). Indeed, birds exposed to radiofrequency magnetic fields (0.1 MHz to 80 MHz) were disoriented (Ritz et al., 2004, Leberecht et al., 2022), while 0.1 MHz or less had no disorienting effect, suggesting the lifetime of the spin-correlated state in the radical pair is less than 10 µsec (Kobylkov et al., 2019). When the radical pair mechanism was put forward by Schulten et al., 1978, no concrete molecule was known that could play host to the mechanism. This changed with a follow up paper by the Schulten group (Ritz et al., 2000), suggesting the then newly discovered flavoprotein cryptochrome as candidate molecule. Of the various Avian cryptochromes, Cry4 is considered most suitable (Xu et al., 2021). Further, Ritz et al., 2000 suggested that radical pair based magnetoreceptor cells, when distributed uniformly over the retina hemisphere, would produce a spatial representation of the magnetic field, which in connection with a visual pathway would allow birds to literally see the magnetic field. Such field-induced visual modulation patterns (simulated in Ritz et al., 2000; Wang et al., 2006) would allow birds to determine also the inclination angle visually. However, they fall short of explaining the functional window. Birds kept in an intensity of 46 µT were not oriented at 34 µT and 60 µT (Wiltschko and Wiltschko, 1996), while according to the simulations by Ritz et al., 2000, at least, a doubling or halving of the sensed intensity seems necessary to perturb the visual modulation pattern.

The third and last hypothesis for the compass sense mechanism is the mechanical transduction by magnetite particles, which was clearly inspired by the discovery of magnetic bacteria (Blakemore, 1975) that biomineralize single-domain magnetite particles (Frankel et al., 1979) and use it for aligning with magnetic field lines. Single domain particles have homogeneous and stable magnetization which can effectively act as a nano-scale bar magnet. There are several theories and models regarding how these bar magnets can excite the sensory cell and thus convey the magnetic field information to the bird. These models include, but not limited to, the torque model (Winklhofer and Kirschvink, 2010) and the variance model (Walker, 2008). In the torque model, the interaction between

these nano-magnets and the magnetic field would produce a torque that can excite cells via mechanically gated ion-channels (Winklhofer and Kirschvink, 2010). In the variance model, the variance of the motion of a thermally agitated chain of single domain particles will depend on the magnetic field intensity. This chain is connected to various mechanically gated ion channels, and thus the interaction between the field and the thermally agitated chain will open and close varying amount of ion channels. The amount and rate (of opening and closing) will depend on the field intensity. Integration of the time varying activity of those channels (which depends on the activity of the chain) will lead to an estimation of the field intensity. The second hypothesis for the mechanical transduction is based on the deformation of Superparamagnetic magnetite (SPM) clusters. Magnetite crystals with sizes well below 50nm do not possess permanent magnetization at room temperature (Frankel et al., 1979; Hanzlik et al., 2000; Tian et al., 2007). Hence, they can't act as torque transducers, but clusters of SPM can affect mechanically sensitive ion channels by the structural deformations induced by the magnetic field (Shcherbakov and Winklhofer, 1999; Davila et al., 2003). Although it is widely accepted that the ophthalmic branch of the trigeminal nerve (Heyers et al., 2010) mediates the magnetic field information of this sensor, the precise location of these magnetite structures remains elusive (Curdt et al., 2022)

2.3 The cognitive map

A compass alone is not sufficient for successful navigation to a target destination if the current position is drifting sideways from the route. Indeed, juvenile startlings and chaffinches that were actively displaced during their first autumn migration, kept their original compass route and ended up in a new location, while adults compensated for the displacement and reached the target destination (Perdeck, 1958). To explain true goal orientation in adult songbirds, a cognitive map has been postulated, and recent research suggests that magnetic parameters contribute to it as well (Chernetsov et al., 2008; Kishkinev, 2015). A cognitive map appears necessary for birds to cope with "nuisance factors", for example, uncertainty in the measurement of the compass cue, which leads to accumulated error with time. Without corrective behaviors, this error would drastically displace the bird from its normal course and subsequently, impairs the bird's ability to reach its target destination. External nuisance factors include weather conditions, like strong winds, which can displace the birds, or a complete absence of any orientation cue. The influence of these factors can be mitigated by the possession of some form of a map or positional information. Knowing the current location relative to a goal corrects for any error induced by internal or external factors.

Although adult birds are apparently able to compute positional information (within limits), there is still debate regarding the nature of the navigational map that birds might possess. In contrast, mammals have space-coding cells in the hippocampus, which include place cells (O'Keefe, 1976) and head direction cells (Taube et al., 1990). Place cells fire when an animal passes a certain location in an environment and head direction cells are tuned to a specific head direction. Although, spatial tunings similar to the one found in the mammalian hippocampus has not been found in birds, there is evidence that birds might possess spatial tunings albeit with a different characteristics (Colombo and Broadbent, 2000, 2000; Sherry et al., 2017). Also, there is the observation that Japanese quails possess head direction cells (Ben-Yishay et al., 2020). It should be noted that, in the navigational map literature, by map it means the large scale (up to 1000s of kilometers) maps that is used for navigation. This map should not be confounded with an indoor (small environment) map. Hence, it is not clear whether the spatial tunings in the bird's hippocampal formations are for large scale navigation, indoor environments or both. It seems that the only spatially tuned cell type that is invariant of the spatial scale is the head direction cells, which can fire in environments with varying scale. In this study, we discuss the large-scale navigational map. In this regard, there is no evidence that birds possess an explicit representation of space like mammalians do. For a discussion regarding the confusion associated with the word 'map' and its meaning see Lohmann et al., 2007.

Regarding the ontology of the map mechanism, it is agreed that it is a learned behavior. Thus, it is a navigational property of adult birds and not of juvenile (first autumn for Northern hemisphere) ones. For juvenile birds, it thought that they use a genetically coded vector-based navigational strategy (Berthold, 1988; Helbig, 1991). This is akin to a clock and compass strategy, where a bird chooses a compass direction and flies in that direction for a certain duration. As a counter argument, some studies challenge the concept of pure clock and compass for juvenile birds (Thorup et al., 2011). In this regard, juvenile birds might possess a crude form of navigational capabilities. However, it is not clear if these capabilities are learned or inherited. A recent study by Thorup et al., 2020 showed that common cuckoos (Cuculus canorus) compensate for displacements albeit after some migratory distance (or traveling time). This finding may tilt the argument towards learning by juvenile birds during their migratory trajectories. Learning is an ongoing continuous process during migration.

Several candidate environmental cues can be utilized for navigation. Infrasound waves generated by mountain ranges or coastal lines can act as a navigational cue. However, there is no direct experimental evidence. The only evidence available is correlative evidence; for example, disturbance of the homing performance of pigeons by atmospheric

fluctuations (Hagstrum, 2000). Another cue that is considered for navigation is gravitational cue, due non-uniformity of the Earths crusts causing fluctuations in the gravitational field (Blaser et al., 2013; Blaser et al., 2014). One theory is that birds possess a pair of gyroscope-like receptors. One measures a location once and memorizes it for life, while the other measures the current field and compares it with the first. The first receptor is typically used to store an important location, like the home base. Another cue is the celestial cue, which assumes that birds can determine location from the location of the sun or the pattern of the stars. Regarding this possible cue for navigation, little literature/experiments are available.

There are various theories regarding the physical nature of the magnetic map. The bi-coordinate theory postulates that birds possess an explicit representation of a magnetic bi-coordinate grid (Benhamou, 2003, Kishkinev et al., 2021). In this grid, the birds measure the local values and compares them to the goal values. In that case, the birds assume the vector direction joining the two points using the compass, or just move in a direction such that to decrease the difference. If traveling is more or less linear, like turtles traveling along the coastline, then a single coordinate is sufficient for reliable navigation. There is also traveling along an isoline, though this technique is scarcely talked about in the bird navigation literature. Lastly, there is the magnetic waymark navigation (Wynn et al., 2022). In this method, the bird (or animal) makes an association between particular magnetic field parameters and an orientation direction. In that case, navigation is a sequence of steps towards a list of waymarks and in each waymark, a new orientation is chosen. Finally, it should be noted that the map sense is thought to be mediated by the ophthalmic branch of the trigeminal nerve (V1)(Kishkinev et al., 2013), although the magnetoreceptor structures remain elusive (Curdt et al., 2022).

2.4 Pulse experiments

These experiments are utilized as a diagnostic test for the magnetite hypothesis. The motivation came from pulse experiments on magnetotactic bacteria (Kalmijn and Blakemore, 1978), where it was found that a sufficiently strong, but brief, magnetic pulse would reverse the orientation of these bacteria. The brief nature of the pulse is to avoid rotation and/or permanent damage to the particles. These bacteria orient along the geomagnetic field using a chain of single domain magnetite particles. Single domain particles possess a stable dipole moment and in a chain the dipole moments add up to boost its strength. This added strength enhances the sensitivity to the geomagnetic field. A pulse applied, predominantly, along the main axis of the chain but with opposite polarity to it, would reverse the dipole moments of the single domain particles and hence all the chain. In a

similar manner to magnetotactic bacteria, if birds utilize single domain magnetite particles for orientation or navigation, a strong, magnetic pulse would alter the bird's natural behavior in a way to warrant further analysis. From the work on magnetotactic bacteria, one may think that a pulse could also reverse the orientation of birds, when tested in Emlen funnels during migratory restlessness. However, as seen below, this was not the case. This led to extended discussions in literature on the nature of the magnetic material, its composition, structure, location and role. Even the methodologies of the experiments themselves was put into question.

2.4.1 Pulse experiments on caged songbirds

Beason et al., 1995 pulsed (5 ms, 0.5 T) bobolinks (Dolichonyx oryzivorus) in three different orientations and then tested them in Emlen funnels. After the application and testing of the first pulse, a second one was applied with opposite polarity. The experiments were conducted when the birds showed migratory readiness behavior, so as to compare the experimental birds with the control ones which show normal migratory orientation. In the first set of pulse experiments, the experimental setup orientations were north anterior, south anterior, and north up. In the north-anterior case, the orientation of the pulse as quoted "The north-anterior birds were magnetized such that, if the bill were made of iron, the tip would attract the south end of a compass." The south-anterior was with opposite polarity and in the north-up case, the pulse was applied vertically through the birds head. In the north-anterior case, the birds were deflected to the left at 255° compared to the control at 0°. In the south-anterior case the birds were deflected to the right at 55°, while the north-up case the birds were oriented in axial bimodality along the 145–325° axis. In the second set of experiments, a pulse applied with an opposite polarity to the first one resulted in random orientations for the different bird groups. The mean vector lengths 'r' for the first set was (0.39, 0.4, 0.36), while for the second set (0.18, 0.1, 0.3).

In a follow up study, Beason and Semm, 1996 found that the reorienting effect of a pulse (delivered north anterior) can be abolished by applying a local anesthetic to the upper beak, aimed at blocking the ophthalmic branch of the trigeminal nerve, which in a previous electrophysiological study by the same authors (Beason and Semm, 1987) was reported to convey magnetic intensity information.

Wiltschko et al., 1994 pulsed (4 ms, 0.5 T) Australian Silvereyes indoors. The orientation of the pulse was as quoted "The physical north pole of the induced field was directed towards the end of coil where the heads of the test birds were placed." In comparison to the Beason terminology, this implies north-anterior as after the application of the pulse, the bill would attract the south end of a magnet. Before treatment, the mean heading was 24°, while after treatment, in the first day, there was roughly a 90° clockwise rotation of

the mean heading. Testing on subsequent 4 days showed a scatter in orientation and then a gradual return to the natural original heading. On the 8th day, there was no more shift in orientation. One of the results of this experiment is counter intuitive to the expected results from pulsing experiments; a reversal in polarity of the magnetic moment of single domain magnetite particles should be permanent and not temporal. It should be noted also that the shift in orientation of the sliver eyes was opposite (clockwise) compared to the counter-clockwise shift of the bobolinks with the north-anterior setup.

Munro et al., 1997a pulsed adult and juvenile Silvereyes indoors. It was shown that the pulse altered the orientation of the adult group but not the juvenile ones. Subsequently, it was argued that since one of the main the differences between adults and juveniles is the experience gathered during migration and that the map sense depends on experience; the pulse affected the map sense and that the magnetite-based receptor provides, at least, one coordinate of the navigational map.

Wiltschko et al., 1998a pulsed (4-5 ms, 0.5T) Australian Silvereyes indoors during their spring migration when they are headed southward. The orientation of the pulse was as quoted "The bird was placed into the coil with its head pointing straight forward to the end where the magnetic south pole of the pulse field was induced ('south-anterior' as defined by Beason et al. 1995, 1997)." Before treatment, the control birds oriented in their natural migratory direction at 182°. In the first day after treatment, they oriented to the east at 73°. This orientation continued unchanged for 4 days. From days 5 to 8 and in accordance with the previous Silvereyes study, there was scatter with insignificant orientation vectors. After day 10, the birds returned to their natural migratory direction southwards. In this study, it was also argued that the affected sense is the map sense, as the tested birds had migratory experience. Wiltschko et al., 2007 did a similar experiment to this one with the addition of a second pulse applied 16 days after the first one. The second pulse, and in contrast to the first one, led to scatter in orientation with weak tendency towards the natural migratory direction. Also, this effect lasted only for 2 days. These results indicate that the birds do not return to the same state after 10 days of the first pulse (when they resume normal orientation), but the new state is a combination of a dynamic process that is likely to alter the affected receptors (for example repairing the damaged ones) and mental process that causes the bird to interpret the altered input in a new manner. In other words, there are physiological and psychological changes happening in the bird in order to orient in the normal migratory direction.

Wiltschko et al., 2002 pulsed (4-5 ms, 0.5 T) Australian silvereyes indoors during their autumn migration when they are headed northward. In contrast to previous work, the test birds were exposed to a 1 mT static biasing field while getting pulsed. The intuition behind the biasing field is the following: if the magnetic particles are free to

move, they would orient along the biasing field. Hence, different combinations of biasing field and pulse directions should produce differing results. The orientation of the pulse was in the south-anterior manner. The biasing field was applied in two directions, parallel (PAR) and anti-parallel (ANTI) to the pulse. Both the control and the biasing field-only treatment, showed normal orientation towards the north with the ANTI case having more scatter. However, after the application of the pulse in the presence of the biasing field, both the PAR and ANTI groups showed axial bimodal orientation in the east-west axis. One of the main outcomes of this experiment is the hypothesis that the magnetic particles are not free to move to orient with the biasing field.

Wiltschko et al., 2009 again tested pulse effects on Australian silvereyes, now applying a local anesthetic to the upper peak after the pulse application and before testing, just as Beason and Semm, 1996 had done on bobolinks. However, in the meantime, structures containing superparamagnetic magnetite were reported in the upper beak (Hanzlik et al., 2000; Winklhofer et al., 2001), and – being associated with nerves – considered putative magnetoreceptors, (Fleissner et al., 2003). Hence, a local anesthetic would temporarily deactivate the receptors which, although affected by the pulse experiments, would no longer produce distorted field readings. In a rare occurrence in science, the intuition came true: the birds without anesthesia demonstrated the typical shifted orientation in accordance with previous experiments, while the birds with anesthesia, applied to their peak, maintained their natural southward orientation. These results supported the hypothesis that the superparamagnetic structures in the beak might be responsible for the magnetic transduction in the trigeminal system. However, in the same year, the very structures containing the superparamagnetic particles turned out to be immune cells, not neurons (Treiber et al., 2012). Also, the local anesthetic used in the study (xylocaine, aka lidocaine) has been found unreliable (Engels et al., 2018).

2.4.2 Studies on songbirds tracked in free flight after pulsing

With the advent of lightweight radio-tracking devices, it became possible to study the navigation performance of songbirds in free flight after pulse treatment. (Holland et al., 2009) pulsed catbirds (0.1 ms, 0.1 T) south anterior, but found no effect on orientations. Later, Holland, 2010 pulsed (0.1 ms, 0.1 T) European robins (Erithacus rubecula) and reed warblers (Acrocephalus scirpaceus). In addition and in a similar manner to Wiltschko et al., 2002, a 320 uT biasing field was added to the basic pulse experiment. The biasing field was applied perpendicular, parallel and anti-parallel relative to the pulse direction. The orientation of the pulse was as quoted "The pulse coil was aligned with the direction of the pulse west to east and the birds were placed in the coil with their heads facing the direction of the pulse, 'south-anterior', as defined by Beason et al.(1995)." For

the perpendicular case, both European robins and reed warblers showed a clockwise shift in the departure bearing relative to the controls. For the parallel case, there was no significant difference in the departure bearings between the test and control birds. Although, for the anti-parallel case, there was a significant difference between the test and control groups, where the orientation of the test was bimodal in an axis almost perpendicular to the departure bearings of the control. In a follow up experiment, Holland and Helm, 2013 studied the difference in departure bearings between juvenile and adult european robins after the application of a pulse. The pulse (0.1 ms, 0.1 T) was administered through a south-anterior configuration. In addition to the pulse, there was an anti-parallel (relative to the pulse direction) biasing field of 320 µT. As for the results, although the mean departure bearings of both the juvenile and adult birds didn't deviate much from control, the mean vector length 'r' of the treated adult group was significantly smaller than the control group (0.872 vs. 0.475), while for juvenile the case was (0.501 vs. 0.578). Thus, there was more scatter in the departure bearings of the treated adult group compared to control. Also, the scatter in the departure bearings of the treated adults seemed to fade away after 10 days having a meaning vector length of 0.871 (compared to the 0475 after treatment). There are two side notes to this experiment: i) the decrease in scatter within 10 days after treatment seems in accordance with the work on silvereyes by Wiltschko et al., 1998a and related work. ii) In the previous study (Holland, 2010), the anti-parallel group had a bimodal orientation, but in this case, there was more scatter with a unimodal orientation. As Karwinkel et al., 2022b point out, the range over which birds were traceable in free flight in the studies of Holland, 2010 and Holland and Helm, 2013 was too short to decide if they were just exploring the stopover area or indeed resumed their migratory program.

Karwinkel et al., 2022a&b performed two pulse studies on the off-shore island Helgoland in the North Sea, where songbirds leave for good when they depart, thereby observing them in the act of migrating. Karwinkel et al., 2022a pulsed (1 ms, 0.1 T) juvenile and adult wheatears (Oenanthe oenanthe), where the orientation of the pulse was as quoted "The magnetic field lines of the pulse were perpendicular to the beak, the latter pointing south anterior." (south left in Beason's nomenclature). Both the experimental and testing phases were conducted outdoors. In the testing phase, the bird trajectories were tracked through the equipped radio transmitter. The results of the pulsing was assessed in through departure probability, departure timing within the night, departure direction and consistency in flight direction. For all four cases, there was no statistically significant difference between the control juvenile and treated juvenile, in line with previous pulse and map studies, but surprisingly, also no difference between the control adults and treated adults. The outcomes of this experiment was hypothesized to

be the result of: i) the birds ignoring the new faulty input from the affected/impaired magnetic field sensor. ii) the magnetic particles were unaffected/unaltered, which was described as less likely than the first possibility. In a follow up experiment, albeit with a different species, Karwinkel et al., 2022b pulsed (0.1 T) European robins (Erithacus rubecula) during spring migration at their stopover on Helgoland. The pulse orientation was as quoted "The head of the bird pointed southwards and the magnetic field lines of the pulse were aligned perpendicularly to the bird's head, with the magnetic North pole pointing towards the bird." Also, like in the previous study, the birds were not tested indoors but in free flight using radio tracking. In an almost similar manner to the previous study, there was no effect on departure probability, nocturnal departure timing, departure direction or consistency of flight direction after pulse application.

2.4.3 Pulse experiments on homing pigeons, bats, and aquatic animals

Beason et al., 1997 pulsed homing pigeons and found that the headings of the treated pigeons differed from the control ones. This shift in heading was affected by distance. Also, the direction of the pulse affected the heading direction, with both the south-anterior and south-left treated pigeons having headings on the opposite sides of the control. However, A pulse study on homing pigeons in Italy conducted by Holland et al., 2013 found no effects. Holland et al., 2008 pulsed bats and found the anticipated effects. Irwin and Lohmann, 2005 pulsed loggerhead sea turtles. It was found that turtles that were free to orient in darkness, were disoriented after pulsing (r=0.15), while controls were oriented. Ernst and Lohmann, 2016 pulsed Caribbean spiny lobsters. The treated lobsters were divided into two groups depending on the direction of the pulse relative to the local geomagnetic field. In one group the pulse was administered anti-parallel to the geomagnetic field, while in the other, the pulse was parallel to the geomagnetic field. In this experiment, it was found that the control group showed no significant orientation, while both the anti-parallel and parallel groups were oriented towards the 47° and 259° directions respectively. Fitak et al., 2020 pulsed juvenile rainbow trout (Oncorhynchus mykiss) and reported that the pulse can elicit orientation behavior in the fish, however, this effect was day and time dependent. For example, it was hypothesized that the daily variation of the solar electromagnetic activity might have an effect on the orientation behavior as seen from the multiple circular-linear regression. Naisbett-Jones et al., 2020 pulsed juvenile Chinook salmon. The control and treated groups were tested in two different magnetic field conditions: the local field and the field that would be present near the southern limit of the species range in the Pacific. In the local field, the control group was significantly

oriented (r=0.55), while the treated group showed statistically insignificant orientation (r=0.37), similar to most results on songbirds. Surprisingly, the opposite was true on the other site, with the control group having scattered orientation (r=0.13), while the treated group having a significant orientation towards the east-northeast (r=0.51). Put differently, the latter experiment (i.e., on virtually displaced fish), was clearly aimed at testing for the involvement of magnetic particles in detecting magnetic map information, but yielded results that were exactly contrary to expectations.

2.4.4 Summary of pulse experiments

The majority of experiments reporting pulse effects on orientation have been conducted on songbirds in orientation cages, mostly on silvereyes and bobolinks, and one on European robins. Taken all together, they clearly suggest an effect of the pulse on directional preferences of experienced migrants, albeit in varying degrees. In these experiments, birds were deprived of non-magnetic cues and had to rely exclusively on magnetic cues for orientation. In contrast, experiments on birds free to fly after the pulse treatment (homing pigeons, catbirds, European robins, reed warblers, wheatears) have yielded incongruent results. Non-magnetic cues were impossible to control in the experiments conducted in free flight, making it difficult to isolate pulse effects in the observed behavior. Therefore, in our mechanistic modeling study, we seek to explain the results obtained on caged migratory birds, which provide a more direct access to the sensory detection mechanisms involved. These can be summarized as follows: Adults, but not juvenile birds are affected by the pulse. The behavioral outcome might be due to an alteration of the magnetic input to the cognitive map. The pulse affects the information conveyed by the trigeminal system. The deflections depend on the pulse directions. There are clockwise, counter-clockwise, and bimodal orientations. After the pulse-altered orientations, there is a period of orientation followed by restoration of the natural alignment towards the migratory direction. It seems that the behavior of southern migrants is reversed compared to the northern ones. An attempt will be provided through this work to explain some of these observations through the tools of simulations and reasoning.

2.5 A brief of modeling in biology

Experimental studies are limited by resources and time. Yet, they convey the truths and facts about nature in them. Hypothesis surviving experiments lead to a theory and from that theory a mathematical model can be built. In return, models guide future experimentation that can disprove the theory or refine it. This cycle can be exemplified by the

archetypal model of the Hodgkin-Huxley equations (Hodgkin and Huxley, 1952). It was discovered that these equations lead to hysteresis behavior (Rinzel, 1978; Best, 1979) and this prediction was subsequently verified by Guttman et al., 1980. There are a plethora of branching sub-fields of modeling in biology. Here, we will focus on the relevant sub-fields for this work, namely: rate models from the sub-field of computational neuroscience, navigational modeling of biologically-inspired artificial agents and the emerging field of reinforcement learning.

2.5.1 Rate models

As is in its name, rate models (RM) study, explain and predict the dynamics of neural circuits in terms of their firing rate. Traditionally in a RM study, a neuron is represented as a differential equation of its firing rate with respect to time. RM model cortical circuits with a group of such neurons. In this regard, RM were able to give an insight into motion perception (Yo and Wilson, 1992; Wilson and Kim, 1994); see Wilson, 1999 for further examples. The work on rate models lead the emergence of attractor networks. Attractor networks are one of the ubiquitous tools that are used to describe how spatially tuned cells in the medial entorhinal cortex and the hippocampus can arise from path integration (McNaughton et al., 2006; Rolls, 2007). Specifically, continuous attractor network models (CANN) were able to describe head direction encodings (Ben-Yishai et al., 1995) and working memory (Berlemont et al., 2020). Si et al., 2014 utilized an attractor network to demonstrate the selectivity of grid cells for the conjunctive inputs of position and velocity. Even under random perturbations, the model was able to accomplish robust path integration. Shipston-Sharman et al., 2016 showed that attractor networks can explain grid firing patterns through the synaptic interactions between excitatory and inhibitory cells. In addition, the model was able to account for theta-nested gamma oscillations and it was shown how modulating gamma oscillations can be achieved separately from spatial computations. In a more abstract sense, a Recurrent Artificial Neural Network (R-ANN) exhibited gird-like patterns when trained on place cells and head direction cells activity-vectors; these vectors symbolize the various positions and head directions in an environment (Banino et al., 2018). It should be noted that machine learning was essentially a divergent branch from computational neuroscience and one can argue that feed forward networks are an abstraction of the RM.

2.5.2 Modeling of magnetic navigation

In most cases shown here, navigational modeling will imply replication of trajectories undertaken by animals. Modeling navigation is a daunting task, it is not just going from

point A to point B; if it was the case, every model would be a linear model. Navigation depends on a large amount of intertwined external and internal factors. Internal factors can be divided into mental and mechanical. Mental factors mainly include motivation and needs which can be individual, group or species based. Mechanical factors imply the ability to do a navigational step (birds can fly so they can overcome certain terrain obstacles) or the ability to sense an aspect of the environment (sensing or not sensing the magnetic field). External factors are very numerous and include: wind for birds or currents for aquatic animals, environmental obstacles, unsafe terrain, foraging location, etc... Mouritsen and Mouritsen, 2000 modeled the directional distribution of birds along the migratory path when birds are assumed to utilize a clock and compass strategy. In this case, a mathematical expectation formula (based on a Gaussian/normal distribution) is used. It was found that a simple parabola can explain the spread of the migratory birds along their trajectories.

Benhamou, 2003 discussed that a the mathematically exact solution for bi-coordinate navigation (using gradient fields) is sophisticated and might be above the mental abilities for most animals. This is the case because such a solution needs to take both gradient fields simultaneously. In the same study, it was argued that directional biases generated by approximate solutions to bi-coordinate navigation might give insights into the nature of the gradients producing these biases. Wiltschko and Nehmzow, 2005 simulated the pigeons homing capabilities based on Kramer's 'Map and Compass' model. In their work, the environment consisted of two intersecting gradients with the bird model possessing a compass sense and a map sense (an internal representation of the gradients). Postlethwaite and Walker, 2011 also studied homing in pigeons. In their work, they also assumed that pigeons have an internal representation of the environment (a cognitive map). However, it was assumed that the bi-coordinate grid of the cognitive map is orthogonal. Hence, there are systematic errors in the pigeon trajectories when they face contour lines deviating from orthogonality in real environments. A mismatch between the ideal cognitive grid and real-world grid lines.

Putman et al., 2012 simulated young loggerhead sea turtles in a resolution ocean circulation model. It was found that turtles can reach their target foraging area with minimal directed swimming per day (1-3h) and this is 43–187% more likely than passive drifting. Zhao et al., 2014 and Qi et al., 2017 utilized the Extended Kalman Filter technique to simulate long distance navigation. Their main assumption was that the animal is able measure the spatial angle between the geomagnetic field lines and the local geographic direction (true north). Based on the locally measured angle, the animal will move in such a direction to minimize the difference between the measured angle and the memorized goal angle. In their work, they simulated the north-south trajectories

of an osprey between Europe and Africa. In a related manner to Putman et al., 2012, Painter and Hillen, 2015a studied the trajectories of individual based models (IBMs) in a flow environment. This was achieved by inserting a Lagrangian-based particle model into the environment and studying the various trajectories of the IBMs according to their individual navigational abilities. For example, the difference between passive drifters and active navigators.

Taylor, 2018 simulated navigation between various signature way points (landmark navigation) in environments that act as a proxy to the true geomagnetic field. The proxy environments were created by using the velocity potential contours and streamlines of an aerodynamic lifting cylinder. The navigational strategy is based on following a goal vector formed between the discrepancy of the measured local field properties and the home field properties. At each time step, the goal vector is computed and the adjusted navigational direction is acquired. Aside from the core navigational strategy, the model allows interference from white noise and fluid currents. Taylor et al., 2021 studied the ability of an animal to perform multiple transequatorial migrations via the systematic measurement of the inclination angle which acts as a synonym for the latitude. They utilized a kinematic model that performs sequential measurements of the inclination angle and compare it with the goal inclination. Subsequently, the model stops movement when the measured inclination and the goal inclination coincide in value. It found that such a model can tolerate magnetic field reversals and perform migrations between the southern and northern hemispheres. In a similar manner to Taylor, 2018, Pizzuti et al., 2021 simulated signature-based navigation. The strategy is the same; the agent computes the goal vector from the difference between the locally measured cues the goal cues. This is performed sequentially till the agent arrives at the desired goal. The additions to this work were a comparison between simple and complex simulated environments, and modeling of physical devices in real world environments.

2.5.3 Reinforcement learning in biology

A new and emerging approach to studying behavior is reinforcement learning (RL). RL is branch of machine learning (ML). ML is gaining traction and is deployed to study biological data (for a review see Greener et al., 2022). RL is considered as an evolutionary step in modeling behavior. Previously, to model behavior, one has to engineer (hand code) the desired behavior in an agent and then observe whether the agents interaction with the environment produced the correct trajectories (or correct sequence of actions). This approach has limitations, because various assumptions have to be made when designing the agent. The down side of that is that the simulations is more prone to errors and greater time is needed to fine tune the model parameters. RL mitigates

these problems through learning. Instead of hard wiring the desired behavior, an agent learns the correct behavior itself by interacting with the environment. This learning is motivated by a desired goal that the agent needs to achieve. The behavior of the agent is shaped mainly by the environment and goal designs. In this work, the agent is a neural network. Although neural networks are a great abstraction of the real neurons, they offer rival representations to the real neural networks (Cadieu et al., 2014; Cichy et al., 2016). The greater challenge in neural networks is not the representation but the learning algorithm, which is a topic outside the scope of this work. Another major advantage of RL is the emergent behaviors. They are behaviors that are not explicitly programmed in the agent, but emerge spontaneously/organically from the interaction of the agent with the environment. Emergent behavior can be very powerful, because they can be behaviors that are not normally undertaken by the animal/agent in real environments under normal circumstances. Thus, they can guide experiments where an environment can be carefully constructed to reproduce the simulated emergent behavior and subsequently rich insights can be gained from such experiments.

Yamaguchi et al., 2018 utilized inverse reinforcement learning (IRL) as a way to discover an animal's behavioral strategies from their behavioral time-series. This approach was applied to the thermotactic behavior of C. elegans. When cultivated under constant temperature, the worms under study were divided into two groups: fed worms and un-fed worms. Using IRL, it was found that the fed worms utilized two strategies. One, directed migration along the temperature gradients, where the worms reached the desired specific temperature. Two, isothermal migration, where the worms followed a specific temperature. In contrast, the un-fed worms avoided the cultivation temperature while utilizing the absolute temperature not it's temporal derivative. Miranda et al., 2020 studied a combined approach of model-free (MF) and model-sensitive (MS) strategies to study the behavior of rhesus monkeys in a two-step decision task. It was found that the task structure and the history of the rewards had high influence on the choices taken. Also, a detailed trial by trial computational analysis demonstrated that there is great influence from the specific form of model sensitivity over the choices (as a combination of strategies) taken that lasted for weeks of testing. Treloar et al., 2020 studied an RL approach for the control of microbial co-cultures inside continuous bioreactors. Several discoveries have been made in this study, including: reinforcement learning is able to directly optimize the product of co-culture bio-processes and that feedback from an agent trained by reinforcement learning can be utilized to contain the microbial populations at the required levels.

Rigoli et al., 2021 studied the difference and degree of equivalence in navigation and trajectory selection between RL and human agents. This was done in simple obstacle-

filled virtual environment. Yu et al., 2021 utilized an inverse reinforcement learning approach to investigate the potential reward functions of animals as a means to understand their collective behavior. In this study, the IRL problem was formulated as a homogeneous Markov game. Wispinski et al., 2022 applied deep reinforcement learning to understand the ecological patch foraging tasks. It was found that RL agents can patch forage in an adaptive manner similar to their biological counterpart. In addition, they were near optimal foraging behavior when the RL agent used a high temporal discounting rate thereby not focusing on short-term rewards but pursuing a long-term strategy. Also, they discovered emergent internal dynamics in the RL agents that is similar to single-cell recordings from non-human primates while foraging. Frankenhuis et al., 2019 provided several arguments for the advantages of RL methods over stochastic dynamic programming (SDP) methods for modeling behavior. Specifically, how RL methods, unlike SDP, can overcome the curse of dimensionality and the curse of modeling. Also, several success cases for behavioral modeling with RL are provided in this study. Neftci and Averbeck, 2019 reviewed the advances in both fields of artificial and biological RL. Also, they investigated the information follow between them and how each field can benefit from the discoveries in the other.

Chapter 3

Methods

3.1 Dynamic neural fields

3.1.1 Theory, math and properties

Dynamic neural fields is a theory that aims at investigating and explaining the dynamics of various cortical neural circuits. The 'field' in the name is because it deals with a continuum of neurons. Thus, as will be shown below, the equations for this theory takes, initially, an integral form. However, with some tweaks, the theory can be extended to a discrete form. The theory takes various forms; here, the equations will be detailed as presented by Trappenberg, 2010 (TE) and Wilson, 1999 (WE). The former is described by equations (3.1). Those equations are labeled the dynamic neural field equations.

$$\tau \frac{\partial \mathbf{u}(\mathbf{x},t)}{\partial t} = -\mathbf{u}(\mathbf{x},t) + \int_y \mathbf{w}(\mathbf{x},\mathbf{y}) g(\mathbf{u}(\mathbf{x},t)) d\mathbf{y} + I^{ext}(\mathbf{x},t) \tag{3.1}$$

In this equation, the bold face indicates vector and matrix quantities. $\mathbf{x}$ represents the spatial dimensions. $\mathbf{u}(\mathbf{x},t)$ is the membrane potential as a function of space and time (Trappenberg, 2010 calls it the internal activation). In this theory, the membrane potential can be attributed to a single neuron or tagged as the average membrane potential of a group of neurons (nodes). The choice of the description depends on the problem being investigated. τ is the membrane time constant. $\mathbf{w}(\mathbf{x},\mathbf{y})$ is the weights matrix, which dictates the strength of the interactions between neurons. $g(\mathbf{u}(\mathbf{x},t))$ is the activation function. Finally, $I^{ext}(\mathbf{x},t)$ is the external stimulus which drives the neuronal network. The discrete form for one spatial dimension, which is used in this work, is shown below as (3.2).

$$\tau \frac{\Delta u_i(t)}{\Delta t} = -u_i(t) + w(x) * g(u(x,t)) + I_i{}^{ext}(t) \tag{3.2}$$

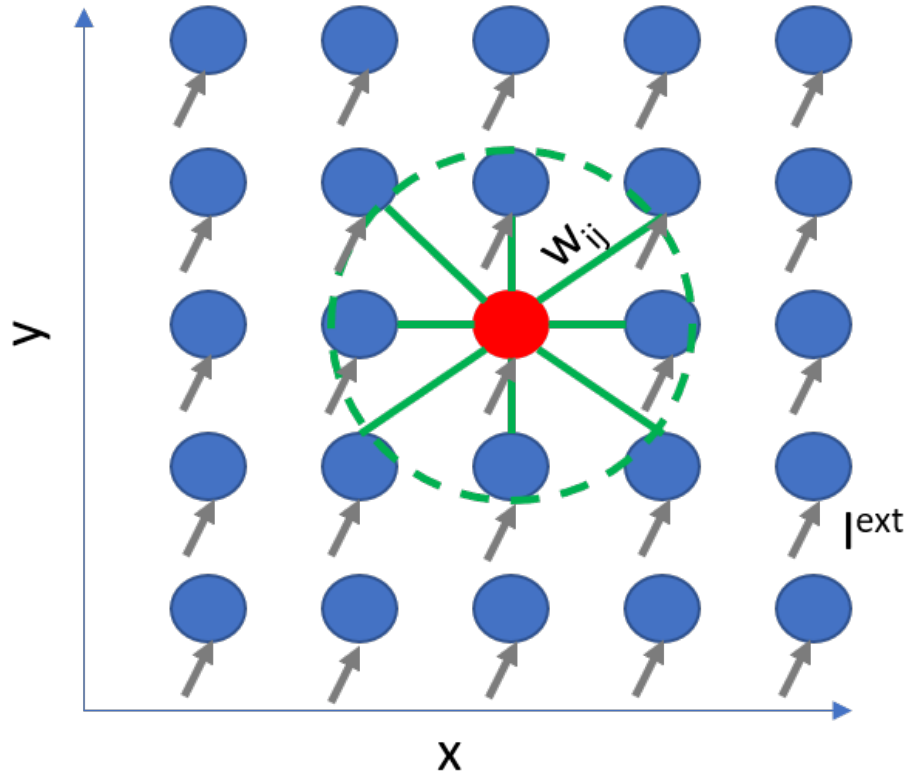

Fig. 3.1: 2D representation of the essence of the dynamic neural fields theory. The blue nodes are neurons (or population of neurons). These nodes are stimulated by an external current I^{ext}. The nodes interact reciprocally with weights $w_i j$. The length of the interactions is exemplified by the dashed green circle.

In this equation, $w(x) * g(u(x,t))$ denotes the spatial convolution between the weights matrix and the activation of every other neuron in the network. This represents the influence of other neurons on the neuron under current consideration. Sometimes, the range of interactions does not involve the whole network, but a small fraction of neurons around the target neuron. The above equations can be visualized by observing Fig. 3.1. Shown in this figure is a 2D representation of the equations. The blue nodes are the neurons (or population of neurons) which receive external stimulus I^{ext}. Also shown are the connections between the middle node and the nearest nodes. The green dashed circle exemplifies the range of interactions, which in this case spans only the nearest nodes. The weights matrix, or the interaction kernel, can take various form depending on the problem under investigation. One ubiquitous form is the Gaussian kernel (or also called the Mexican hat). This kernel is represented in 2D by equation (3.3).

$$w_{ij} = A(e^{\frac{-(x_i-x_j)^2+(y_i-y_j)^2}{4\sigma^2}} - C) \tag{3.3}$$

In this equation, A and C are the scale and shit constants respectively. σ is the

space constant which dictates the span of the interactions between the nodes. Finally, the last important function of these equations is the activation function. This function takes various forms across computational neuroscience and machine learning, and these forms include: the sigmoidal, *tanh*, threshold activation functions. Equations (3.4) and (3.5) show the sigmoidal and threshold activation functions respectively.

$$g(u) = \frac{1}{1 + e^{-u}} \tag{3.4}$$

$$g(u) = \begin{cases} 0 & \text{for } u \leq V \\ 1 & \text{for } u > V \end{cases} \tag{3.5}$$

In the above equations, V is the membrane threshold. The equations of the dynamic neural field theory (DNFT) can take another form as shown in Wilson, 1999 (WE). In that case, there is two species of neurons: excitatory and inhibitory neurons as shown in equations (3.6), (3.7), (3.8), (3.9). These equations are also named the Wilson-Cowan equations.

$$\tau \frac{\mathrm{d}E(x)}{\mathrm{d}t} = -E(x) + S_E(\sum_x W_{EE}E(x) - \sum_x W_{IE}I(x) + P(x)) \tag{3.6}$$

$$\tau \frac{\mathrm{d}I(x)}{\mathrm{d}t} = -I(x) + S_I(\sum_x W_{EI}E(x) - \sum_x W_{II}I(x) + Q(x)) \tag{3.7}$$

$$w_{ij}(x - x') = b_{ij} \exp\left\{ \frac{-|x - x'|}{\sigma_{ij}} \right\} \tag{3.8}$$

$$S(P) = \frac{100P^2}{\theta^2 + P^2} \tag{3.9}$$

In these equations $E(x)$ and $I(x)$ are the mean firing rates of the excitatory and inhibitory neurons respectively. S is the Naka-Rushton function, which is an activation function close in shape to the sigmoidal one. $P(x)$ and $Q(x)$ are the external stimulus to the excitatory and inhibitory neurons respectively. TE and WE might look different, but in essence, they are the same. One can drive the WE equations by applying an activation function to the TE equations. In their core, both convey the same message: The change in the neuronal activity (voltage/internal activation or firing rate) depends on the current value plus the weighted influence of the connected efferent neurons (neurons that provide input through the dendrites or soma). One can not deny the importance of the external stimulus in shaping the network dynamics, however the greater richness in dynamics arises due to the network architecture and the constants that define it . DNFT can accommodate as many neuronal species and spatial dimensions as desired,

but practically one or more neuronal species in a 1D or 2D setting is sufficient to simulate various cortical circuits. The main differences between DNFT networks are the equation constants, their architecture and the stimulus function.

3.1.2 Implementation

Coding and simulating the DNFT equations was performed in Python with the help of the Scipy and Numpy libraries. Here, we will present the important parts of the code that are relevant for solving the DNFT equations.

```
def node_rk45_field(self, t, u):
    # Inputs:
    # t: time, the variable we differentiate with respect to
    # u: the voltage or internal activation

    # Calculating the activations
    g = 1 / (1 + np.exp(-u))

    # Convolvtion of the activations with the weights matrix
    con = conv_wrap(g, self.w)

    # The differential equation (Similar to Eq. 3.1)
    du_dt = (-u + self.i_ext + con) / self.tau_u
    return du_dt

```

Here, we define the function that will create for us the differential equation $\frac{du}{dt}$ while taking as input the state variable u and time variable t (we differentiate with respect to t). The ingredients to this differential equation are the activations g and the convolution of the weights matrix with the activations *con*. The implementation of the *conv_wrap* is given by the following function.

```
def conv_wrap(fun, mask):
    # Inputs:
    # fun: the activations
    # mask: the weights matrix

    size = fun.size
    res = np.zeros(size)
    for i in np.arange(0, size, 1):
        conv_sum = 0
        for j in np.arange(0, size, 1):
            conv_sum += fun[j] * mask[i, j]
    res[i] = conv_sum
    return res
```

```

```

In this function we do the convolution integral between the weights matrix and the activations. Where the weights matrix is retrieved from the following function.

```
def weight_function(nodes_number, nodes_distribution, std=0.6283):
    # Inputs:
    # nodes_number: number of neurons/nodes in the network
    # nodes_distribution: their position in the network (angular position)
    # std: standard deviation of the space constant for the wieght function

    # Get the weight function
    f = WeightFunctions(scale=2, std=std, divisor=2, y_shift=0.5).gaussian_1d

    # Calculate the distance between neurons/nodes
    distance_matrix = np.zeros((nodes_number, nodes_number), dtype=float)
    for h in np.arange(0, nodes_number, 1):
        for q in np.arange(0, nodes_number, 1):
            distance_matrix[h, q] = (np.pi / 180) * np.minimum(
            np.abs(nodes_distribution[h] - nodes_distribution[q]),
            360 - np.abs(nodes_distribution[h] - nodes_distribution[q])
    )

    # Calculate the weights matrix
    weight_temp = np.asarray(f(distance_matrix))
    return weight_temp

```

Finally, we solve the differential equation with the Runge-Kutta technique as applied by the *solve_ivp* function from the Scipy library. This is demonstrated in the following line of code.

```
self.sol_field = solve_ivp(self.node_rk45_field, [0, 100], np.zeros(int(g),
                           float), t_eval=np.arange(0, 100.5, 0.5))

```

3.2 Reinforcement learning

3.2.1 Theory, math and properties

Reinforcement learning (RL) is a branch of machine learning. As its own field, it encompasses a class of solutions that deal with solving a specific kind of problem; this problem is defined as "automatic learning of optimal decisions overtime" Lapan, 2018 or "optimal control of incompletely-known Markov decision processes" Sutton and Barto, 2018. RL was motivated from behavioral biology. RL in it's essence is about learning from experience, like in conditioning animals in a lab. An animal's behavior (sequence of actions) can be either rewarded or punished depending on the desired outcomes. Both reward and punishment reinforces the probability of certain actions and diminishes others. Thus, with experience (trial and error) an animal ought to learn the desired behavior. Even for humans, we learn from experience. If we touch a hot kettle, we are negatively reinforced by the painful sensation and next time we touch it when it cooled down. If we get a high score in a subject we are positively reinforced by our parents, teachers and friends. Learning through interaction is one form of the fundamental ways of adapting to an environment. In a similar manner, RL solutions attempt to solve the problems stated above by engineering the problem as an agent/s interacting with an environment (and maybe with each other) in order to learn the desired behavior. The agents actions are reinforced with an engineered reward when the specified goals are reached.

RL is different from supervised learning. In supervised learning, the desired outcome is provided by an external teacher, but in RL it is learned. Also, RL is different from unsupervised learning, with the goal of the latter being to unearth hidden structure in the data and not to enforce behavior. The basic elements of a RL problem can be visualized as seen in Fig. 3.2. These elements include: the agent, the actions, the environment, the observations and rewards. The agent is the entity that interacts with an environment. The agent performs actions in the environment and these actions transform/perturb the (perceived)environment. After the action, the agent absorbs the new state of the environment as an observation, while also taking in rewards/punishments according to the action taken. Then, the agent outputs a new action according to this new observation and so on. The environment is formally defined as everything outside of the agent. The agent's representation does not have to be based upon a human or an animal, it can take several forms. The agent can be smart car learning to auto-drive, or a spam detection algorithm, or an entity in a video game (In Super Mario, Mario is the agent and the level is the environment).

Markov decision process is the theoretical foundation upon which the RL is defined. Here, we will start with the definition of the Markov process, then proceed to define

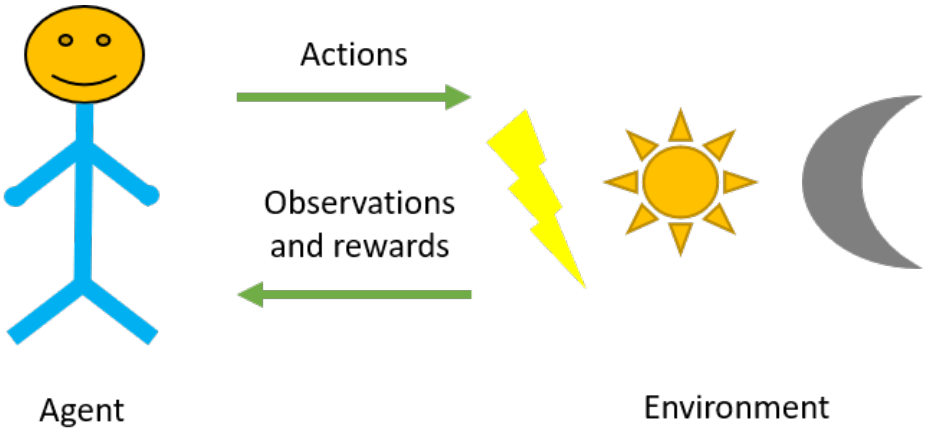

Fig. 3.2: The RL problem showing the agent environment interaction with the follow of actions, observations and rewards between them.

Markov reward process and Markov decision process. Markov process (MP) defines the dynamics of a system isolated from outside influence. The core of the MP can be visualized with the aid of Fig. 3.3. The basic elements of a MP are the state and the edge (the edge also implies the associated probability). The MP is a stochastic system that is completely defined by its transition table. The probabilities in the transition table are conditional probabilities; for example, from $S3$ to $S1$ $P(S1|S3) = 0.2$ (read as: probability of $S1$ given $S3$).

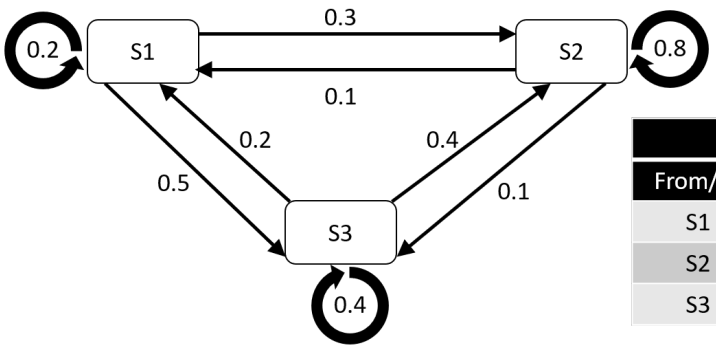

Transition table			
From/To	S1	S2	S3
S1	0.2	0.1	0.2
S2	0.3	0.8	0.4
S3	0.5	0.1	0.4

Fig. 3.3: A Markov process of three states. Some exemplary transition probabilities are shown on the edges. In addition, the transition table is shown with the designated probabilities. The system is isolated, so that the probabilities along each column add up to one, e.g.., $\sum_i P(Si|S1) = 1$. The sum of probabilities along a row indicate how favorable a state is relative to the other ones, here $\sum_j (P(S2|Sj) > \sum_j (P(S3|Sj) > \sum_j (P(S1|Sj)$, i.e. the system has the highest likelihood to be in state $S2$.

A MP ought to possess the Markov property. This entitles that only the current state of the system is needed to describe its future dynamics. In other words, the dynamics of the system does not depend on the state history, but only on the current state. The Markov property implies that all states of the system are unique and distinguishable from one other. Another requirement of the MP is that the probability distribution of

any state is stationary and doesn't change with time. For example the distribution of $S1([0.2, 0.3, 0.5])$ should be time independent. If this was not the case, then there is a hidden dynamical property that affects the distribution with time. Thus, the future dynamics of the system does not only depend on the current state, but also on the history, which breaks the Markov property. Practically, this problem can be circumvented by unearthing the hidden variable, or redefining the MP so as to group several states as a new state (which includes all the information needed to define the future dynamics).

A direct upgrade to the MP is the Markov reward process (MRP). The new addition is a scalar value called the reward. The reward can be assigned to a state or to the state-state transition, i.e., $R_t = f(s_t)$, or $R_t = f(S_t, S_{t-1})$. In this chapter, we discuss the reward as a function of the state transition pair, but later, in the second manuscript (chapter 5), it depends only on the associated state. The reward is a central concept in RL and another point needs to be added; the reward on most RL applications is assumed to be constant and given by the environment (external from the agent). Rewards are not feelings, when talking about humans for example. Feelings are internal to a human agent and changes from time to time. Back to the discussion at hand, the MRP can be illustrated with Fig. 3.4. In this figure, the edges are updated with the associated reward. In addition, a rewards table is provided.

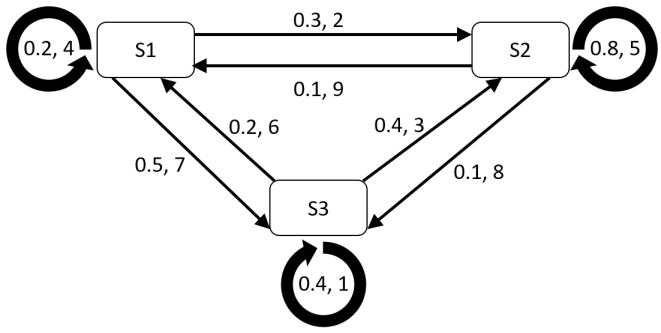

Transition table			
From/To	S1	S2	S3
S1	0.2	0.1	0.2
S2	0.3	0.8	0.4
S3	0.5	0.1	0.4

Reward table			
From/To	S1	S2	S3
S1	4	9	6
S2	2	5	3
S3	7	8	1

Fig. 3.4: A Markov reward process of three states. The transition probabilities and rewards are shown on the edges. In addition, the transition and reward tables are provided.

For an animal in a reward-learning paradigm, the reward must occur timely in response to the desired behavior (action) so that the animal can learn from the rewarding outcome of its behavior. If instead the reward comes too late, the animal might not associate the reward with the behavior and the behavior does not get reinforced. In RL, there is more flexibility as to the timing of the reward. An action can be rewarded immediately with the full reward. But the reward can also be distributed over time to focus on the strategic return in the long run. In RL, this flexibility is achieved with the so-called discount factor γ ($0 <= \gamma < 1$), defining the factor by which the reward diminishes from one time step

to the next, i.e.,

$$G_t = R_{t+1} + \gamma R_{t+2} + \gamma^2 R_{t+3} + ... = \sum_{k=0}^{\infty} \gamma^k R_{t+k+1} \tag{3.10}$$

In this equation, G_t is the discounted reward at time step t. Since $\gamma < 1$, the total reward (over all times) can be expressed by a geometric series and converges to $\frac{R}{(1-\gamma)}$. The discount factor γ can be considered a measure of the predictive power of the agent. A God-like agent will have a $\gamma = 1$ or an absolute predictive power, and will be able to predict all the future rewards to eternity with pinpoint accuracy. Alternatively, a $\gamma = 0$ means the agent is shortsighted and can only see under their feet. The discounted reward is associated with a trajectory, which is a sequence of states. For example, starting at S_1 and with $\gamma = 1$, the trajectory $(S_2 S_1 S_3 S_2 S_1 S_1)$ will have a $G_t = 34$.

Although G_t is a conceptual upgrade to R_t, it is still not very handy in practice. Thus, we arrive at arguably the most important concept in RL; that being the value of the state $V(s)$. As the name implies, the value of the state is a measure of how good it feels to be in that state and mathematically it is given by (3.11).

$$V(s) = E(G|S_t = s) \tag{3.11}$$

$V(s)$ is the expected return of a state. In large processes (or environments), one arrives at the value of the state (VoS) by averaging a huge number of trajectories. VoS is so important to RL because, unlike rewards, it can be associated with all states, even states that would give zero rewards. Rewards can be discrete and sparse. For example, in college, the reward is graduating, which we assume is the last day of the last semester. However, in one's first year in college this is a very far away reward and one can get demotivated. Every day before the last day has zero reward. However, every day doesn't have a zero $V(s)$. The closer a day is to the graduation day, the higher its value. One can argue that most tools in RL is about estimating VoS, because once one knows it, making decisions is easy. One has to always go to the state with the highest $V(s)$. As a concrete example, lets calculate $V(s = S_1)$ when $\gamma = 1$ for the process in Fig. 3.4: $V(s = S_1) = 0.3 * 2 + 0.5 * 7 = 4.1$.

The next upgrade to the MRP is the Markov decision process (MDP), which is the final stage of the theoretical framework for RL. MDP extends on MRP by adding actions to the transition table/matrix and converting it to a 3D matrix as shown in Fig. 3.5. This is a six states MDP with six actions. Choosing a source state is equivalent to choosing the red vertical slap. Then, choosing an action is equivalent to choosing a column in that slap (the intersection of red and cyan slaps). Lastly, choosing a target(sink) state is equivalent to choosing a cell in the resulting column.

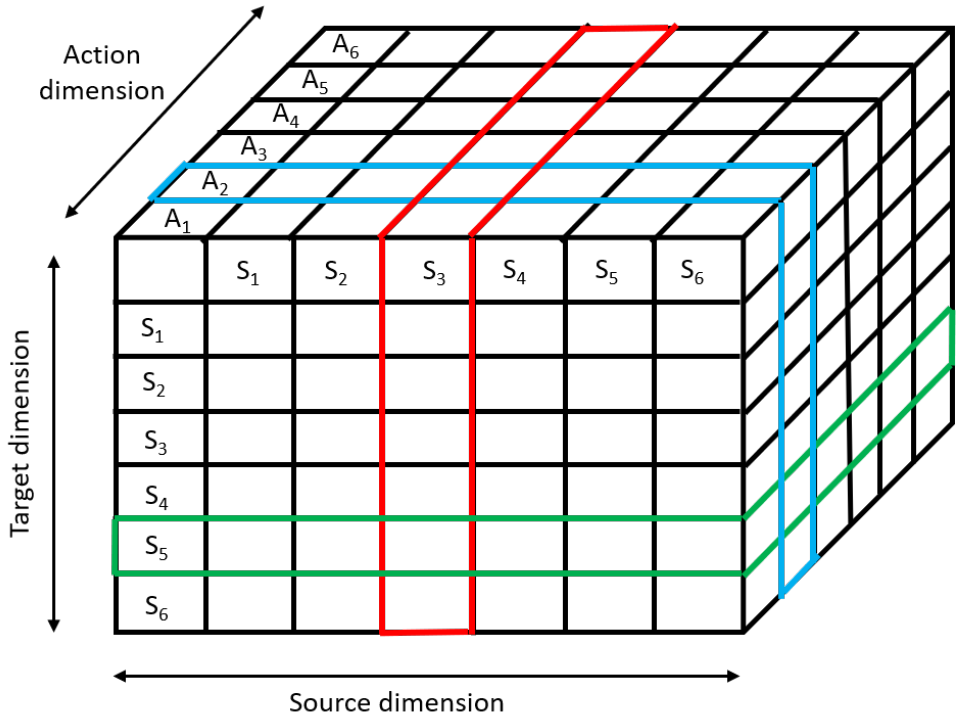

Fig. 3.5: A Markov decision process as exemplified by a 3D transition matrix. The columns are the source states, the rows are the target states and the depth is the actions. The probability of a transition is the cell resulting from the intersection of the three colored slaps (green, red and cyan).

The rewards are calculated in similar manner from a separate 3D matrix. Rewards can be either assigned to target state, state pairs or state pairs and an action. The action's effect on a reward by shown via an example: let us assume someone is trying to reach a water well in the middle of the desert. This person knows the location of the well, but does not know that the well's water evaporate with time. This person has two options to reach the well, on foot or riding a camel. The action taken will affect how much water has remained in the well at arrival, and thereby the reward.

Finally, we arrive at the competitor (compared to the VoS) for the most important concept in RL, the policy. The policy is the set of rules that governs the actions/behavior of an agent/s in a MDP. For a navigating agent, rules can be as simple as the 'moving forward' only action or as complicated as a multilayered neural network with hundreds of possible actions. The policy, as one might expect, affects the discounted reward over time. Therefore, different policies will accumulate different number of rewards over time. The formal definition of a policy is the action's probability distribution for every state as shown in (3.12).

$$\pi(a|s) = P[A_t = a|S_t = s] \tag{3.12}$$

Before detailing how a RL problem can be solved, few extra secondary concepts need to be defined; starting with the Bellman equation of optimality (BeoP). BeoP defines a method that links the optimal value of a state with the values of the adjacent states and is given by (3.13).

$$V(s)_o = \max_{a \epsilon A} E_{s' \epsilon S}[r_{s,a} + \gamma V_{s'}] = \max_{a \epsilon A} \sum_{s' \epsilon S} p_{a,s->s'}(r_{s,a} + \gamma V_{s'}) \tag{3.13}$$

In this equation, s is the state whose value we want to update, s' are the adjacent/next states, S and A are the set of all possible states and actions, respectively. As seen from the equation, $V(s)_o$ is equal to the action that maximizes the expected value of $r_{s',a} + \gamma V_{s'}$, which is the reward and the discount value obtained in the next state as the result of an action. The BeoP which is used to define the optimal VoS is fundamental not only in RL, but also in general dynamic programming. However, the optimal VoS is the not the most widely used quantity practically, instead we use the traditional VoS, which is given by (3.14).

$$V(s) = \sum_a \pi(a,s) E_{s' \epsilon S}[r_{s,a} + \gamma V_{s'}] = \sum_a \pi(a,s) \sum_{s' \epsilon S} p_{a,s->s'}(r_{s,a} + \gamma V_{s'}) \tag{3.14}$$

Which is the expected reward from all possible actions from that state. Another quantity that is used in RL and related to the VoS, is the value/quality of the action (VoA) and is parameterized by equations (3.15). VoS and VoA are related by (3.16).

$$Q(s,a) = E_{s' \epsilon S}[r_{s,a} + \gamma V_{s'}] = \sum_{s' \epsilon S} p_{a,s->s'}(r_{s,a} + \gamma V_{s'}) \tag{3.15}$$

$$V(s) = \sum_a \pi(a,s) Q(s,a) \tag{3.16}$$

Another useful quantity which will be used in this work is the advantage of the action (AoA) and it is given by equation (3.17). AoA is a measure for the performance of an action, higher AoA means the action chosen, on average, will lead to higher accumulated future rewards.

$$A(s,a) = Q(s,a) - V(s) = Q(s,a) - \sum_a \pi(a,s) Q(s,a) \tag{3.17}$$

Having defined the RL formalism and some secondary concepts, we now proceed to illustrate the method by which we solve the RL problem. This method is the proximal policy optimization (PPO). PPO is one of the most powerful and efficient RL-solving algorithms out there. It is based on the Actor-Critic method (if the reader wanted more

history). There are three main components for such an algorithm: i) the anatomy of the agent, ii) the experience gathering algorithm and iii) the training algorithm. The agent is fundamentally made up of a policy head and a value head as shown in Fig. 3.6. This is a neural network. At each time step t, the network takes on observations/states S_t and outputs actions A_t and $V(s)_t$. The observation is what the agent 'sees' and it is not the same as the state of the environment. They are equal when the whole RL problem has the Markov property, and thus the environment is fully observable. In that case, the agent sees the whole environment and the observation is the state. In this work, we assume that the Markov property is fulfilled.

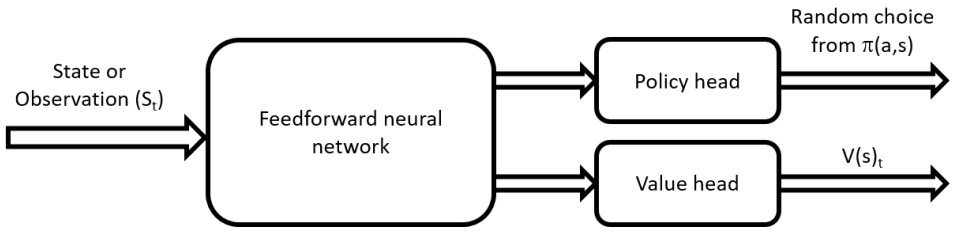

Fig. 3.6: The agent of the PPO algorithm. It has three parts, the common feedforward network, the head network and the value network. The head network output the action to be taken and the value network outputs the current VoS.

The agent gains experience by interactions with the environment. Initially, the network is initialized randomly. This leads to random behavior in the environment, which is improved with training. The agent gathers experience in the form of a trajectory. A trajectory is the path of the agent in an episode, which is the path taken from the birth of the agent in the environment ot its success or failure. We gather hundreds or even thousands of trajectories for a single training step. Trajectories are presented in the form: $(S_0, A_0, R_1, S_1) -> (S_1, A_1, R_2, S_2)...$ From these data, we calculate the parameters that are needed for training, including the advantage of the action and the value of the state.

Finally, we arrive at the training algorithm which is backpropagation of loss/error. The beauty and power of the PPO algorithm comes from how the objective is calculated for the policy head, which is given by equations (3.18) and (3.19).

$$L(\theta) = \frac{\pi_\theta(a,s)}{\pi_{\theta old}(a,s)} \tag{3.18}$$

$$J^{clip}(\theta) = \hat{E}[min(A(a,s) * L(\theta), A(a,s) * clip(L(\theta), 1-\epsilon, 1+\epsilon))] \tag{3.19}$$

In these equations, $L(\theta)$ is the ratio between the probabilities of the new policy $\pi_\theta(a,s)$ to the probabilities of the old policy $\pi_{\theta old}(a,s)$. $J^{clip}(\theta)$ is the clipped objective and the extent of clipping is determined by the parameter ϵ. ϵ controls how much the new policy will diverge from the old policy. A large ϵ will allow for a larger update to the new policy.

The clipped objective is to be maximized, and thus during loss calculation it is negated then backpropagated. Aside from the objective function, the advantage of the action is also calculated differently in the PPO algorithm as shown in equations (3.20) and (3.21). In this equation, λ is a discount factor like γ and T is the trajectory length. Lastly, it should be stressed that, the above objective function is for the policy head. The loss of the value head is calculated from the mean square error MSE between the VoS from the network output and the reference VoS as shown later in the implementation section.

$$A_t = \sigma_t + (\gamma\lambda)\sigma_{t+1} + (\gamma\lambda)^2\sigma_{t+2} + ... + (\gamma\lambda)^{T-t+1}\sigma_{T-1} \tag{3.20}$$

$$\sigma_t = r_t + \gamma V(s_{t+1}) - V(s_t) \tag{3.21}$$

3.2.2 Implementation

In this section, we will show some of the code that is relevant for the PPO algorithm, and including the code for the agent. The code is written in the Python API and will be uploaded to Github as soon as the documentation is finished. We only focus on code snippets from Python. Because the Python code alone is about 1800 lines. The *c#* code is for environment handling and not so critical for the PPO algorithm. Here, we will start with the agent class which inherits from nn.Module class from the Pytorch machine learning library.

```
class ModelActorCritic(nn.Module):
    def __init__(self, color_gray, im_dim, act_size, memory_length=1):
        super(ModelActorCritic, self).__init__()

        # Convolution layer parameters
        self.color_gray = color_gray  # Number of image channels
        self.im_dim = im_dim  # Image height and width
        self.seq_length = memory_length  # Number of observations to
   form
        # a state

        # LSTM, value head and policy head parameters
        self.hidden_dim = 512
        self.num_layers = 1

        # Create the convolution layer
        self.conv = nn.Sequential(
        nn.Conv2d(self.color_gray, 32, kernel_size=4, stride=1),
        nn.ReLU(),
```

```
        nn.Conv2d(32, 64, kernel_size=4, stride=2),
        nn.ReLU(),
        nn.Conv2d(64, 128, kernel_size=4, stride=2),
        nn.ReLU(),
        nn.Conv2d(128, 256, kernel_size=4, stride=2),
        nn.ReLU()
        )

        # Capture the convlution layer output size since it is variable
        conv_out_size = self._get_conv_out((self.color_gray,
                                            self.im_dim, self.im_dim))

        # Create the LSTM layer
        self.rnn = nn.LSTM(conv_out_size, self.hidden_dim,
                           self.num_layers, batch_first=True)

        # Create the policy head (a feedforward layer)
        self.mu_actor = nn.Sequential(
        nn.Linear(self.hidden_dim, 64),
        nn.ReLU(),
        nn.Linear(64, act_size)
        )

        # Create the value head (a feedforward layer)
        self.mu_critic = nn.Sequential(
        nn.Linear(self.hidden_dim, 64),
        nn.ReLU(),
        nn.Linear(64, 1)
        )


    # Handles the forward pass through the layers of the network
    def forward(self, x):
        batch_size = int(x.size(0) / self.seq_length)  # Get batch size

        # Initialize the LSTM hidden layer
        hidden = self.init_hidden(batch_size)

        # the convolution layer pass
        conv_out = self.conv(x).view(batch_size, self.seq_length,  -1)

        # LSTM layer pass
        rnn_out, hidden = self.rnn(conv_out, hidden)

        # Reshape and get the last element of the sequence
```

```
        rnn_out = rnn_out[:, -1, :].view(rnn_out.size()[0], -1)

        # Return the policy and value head outputs
        return self.mu_actor(rnn_out), self.mu_critic(rnn_out)

    # A dedicated function to get the output size of the convolution
    layer
    def _get_conv_out(self, shape):
        o = self.conv(torch.zeros(1, self.color_gray, self.im_dim,
                                  self.im_dim))
        return int(np.prod(o.size()))

    # A function to initialize the hidden layer of the LSTM
    def init_hidden(self, batch_size):
        hidden_state = torch.zeros(self.num_layers, batch_size,
                                   self.hidden_dim).cuda()
        cell_state = torch.zeros(self.num_layers, batch_size,
                                 self.hidden_dim).cuda()
        hidden = (hidden_state, cell_state)
        return hidden
```

The above class can be daunting, but a careful inspection of the code with the commentary will reveal that it is just a straightforward stack of layers. These layers being a convolution layer, since the observations are images. A long short term memory (LSTM) layer which represents memory of the observations. Ending with a fork into two feedforward layers, one for the policy and the other is for the value. The memory is needed to ensure that the RL problem under study is Markov complete, so history is included at each step to account for hidden factors. The length of the history is determined by the variable `memory_length`. Next, we will show the code of how the data from the trajectories are extracted for the calculation of the advantage of the action and the reference value of state. Both these values will be used for calculation of the objective function. The below function will calculate the AoA and VoS as detailed in equations (3.20) and (3.21). The VoS can be easily extracted from those equations as will be shown below in the code.

```
def calc_adv_ref(trajectory, net, states_in):
    # Inputs:
    # trajectory : the whole trajectory transitions
    # net : the neural network
    # states_in : all states in the trajectory

    # Pass the observations through the network and get the values as
```

```
    output
    _, values_in = net(states_in)
    values = values_in.squeeze().data.cpu().numpy()

    adv_temp  = 0.0  # Initialize the advantage of the action
    result_adv = []  # A container for the AoA for every step in the
    trajectory
    result_ref = []  # A contrainer for the reference VoS for every
    step in the
                     # trajectory

    # Looping in reverse since, at every step, the current AoA and VoS
    depend
    # on all rewards and VoS in the future.
    for val, next_val, exp in zip(reversed(values[:-1]), reversed(
    values[1:]),
                                  reversed(trajectory[:-1])):
        # If a step in the trjectory is the end state
        if exp.done:
            sigma = exp.reward - val  # sigma = r - V(s)
            adv_temp  = sigma  # A = sigma
        else:
            # Iterative version of (Eq.21)
            sigma = exp.reward + GAMMA * next_val - val
             # Iterative version of (Eq.20)
            adv_temp  = sigma + GAMMA * GAE_LAMBDA * adv_temp
        result_adv.append(adv_temp)  # Stack the AoA
        result_ref.append(adv_temp  + val)  # Stack the VoS
    adv_v = torch.FloatTensor(list(reversed(result_adv))).cuda()
    ref_v = torch.FloatTensor(list(reversed(result_ref))).cuda()
    return adv_v, ref_v
```

Having illustrated how the experience is handled to extract the AoA and the reference VoS, we now proceed to use these quantities in training the network as shown in the below code.

```
def ppo_net(self, net, trajectory_in, opt, step_idx, agent_id=0):
    # Inputs:
    # net: the nerual network
    # trajectory_in : the full trajectories to be trained on
    # opt: the gradient optimizer
    # step_idx : the step index in the trajectory
    # agent_id : agent number as we use multiple agents for training

```

```
    # We extract the memory (history of states) in a separate container
    traj_states_memory = [t.memory for t in trajectory_in]
    traj_states_memory = np.array(traj_states_memory)
    traj_shape = traj_states_memory.shape
    # Reshaping of the array of the trajectory states
    traj_states_memory = traj_states_memory.reshape(traj_shape[0]*
traj_shape[1],
                                    traj_shape[2], traj_shape[3],
traj_shape[4])
    traj_states_memory = list(traj_states_memory)
    # Just renaming
    traj_states = traj_states_memory

    # Extraction of the actions from the trajectories
    traj_actions = [t.action for t in trajectory_in]
    traj_states_v = torch.FloatTensor(traj_states).cuda()
    traj_actions_v = torch.FloatTensor(traj_actions).cuda()
    # Calculion of the AoA and reference VoS
    traj_adv_v, traj_ref_v0 = calc_adv_ref(list(trajectory_in), net,
                                           traj_states_v)

    # Passing the states through the neural network to get actions
    mu_v, _ = net(traj_states_v)
    # Determing the log probability of the old policy
    old_logprob_v = F.log_softmax(mu_v, dim=1)
    action_old = F.softmax(mu_v, dim=1)

    # Normalize advantages as sometime STD do inf
    traj_adv_v = (traj_adv_v - torch.mean(traj_adv_v)) /
                                          (torch.std(traj_adv_v) + 1e
-7)

    # Droping last entry from the trajectory_in, as our adv and ref
value
    # are calculated without it
    trajectory_in = trajectory_in[:-1]
    old_logprob_v = old_logprob_v[:-1].detach()
    action_old = action_old[:-1].detach()

    sum_loss_value = 0.0
    sum_loss_policy = 0.0

    # The training procedure (the meaty part)
    for epoch in range(PPO_EPOCHES):
        for batch_ofs in range(0, len(trajectory_in), PPO_BATCH_SIZE):
```

```
            # Parsing part of the trajectory according to the batch size
            # The multiplication with memory length for states is because
            # each state is a history of states
            states_v = traj_states_v[(batch_ofs * MEMORY_LENGTH):(batch_ofs *
                                     MEMORY_LENGTH) + (PPO_BATCH_SIZE * MEMORY_LENGTH)]
            actions_v = traj_actions_v[batch_ofs:batch_ofs + PPO_BATCH_SIZE]
            batch_adv_v = traj_adv_v[batch_ofs:batch_ofs + PPO_BATCH_SIZE]
            batch_ref_v = traj_ref_v0[batch_ofs:batch_ofs + PPO_BATCH_SIZE]
            batch_old_logprob_v = old_logprob_v[batch_ofs:batch_ofs +
                                                PPO_BATCH_SIZE]
            batch_action_old = action_old[batch_ofs:batch_ofs + PPO_BATCH_SIZE]

            # Critic or value head training with the mean square error
            opt.zero_grad()
            mu_v, value_v = net(states_v)
            loss_value_v = F.mse_loss(value_v.squeeze(-1), batch_ref_v)

            # Actor or policy head training
            logprob_pi_v = F.log_softmax(mu_v, dim=1)
            action_new = F.softmax(mu_v, dim=1)
            # Probability of the old action
            chosen_action_old = torch.sum(batch_old_logprob_v * actions_v,
                                          dim=1)
            # Probability of the new action
            chosen_action_new = torch.sum(logprob_pi_v * actions_v, dim=1)
            # Ratio of the new action to the old action (L(theta))
            ratio_v = torch.exp(chosen_action_new - chosen_action_old)
            surr_obj_v = batch_adv_v * ratio_v
            # The clipped objective
            clipped_surr_v = batch_adv_v * torch.clamp(ratio_v, 1.0 - PPO_EPS,
                                                       1.0 + PPO_EPS)
            # The loss which is the negative of the objective
            loss_policy_v = -torch.min(surr_obj_v, clipped_surr_v).mean()
```

```
83
84              # Propagate the loss and take an update step
85              total_loss_v = loss_policy_v + loss_value_v
86              total_loss_v.backward()
87              opt.step()
88
89            sum_loss_value += loss_value_v.item()
90            sum_loss_policy += loss_policy_v.item()
```

Again, the above code can be daunting, but it can be divided into two parts: before the for-loop and inside the for-loop. In the former, the code there is for extracting and preparing data from the trajectories to be used in training. In the latter, all the important stuff happen. We iterate over the trajectory in batch-size steps. As we iterate, we extract and calculate relevant quantities for training. In lines 63-65 we train the value head (the critic) using the mean square error loss between the values from the neural network and the reference values extracted from the trajectory. In lines 68-79 we calculate the clipped objective. First, we get the probability distribution of the actions as shown in line 68. Then, we get the probability of the chosen action by multiplying the probability distributions of the actions with the policy output (an array of 1s and 0s) as shown in lines 71 and 74. Then in line 76, we calculate L(θ). In line 79, we calculate J(θ). Lastly, in lines 82-87 we calculate the loss as the negative of the objective and backpropagate the error through the network.

Chapter 4

Manuscript one: magnetic pulse simulations

A neural theory for magnetic pulse effects in magnetic orientation studies

Karim Habashy [1] and Michael Winklhofer [1,2]

[1] Institut für Biologie und Umweltwissenschaften, Carl von Ossietzky Universität Oldenburg, Oldenburg, Germany

[2] Research Centre for Neurosensory Sciences, Oldenburg, Germany

April 26, 2024

Abstract

The magnetite hypothesis for magnetoreception posits ferrimagnetic particles as key agents in magnetosensory cells. To specifically test for the involvement of magnetic particles in magnetic orientation behaviour, several studies have pre-exposed test animals to a brief but strong magnetic pulse aimed at remagnetizing the particles. The observation of altered magnetic orientation in pulsed animals is consistent with the hypothesis, but there is no consensus as to what aspects of magnetic field sensing were actually affected. We here approach this problem theoretically and simulate pulse effects on a network of putative magnetoreceptor neurons described with the mathematical framework of dynamic neural field theory. We assume that the effect of a pulse depends on the relative orientation between pulse-field vector and magnetic dipole moment in a single neural unit, which at the level of the network leads to a subpopulation of units with altered or impaired output. Irrespective whether the network provides compass or intensity information, the anisotropic effect of the pulse on the network can explain key outcomes of the pulse experiments, such as orientations shifted by 90 degrees relative to controls and bimodality. We offer testable predictions for magnetic orientation experiments in a refined pulsing protocol with more diagnostic power.

Keywords: Magnetic pulse , Neural fields, Orientation and navigation, Magnetite, Magnetic field sensor, Computational neuroscience

4.1 Introduction

Magnetic orientation has been demonstrated in various types of migratory animals [Wiltschko and Wiltschko, 2005; Mouritsen, 2018]. Despite the identification of candidate neural pathways for magnetic field perception [Zapka et al., 2009; Heyers et al., 2010; Nimpf et al., 2019; Kobylkov et al., 2020], the nature of the underlying magnetic sensory cells has not been identified yet. The search for candidate structure is guided by three different hypotheses about the magnetically active agent: i) ferrimagnetic particles which can interact significantly with the relatively weak geomagnetic field to produce a mechanical response that in turn could be detected by known mechanoreceptive structures, such as those in the trigeminal nerve system of vertebrates. [e.g., in fish: Walker et al., 1997, in birds: Kobylkov et al., 2020]. This idea is also referred to as magnetite-hypothesis, since magnetite (Fe_3O_4) has the strongest magnetization of all known biominerals. ii) the flavoprotein cryptochrome, which has been shown to host a spin-correlated radical-pair after light excitation and whose reaction rates depend on the magnetic field [Schulten et al., 1978 ; Ritz et al., 2000]. The candidate magnetoreceptor cryptochrome Cry4 occurs in cone photoreceptors of night migratory songbirds [Günther et al., 2018], and may interact with downstream components of the established visual signal transduction pathway [Wu et al., 2020], so that the magnetic field could modulate visual pattern as suggested earlier [Ritz et al., 2000]. iii) the semicircular duct of the inner ear, where magnetic field changes induce an electromotive force that may be detectable by highly sensitive voltage-gated ion channels in vestibular hair cells [Nimpf et al., 2019].

Each hypothesis makes specific predictions regarding the quality of information that a given mechanism can extract from the magnetic field. The radical-pair mechanism is intrinsically insensitive to the magnetic field polarity [Schulten et al., 1978], which is in agreement with the inclination compass of songbirds [Wiltschko and Wiltschko, 1972]. The induction mechanism is only sensitive to field changes, so that it would be blind to an additional magnetic field that is fixed with respect to the head [Jungerman and Rosenblum, 1980] [see also Wang et al., 2019 Winklhofer, 2019]. Last, unlike the other two mechanisms, the magnetite mechanism has no intrinsic restrictions, although there may be practical limitations depending on the realization of the mechanism [Kirschvink and Gould, 1981; Walker, 2008; Winklhofer and Kirschvink, 2010]. In view of such uncertainties, it is desirable to have a diagnostic test, ideally non-invasive, to disambiguate the most likely magnetoreception mechanism responsible for a given behavioural response. The key diagnostic test for the radical-pair mechanism utilizes weak radiofrequency (RF) magnetic fields, designed to directly interfere with the mechanism and therefore being continuously applied while recording spontaneous orientation in the ambient magnetic

field; indeed, songbirds exposed to RF magnetic fields showed significantly larger directional scatter compared to unexposed controls [Ritz et al., 2004; Engels et al., 2014; Kavokin et al., 2014; Schwarze et al., 2016; Pakhomov et al., 2017b; Kobylkov et al., 2019].

The classic diagnostic test for the magnetite mechanism is the magnetic pulse pretreatment, which was inspired by Ad Kalmijn's work on magnetotactic bacteria [Kalmijn and Blakemore, 1978], who pulsed north seeking cells to turn them into south seeking ones. Analogously, animals from the treatment group are pre-exposed to a single magnetic field pulse, sufficiently strong (ca. 100 mT peak field) to polarize all magnetic particles into the pulse field direction, but brief enough (< 5 msec rise time) to avoid physical alignment of the particles with the pulse field. Although the pulse pretreatment brought about significant effects in adult birds, ranging from deflected orientation directions to disorientation (Table 4.1), it did not seem to affect the orientations of young birds that had no prior experience in migration [Munro et al., 1997a, 1997b; Holland and Helm, 2013]. This dichotomic outcome has led to the notion that the innate inclination compass of young birds (inclination compass) is based on a radical pair mechanism, while a magnetite mechanism is involved in obtaining magnetic factors for the navigational map used to determine the position relative to the goal [Wiltschko et al., 2009]. In magnetic map navigation, the full three-dimensional magnetic field vector appears to be involved [Kishkinev et al., 2021], which necessitates access to celestial cues to determine the declination angle between magnetic North and true North. Bearing in mind that pulsed birds were mostly tested in Emlen funnels without celestial cues available, one can argue in hindsight that the indoor test situation was not adequate to interrogate magnetic map navigation. In the only two studies that tracked pulsed songbirds released under open skies, thus allowing for magnetic map navigation, the orientation of adults, but not of juveniles was compromised by the pulse [Holland, 2010; Holland and Helm, 2013], which supports the dichotomic age effect observed earlier in caged birds.

Under the magnetic map hypothesis, the general observation that experienced birds remained oriented after pulsing but showed shifted orientation tendencies may be interpreted in terms of a virtual magnetic displacement such that the pulsed bird perceives a different magnetic field than physically present at the testing site A. If the apparent magnetic field percept at A resembles that at a location B known to the bird from an earlier flight and memorized on the cognitive magnetic map, the bird brain would update its prediction about the location, so that virtual magnetic displacement entails a mental displacement to location B. If the goal direction associated with location B differs from that at site A, then an adjustment of the goal direction prompts different orientation directions. However, in contrast to a controlled virtual magnet displacement study in a

known magnetic field mimicking that of a location known to the investigator (and the birds), a pulse experiment can be regarded as an uncontrolled virtual magnet displacement to a site unknown to the investigator, making it impossible to predict the new goal direction. From the standpoint of hypothesis testing, the lack of a clear prediction is not satisfactory. We here approach the problem by simulating the effect of a pulse on a mathematical model that before pulsing adequately predicts orientation responses to a magnetic field.

We start from the mathematical model for sensing the magnetic field direction by Taylor, 2016 (T16), who simulated the combined neural output function of subpopulations of magnetic sensory cells, where each subpopulation is tuned to a different magnetic field angle. However, the model assumes a fixed head direction in the reference frame where the magnetic field is expressed, as in experiments on head-constrained animals. To allow for arbitrary head orientation, as in experiments on unconstrained animals, we added a head-direction network and a difference-network that computes the angular difference between the sensed magnetic field vector and the head direction. In a further modification of the original T16 model, we reduce the symmetry from circular to bilateral, which as we will show reproduces the Weber-Fechner law without any further constraints on the input functions. We then simulate the effect of a magnetic pulse on the network output functions. Thus far we have no indication how magnetite particles inside the putative sensory structure transduce the field into a receptor potential. Therefore, to test how the model predictions depend on the form of the transducer function, we compared the variance model by Walker, 2008 as used in T16 with the torque model by Winklhofer and Kirschvink, 2010 (WK10). Finally, we offer predictions that may guide future experiments.

4.2 Methods

To account for the behavior of birds after the application of a magnetic pulse is a feat far from simple. The main reason for this is that a behavior is the sum of several processes. These processes, in a basic sense, include: i) sensory functions, where the magnetic field is sensed. ii) integrative functions, where the information from the magnetic field and other cues, like visual cues, are integrated. iii) Motivational functions, where the current needs (motivation) and previous experiences (memory) are taken into account. To provide an adequate explanation for the behavior of birds after pulsing experiments, several assumptions have to be in place in order to aid the model in its explanatory and predictive powers.

Here, the discussion starts with a network model that is similar to T16. Followed by

Reference	Species	Age group	Environment	First pulse effect
Wiltschko et al., 1994	Australian silvereyes	Adults	Indoors	≈90° eastward deflection
Wiltschko and Wiltschko, 1995	European robins	Juveniles (transmigrants)	Indoors	Individual orientations
Beason et al., 1995	Bobolinks	Adults	Indoors	Bimodality, eastward and westward deflections
Munro et al., 1997a	Australian silvereyes	Adults and juveniles	Indoors	Adults: eastward deflection, juveniles: no effect
Munro et al., 1997b	Australian silvereyes	Juveniles	Indoors	No effect
Wiltschko et al., 1998	Australian silvereyes	Adults	Indoors	≈110° eastward deflection
Wiltschko et al., 2002	Australian silvereyes	Adults	Indoors	East-west bimodality
Wiltschko et al., 2007	Australian silvereyes	Completed one journey	Indoors	≈120° eastward deflection
Wiltschko et al., 2009	Australian silvereyes	Adults and juveniles	Indoors	Usual deflection, but only in the pharmacologically untreated group
Holland, 2010	European robins and reed warblers	*Adults?	Outdoors	Eastward deflections, normal headings and bimodality
Holland and Helm, 2013a	European robins	Adults and juveniles	Outdoors	Adults: significant reduction in precision of orientation
Beason et al., 1997	Homing pigeons	Adults	Outdoors	Eastward and westward deflections from controls
Holland et al., 2013b	Homing pigeons	At least six months	Outdoors	No effect in orientation and homing performance
Irwin and Lohmann, 2005	Loggerhead sea turtles	Hatchlings	Covered pools	Not significantly oriented in darkness
Fitak et al., 2020	Rainbow trout	Juveniles	Indoors	Daily differential orientation, possibly due to solar activity
Naisbett-Jones et al., 2020	Pacific salmon	Juveniles	Outdoors	Orientation/disorientation depending on the testing field parameters
Riveros and Srygley, 2008	Leafcutter ants	Unknown	Outdoors	Random orientation in overcast days
Ernst and Lohmann, 2016	Caribbean spiny lobster	Juveniles	In lab	Disorientation in controls and orientation in pulsed lobsters
Karwinkel et al., 2022a	Wheatears	Adults and juveniles	Outdoors	No effect in all performance metrics
Karwinkel et al., 2022b	European robins	Adults	Outdoors	No effect in all performance metrics

Table 4.1: A brief summary for some of the pulsing experiments in literature [Wiltschko et al., 1994; 1995, 1998a, 2002, 2007, 2009; Beason et al., 1995, 1997; Munro et al., 1997a, 1997b; Holland, 2010, 2013a, 2013b; Irwin and Lohmann, 2005; Ernst and Lohmann, 2016; Riveros and Srygley, 2008; Fitak et al., 2020; Naisbett-Jones et al., 2020; Karwinkel et al., 2022a; Karwinkel et al., 2022b]. *Inferred from text as it is not explicitly mentioned.

the modified versions that are provided as an attempt to connect between the sensory and cognitive processes. Then, a depiction of the reference frame used in the simulations

is presented. Finally, a description of the pulsing experiments protocols is illustrated

4.2.1 A network for sensing the field's direction

The approach in this section tries to be as faithful as possible to the experiment number one in T16. The main difference is the API used for the modeling. Here, Python is used while in the referenced paper Matlab is used. The tools in this work stems from the topic of dynamic neural fields. A brief overview will be provided here, but a more elaborate and detailed explanation can be found in Wilson, 1999 and Trappenberg, 2010. Neural fields study the response of a continuum of neuronal activity as a function of the input stimulus and network configuration. For the one-dimensional case, this continuum can be described by equations (4.1) and (4.2).

$$\tau \frac{\mathrm{d}v(x,t)}{\mathrm{d}t} = -v(x,t) + w(x) * g(v(x,t)) + I(x,t) \tag{4.1}$$

$$w * g(v(x,t)) = \int w(x-x')g(v(x',t))dx' \tag{4.2}$$

τ is the neural population time constant. $v(x,t)$ is the average membrane potential of a population of neurons at position x and time t. $w(x)$ is the weight function, which represents the strength of the synaptic connections between the respective neural populations. $I(x,t)$ is the input function, or stimulus; it is also a function of position and time. $g(v(x,t))$ is the activation function; typically, it specifies the firing rate of a neuron, but in the context of a neural population, it represents the fraction of the active neurons in a population given a value for the membrane potential. In this study, the sigmoidal activation function, given by (4.3), is used. Finally, $w(\Delta x)$ is the shifted Gaussian weight function which is given by (4.4). In this equation, Δx is the distance between any two nodes, σ is the space constant (standard deviation) and c is the shift/bias factor.

$$g(x) = \frac{1}{1+e^{-x}} \tag{4.3}$$

$$w(\Delta x) = \exp\left(-\frac{\Delta x^2}{2\sigma^2}\right) - c \tag{4.4}$$

To provide a model adequate for sensing the magnetic field direction, several assumptions and constrains are to be applied. i) it is assumed that the nodes (neural populations) form a circular pattern of connections as shown in Fig. 4.1a. ii) the network is fixed relative to the head of the bird; the bird rotates its head and the network rotates accordingly. iii) each population of neurons has a sensitivity direction as indicated by the gray arrows. The nodes fire with the maximum mean firing rate if the magnetic field is aligned with its

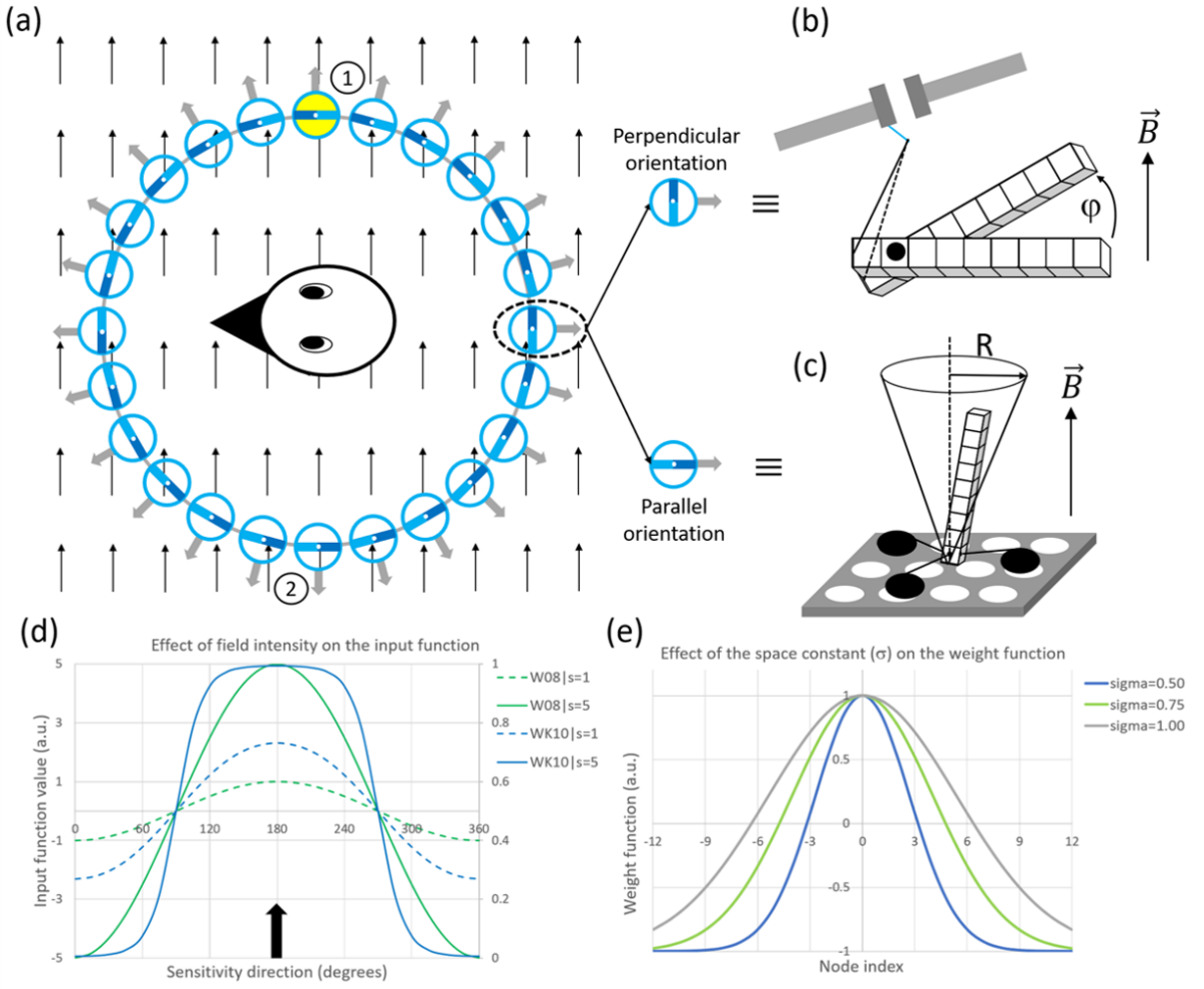

Fig. 4.1: The magnetic field direction sensing network. Each circle is a population of neurons. Each population is attuned to a specific magnetic field direction as indicated by the gray arrows. The light-blue/blue rectangle in each circle resembles the orientation of the magnetite particle relative to the sensitivity direction (gray arrow). In this case, the magnetite particle is oriented perpendicular to the sensitivity direction. The background arrow field is the magnetic field. **(b)** The torque model WK10. φ is the angle of rotation of the magnetosome chain due to the magnetic field $\vec{B}$. **(c)** The variance model W08. R is the base radius of the cone, which is formed due the wiggling of the magnetosome chain around a virtual axis perpendicular the surface of the cell. R depends on the strength of the magnetic field $\vec{B}$ and the temperature. **(d)** Plots showing the effect of the magnetic field intensity on the W08(left axis) and WK10(right axis) input functions. The black arrow represents the magnetic field direction. **(e)** Plots showing the effect of the space constant (standard deviation) on the Gaussian weight function.

sensitivity direction. Hence, each neural population is tuned to sense a specific magnetic field direction. iv) a model for the magnetic field transduction mechanism has to be provided. Here, two models are studied. The torque model by WK10 and the variance model by W08. The torque model assumes that the magnetosome chain to be arranged

perpendicular to the sensitivity direction (Fig. 4.1b) and is given by equation (4.5).

$$I_k(\theta) = \frac{1}{1 + e^{-s\cos(\theta_k - \varphi)}} + e_k \tag{4.5}$$

The variance model assumes the chain to be parallel to the sensitivity direction (Fig. 4.1c) and is given by equation (4.6).

$$I_k(\theta) = s\cos(\theta_k - \varphi) + e_k \tag{4.6}$$

In both equations, θ is the sensitivity direction. φ is the direction of the magnetic field. s is a parameter proportional to the magnetic field strength. k is the node index. e_k is the noise. The noise can affect any component from the simulation. Here, it is simplified and summed up to be added to the input. The noise is added as a white Gaussian noise with zero mean and standard deviation of 0.2.

4.2.2 Modifications to the basic network model

The model in the previous section is not sufficient as a magnetic field direction sensing system. The drawback can be stated as follows: if the bird rotates its head 180° to the right(clockwise), the portion of the network, indicated by (1) in Fig. 4.1a, will rotate accordingly to the new position at (2). The opposite is true for the portion of the network which is initially at (2). Hence, the nodes initially at (1) will be suppressed, while the nodes initially at (2) will be active after the rotation. Consequently, as the bird rotates its head around, different portions of the network will fire accordingly. How can the bird infer the magnetic field direction this way?

Two possible solutions arise if more assumptions and constraints are to be considered. The first solution relies on two extra assumptions. i) the bird possesses an equivalent of head direction cells. To date, there is no universal consensus that birds have an equivalent to head direction cells, although they possess many common spatial processing capabilities compared with the mammalian counterpart [Colombo and Broadbent, 2000; Sherry et al., 2017]. Recently however, it was shown that the Japanese quails have head direction cells[Ben-Yishay et al., 2020]. ii) the head direction network is modeled as a ring attractor network [Xiaohui et al., 2002; Laurens and Angelaki, 2018]. Based on these two assumptions, the basic model can be modified to look as in Fig. 4.2a. This network model will be referred to as the head-direction model. In this model, the inner most network is the magnetic field direction network. The middle network is the head direction network. The outer network is the difference network, which computes the direction of the magnetic field relative to the current head direction. The difference

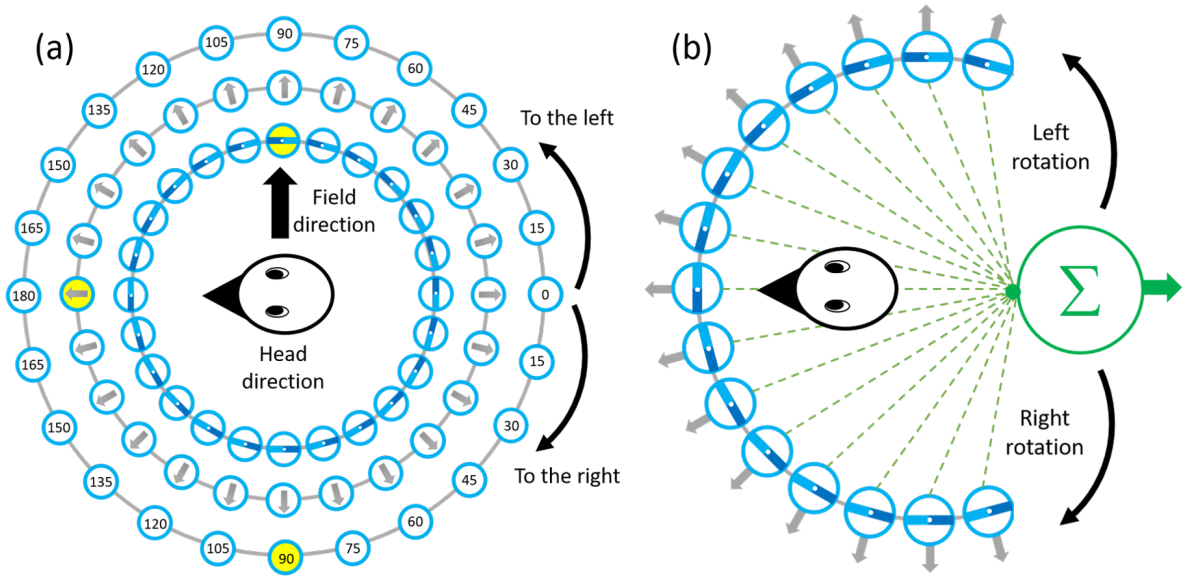

Fig. 4.2: The modified versions of the model by T16. a) the head-direction model: the innermost network is the magnetic field direction network. The middle network is the head direction network. The outermost network is the difference network. The difference network measures the difference between the current head direction and the magnetic field direction. For a head direction at 180° and field direction at 90°, the network computes the field to be at 90° to the right of the head direction. b) the maximum-intensity model: it relies on the asymmetry of the angular distribution of the sensing nodes. The green circle is the integrating node/neuron.

network is described by equations (4.1)&(4.2), with the input given, in discrete form, by equation (4.7).

$$I_k(t) = \sum_{m=0}^{m=n-1} H_m(t) + F_{m+k}(t) \tag{4.7}$$

Where $I_k(t)$ is the input to a node at position k and time step t. $H(t)$ and $F(t)$ are the outputs from the head direction network and field direction network respectively. The position indices m and k run from 0 to $n-1$. n is the number of nodes in the network.

The second solution, as shown in Fig. 4.2b, is also based on two extra assumptions. i) the sensing nodes distribution is not circularly symmetric, but spans a certain angular range. In this work, the simulations are done with 39 nodes spanning an angular range between 85° to 275° (a node every 5°) with the head direction fixed at 180°. While, for clarity purposes, the model illustrations show a 15 node network between 75° and 285° (a node every 15°). ii) the network detects the direction of the horizontal field component by sensing the maximum field intensity in the horizontal. This is done by means of an integrating node/neuron which sums up the activity of the network; the sum is maximum when the head direction points in the same direction as the magnetic field. Due to the asymmetry, the integrated intensity values will vary between a minimum and a maximum. This model will be referred to as the maximum-intensity model and is represented by two

sets of equations: one for the sensing nodes and the other is for the integrating node. For both node types, the state equation is described by (4.8). One of the differences between the node types is the nature of the input $I(x,t)$. For the sensing nodes, the input is the WK10 model as given by (4.4). While, for the integrating node, the input is the sum of the activations from the sensing layer.

$$\tau \frac{\mathrm{d}v(x,t)}{\mathrm{d}t} = -v(x,t) + I(x,t) \tag{4.8}$$

Another difference is the nature of the activation function. In case of the sensing nodes, the activation is two stages: a threshold stage, where the input below 0.5 is set to 0 then an activation stage, which is given by the standard sigmoidal function. For the integrating node, the activation function is modified by the bias b and scale a factors as shown in (4.9). In this equation, v_{sum} is the sum of the activations from the sensing layer. The bias and scale factors can be thought of as subtractive and divisive inhibition. They are needed to improve the representation of the output from the sigmoidal function, but it is beyond the scope of this study to shown how this is achieved mathematically.

$$g_{integrate} = \frac{1}{1 + e^{-a(v_{sum}-b)}} \tag{4.9}$$

4.2.3 The reference frame

The reference frame, as shown in Fig. 4.3, is a fixed frame. It is virtually placed in the room where the experiments are conducted. It aids in quantifying and comparing the various vector quantities used in the simulation. These quantities include the head direction, magnetic pulse direction, the geomagnetic field direction and the landmark orientation (star, chair, etc..). Together, the head direction oriented at 180° and the magnetic pulse directed towards 0° form the south anterior configuration as defined by Beason et al., 1995.

4.2.4 Pulse experiments

Simulated magnetic pulses are applied to the configuration in Fig. 4.2a. The pulse effect depends on two parameters α and β. α is angle between the pulse and the magnetic moment of the magnetite particle, while β dictates the angular range of the various pulse effects. If α is less than $90° - \beta$, the particles will not be affected. If α lies between $90° - \beta$ and $90° + \beta$, the magnetite particles will be impaired (suggested by one of our colleagues, Mouritsen). If α is greater than $90° + \beta$, the magnetite particles will be either impaired, have their magnetic moment reversed or remain intact. These effects are illustrated in

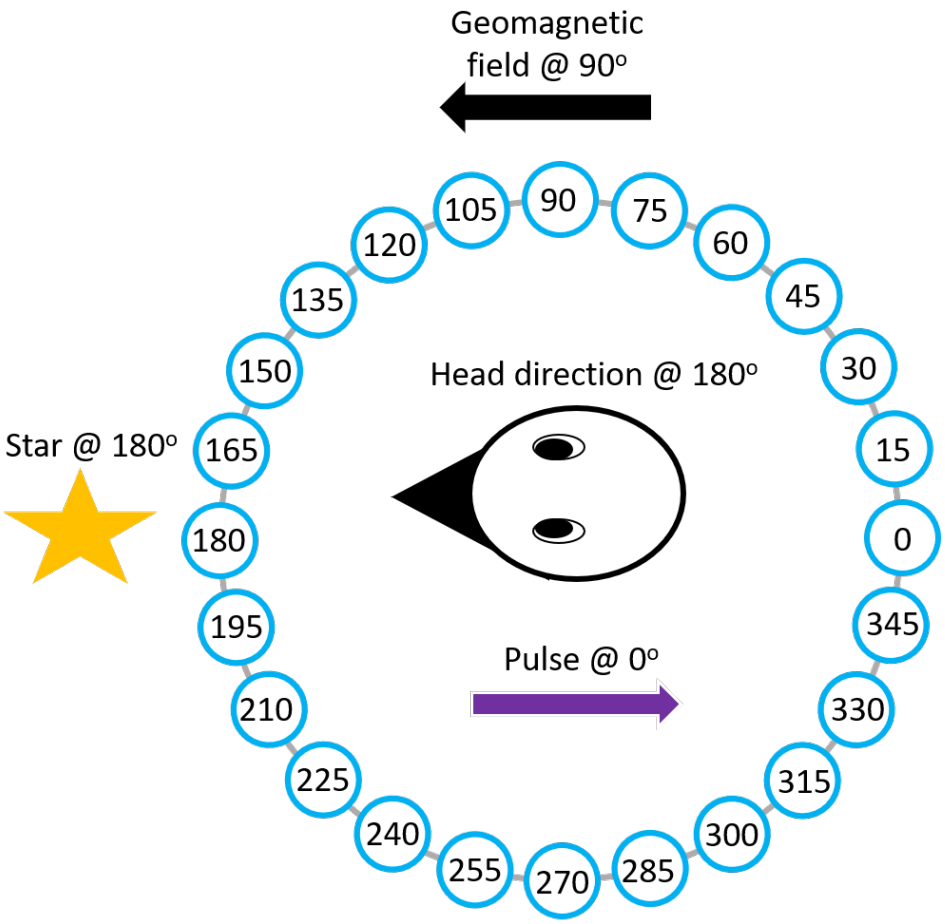

Fig. 4.3: The reference frame. It takes on a mathematical sense, with the 0° being at the right. In this frame, the various vector quantities relevant to this study can be compared.

Fig. 4.4.

Three main types of networks arise according to the presented pulse protocol: i) impaired-networks arise when α is greater than $90° + \beta$ and the nodes are impaired. ii) reversal-networks arise when α is greater than $90° + \beta$ and the nodes are reversed iii) preserved-networks arise when α is greater than $90° + \beta$ and the nodes are intact. Impaired-networks can arise from head-direction and maximum-intensity models, while reversal-networks arise from the former and preserved-networks from the latter.

4.3 Results and discussion

In this section, the results from the simulated pulsing of the head-direction and maximum-intensity models are presented. These results are interpreted into two different ways: i) initially, as an alteration of a compass system that perturbs the bird's sense of direction. ii) later, as a virtual displacement, where the network model in this study is treated as a component of a map sense.

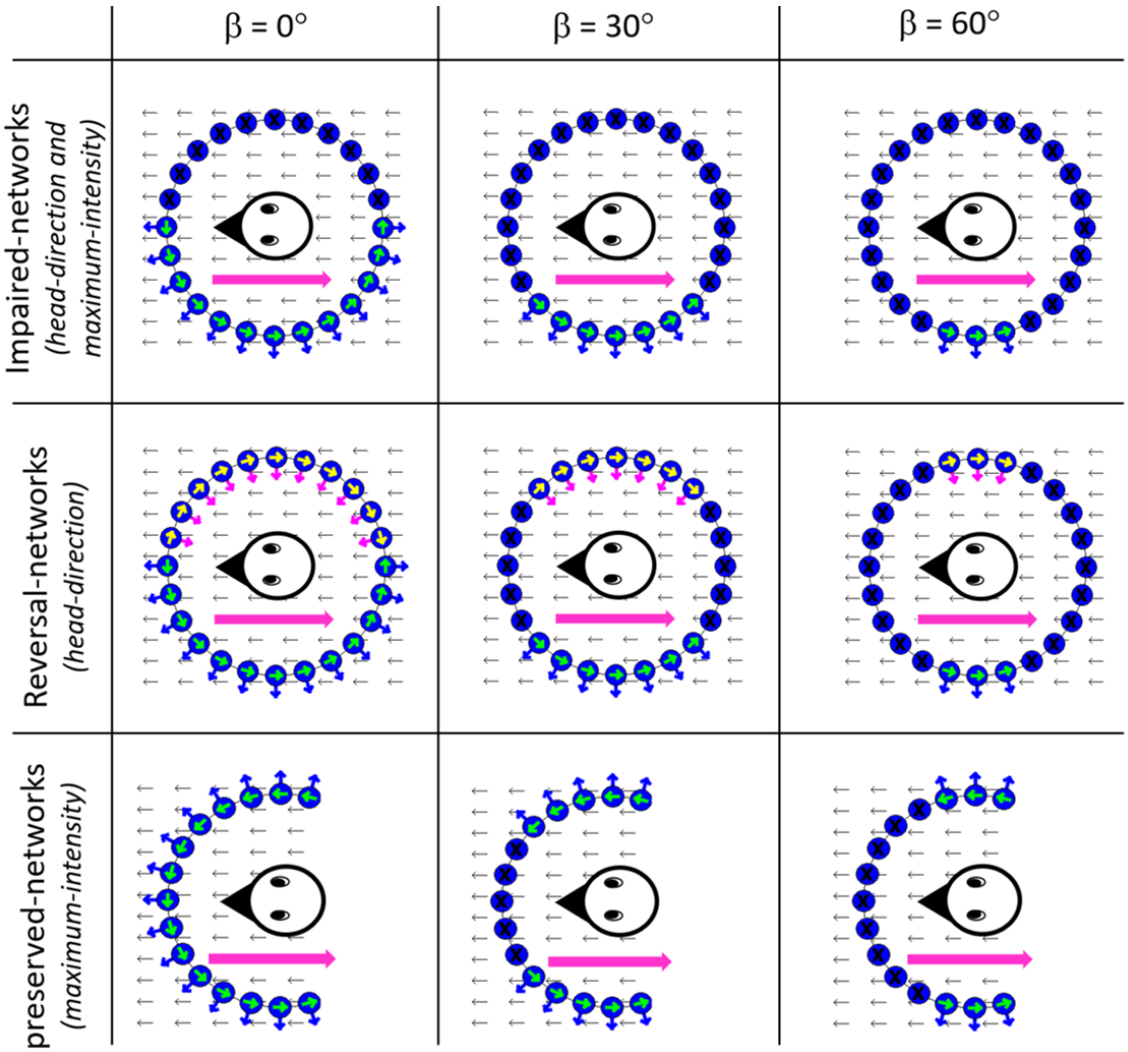

Fig. 4.4: A depiction of the effect of the magnetic pulse on the magnetite particles. It shows the effect of varying the parameter β on the three main network types: impaired-networks, reversal-networks and preserved-networks. The green arrows are the normal orientation of the magnetic moment. Blue arrows are the sensitivity direction. Magenta and yellow arrows are the reversed sensitivity direction and magnetic moment after the application of the pulse. X means that the magnetite particle is impaired.

4.3.1 Pulsing experiments leading to eastward or westward deflection in orientation

In literature, the pulse is applied, mostly, either anti-parallel or parallel to the head direction. The former is termed south-anterior while the latter is called north-anterior. In south-anterior experiments, applying a biasing field perpendicular to the pulse leads to a deflection towards the east/north-east from the northward migratory direction [Beason et al., 1995; Holland, 2010]. Also, for south-anterior experiments, the birds were deflected towards the east/north-east but from a southward migratory direction [Wiltschko et al., 1998a; Wiltschko et al., 2002]. In the case of north-anterior, the birds were deflected to

the west from their northward migratory direction [Beason et al., 1995], but they were deflected to the east from their northward migratory direction [Wiltschko et al., 1994]. It seems that in the cases of bobolinks, european robins and reed warblers, there is a tendency for a deflection to the right of their migratory direction under south-anterior conditions and to the left under north-anterior conditions. However, silvereyes show the opposite trend of deflection to the left under south-anterior conditions and to the right under north-anterior conditions.

Head-direction model

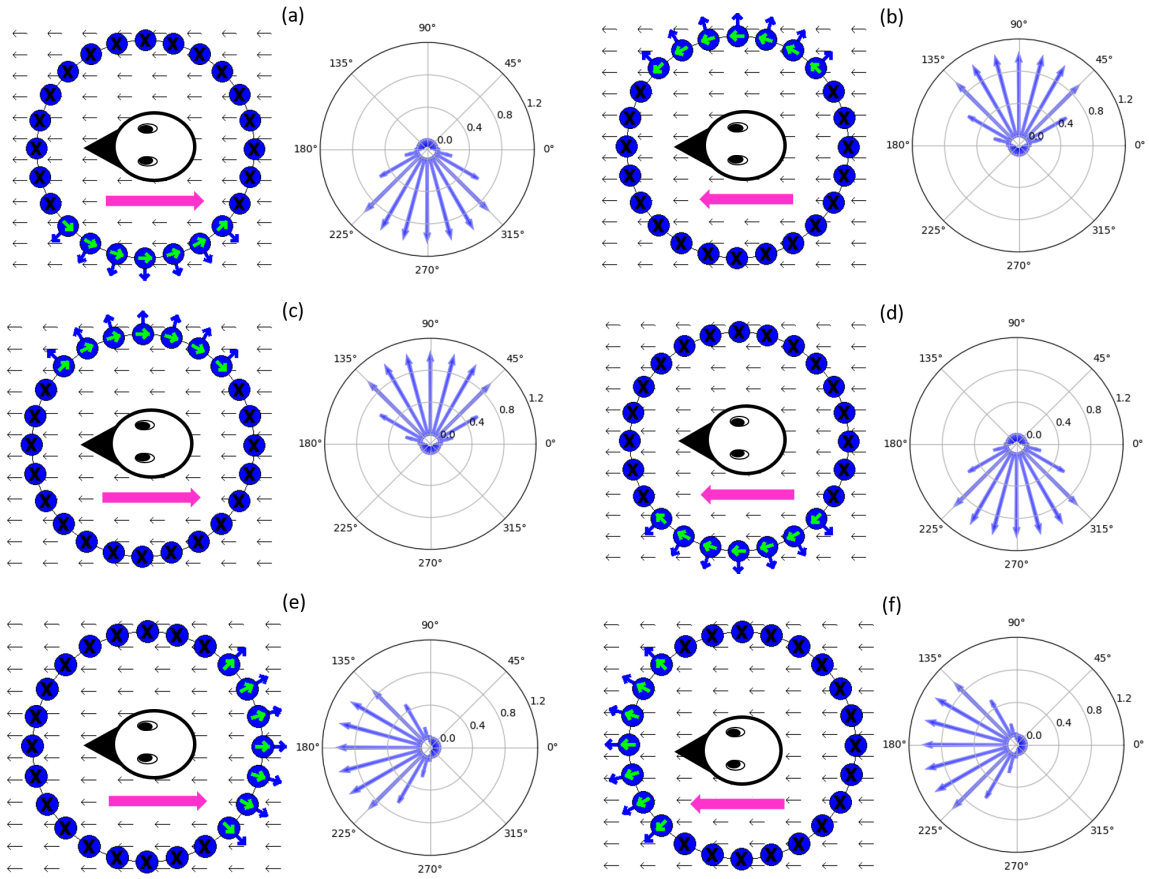

Fig. 4.5: Pulsing experiments under the condition of a fixed head direction and with $\beta = 30°$. The magenta arrows are the pulse. **a)** south-anterior and **b)** north-anterior setups with the WK10 input model having the magnetite particles distributed in a counter-clockwise sense. **c)** south-anterior and **d)** north-anterior setups with the WK10 input model having the magnetite particles distributed in a clockwise sense. **e)** south-anterior and **f)** north-anterior setups with the W08 input model. These types of networks are referred to as impaired-networks since they manifest only impaired magnetite particles.

Under the assumption that the biasing field does not modulate the network or the magnetite-based sensor dynamics, Fig. 4.5 shows impaired-networks that can explain the above observed behavior; this is done for the case where the head direction is aligned

with the true geomagnetic field. The upper networks are based on the WK10 model with the magnetite particles oriented in a counter-clockwise sense. The middle ones are based also on the WK10 model, but with the particles oriented in a clockwise sense. The lower networks are based on the W08 model. Using the altered compass interpretation, the top WK10 networks simulate the silvereyes behavior; the bird senses the geomagnetic field direction to the west relative to the true direction under south-anterior conditions, and to the east under north-anterior conditions. The middle WK10 networks simulate the behavior of the bobolinks, european robins and reed warblers. Finally, The W08 networks sense the true geomagnetic field regardless of the pulse direction.

The W08 network in Fig. 4.5e seems counter intuitive. The network detects a direction opposite from its active nodes. This behavior can be attributed to the fact that the W08 model allows for negative input values by the nature of its cosine weighting. In addition, impaired nodes are assumed to have zero input. Under these conditions, in a winner take all network, zero is higher than negative, so the nods opposite of the negatively activated ones win the competition. Are negative input values biological? Regardless, the simulation is artificial in this regard and further study into the nature of the magnetite sensor is beneficial.

Due to the observations that the W08 model is not affected by the pulse and is biologically implausible, the W08 model will not be discussed further in favor of the WK10 model. The point being made is the dependency of the neural network architecture on the input model. Thus, the results of pulsing experiments are a function of both the neural network architecture and the input model (the magnetite sensor structure).

Still, the networks based on the WK10 model have two shortcomings. First, they do not explain bimodality. Bimodality do not arise in impaired-networks. Second, they do not explain what happens when a bird rotates its head relative to the field. The second issue can be emphasized by the study of Fig. 4.6. This type of plots will be referred to as the head-direction graphs. In a head-direction graph, each point is the vector sum of a polar plot. In Fig. 4.6, the green plot is the true geomagnetic field direction, which is independent of the bird's head direction. The normal(un-pulsed) bird rotates its head and at each direction it senses the field at its true direction of 180°. The black plot is the change in head direction by the rotation of the bird's head. The relation between the black and green plots can be understood through Fig. 4.2a: when the head direction is at 240°, the difference between the black plot and the green plot is the angle required for the bird to rotate its head in order to align with the true field direction. In this case, the angle is 60° to the right. The intersection of the green and black plots marks the direction, in this case 180°, where the birds head direction and the geomagnetic field align.

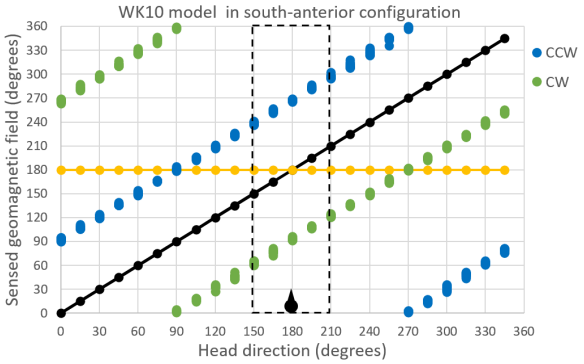

Fig. 4.6: Head-direction graph for the network models in Fig. 4.5a&c. The green plot is the true geomagnetic field direction which is independent of the head direction. The black plot is the change in head direction due to the rotation of the bird's head. The blue and green plots are the sensed geomagnetic field direction after applying the pulse ten times. The dashed box is the decision-window; in this window, the bird perceives the geomagnetic field direction. The back head is the true north (or south) which is coincident with the bird's head direction during the pulsing experiments.

The blue and green plots are the sensed geomagnetic field direction after applying the pulse. These plots are generated by applying the pulse ten times with the configurations in Fig. 4.5a&c. By comparing the blue(green) and black plots, it is evident that, in all head directions, the bird will sense the geomagnetic field to the left(right) of its current heading. The bird will never be able to align with the geomagnetic magnetic field. This might be confusing to the bird and any attempt to reconcile this result with the south-anterior experiments in literature is speculative. Yet, there is the possibility that, while finding the field confusing, the bird can pin the field direction by a landmark which is pointing to the true north (or south), for example the sun or stars. Once a decision is made, with this landmark in sight, the bird ignores any new magnetic field direction information. This method will be referred to as the decision-window method.

By the inspection of Fig. 4.7, some properties of the impaired-networks can be deducted. Varying the parameter β (Fig. 4.7a) has little effect on the sensed geomagnetic field. Thus, the network is robust against impairment of magnetite particles in a bi-cone around the pulse. Also, varying the magnetic pulse direction (Fig. 4.7b) in 90° steps, leads to a similar 90° shift in the sensed geomagnetic field. Utilizing the decision-window hypothesis and for the 270° pulse, the bird will sense the true direction of the magnetic field. While, for the 90° pulse, the bird will sense a field shifted by 180°.

Maximum-intensity model

Before delving into the pulse effects on the maximum-intensity model, it is profitable to illustrate the normal operation of such a model; this is done with the aid of the maximum-

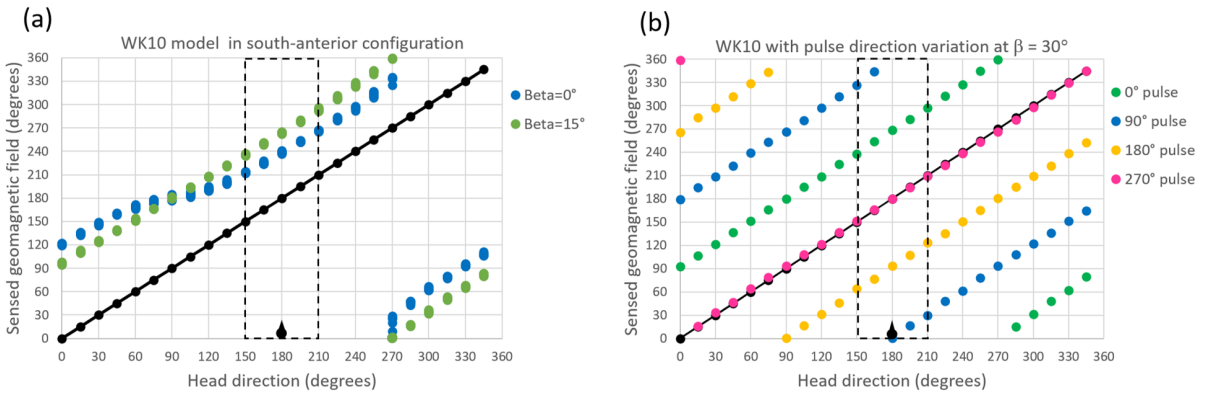

Fig. 4.7: Head-direction graphs for impaired-networks. **a)** Varying β for the counter-clockwise WK10 model in south-anterior (0° pulse) configuration **b)** Varying the pulse direction for the WK10 model with $\beta = 30°$. The dashed box is the decision-window; in this window, the bird perceives the geomagnetic field direction. The back head is the true north (or south) which is coincident with the bird's head direction during the pulsing experiments.

intensity graphs as shown in Fig. 4.8a. These graphs show the variation of the integrated activity from the sensing layer as a function of the head direction. It is evident that there is a region where the integrated activity is maximum and this is where the bird decides upon the direction of the field in the horizontal. The maximum region encompasses the alignment between the true geomagnetic field direction and the head direction. Hence, when a maximum is reached, and by convention, the bird calculates the field direction as its current head direction.

Fig. 4.8a also shows that the integrating node firing rate changes logarithmically with a linear change in the magnetic field intensity. This might be related to the observation by Semm and Beason, 1990 that the number of spikes from the trigeminal ganglion increased logarithmically with the field intensity. This logarithmic behavior can arise mathematically from the activation functions and/or the input function (the WK10 model). Finally, this model can be expanded effortlessly to encompass the change of the field in the vertical; this is done by the means of a kind of a hemispherical distribution of sensing nodes. However, for brevity, the study will focus only on the horizontal field component.

Regarding the pulsing simulations, east and west deflections can arise from the maximum-intensity model as shown in Fig. 4.8b&c. Pulsing in south-anterior configurations leads to eastward deflections from the true field direction, while pulsing in north-anterior configurations leads to westward deflections. As in the head-direction model, the results from these two configurations can be swapped by changing the sense of the magnetite particles from counter-clockwise to clockwise. The results from these simulations can be verified by visual inspection of the illustrative model in Fig. 4.9a; when the birds head direction is at 90°, the active nodes will be pointing in the field direction and the integrated activity is maximum.

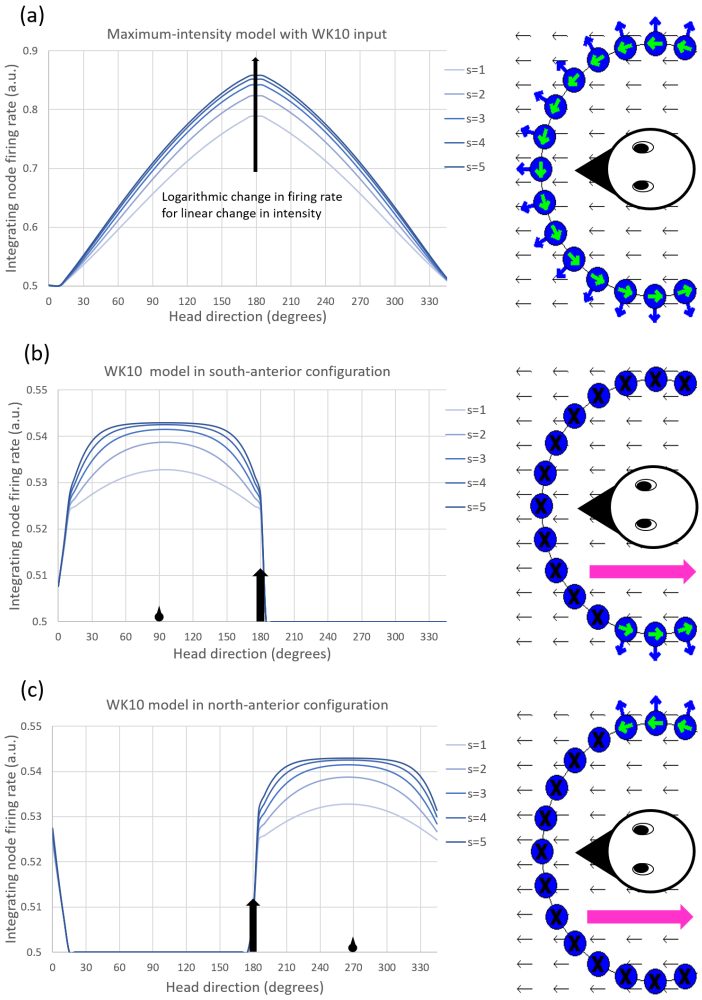

Fig. 4.8: Maximum-intensity graphs with the corresponding network illustrations. These graphs show the variation of the summed/integrated activity as a function of the head direction; this was done for various values of the field intensity parameter s. **a)** the un-pulsed (normal) network. **b)** south-anterior and **c)** north-anterior configurations with the WK10 model. The short black arrow is the true field direction. The black head is the sensed field direction. These simulations were done with 39 nodes in a 85° to 275° angular distribution and with $\beta = 80°$.

4.3.2 Pulsing experiments leading to bimodal orientation

In south-anterior experiments, bimodality arises in various bird species [Wiltschko et al., 2002; Holland, 2010]. Here, we show that bimodality can arise in the both head-direction and maximum-intensity networks, albeit with different network settings and assumptions.

Head-direction model

Simulations of the south-anterior and north-anterior experiments that show bimodality are shown in Fig. 4.9; this is done with the assumption that the biasing field has no effect. Bimodality arises because applying a pulse leads to two competing half circles

(Fig. 4.9b&c); for each sensing node there is a similar 180°-shifted node competing for the same field direction. These node-pairs will have the same input and this leads to bimodality. Also, bimodality is independent of the sense of the magnetite particles distribution (counter-clockwise or clockwise).

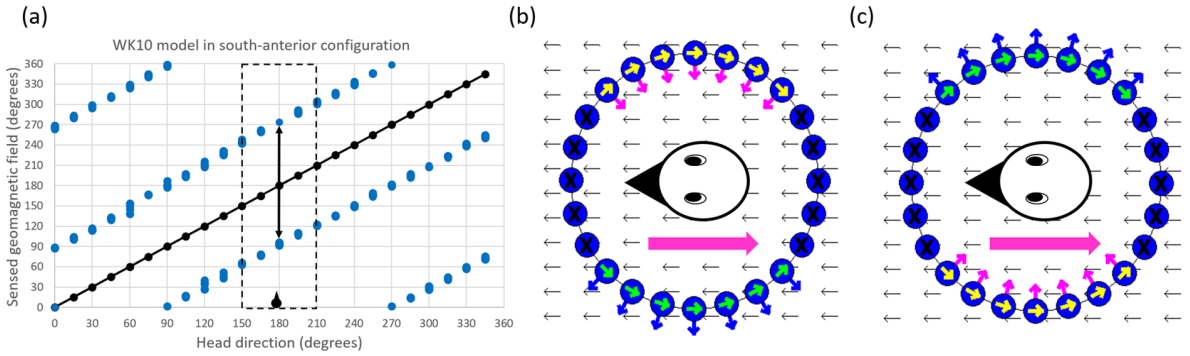

Fig. 4.9: Head-direction graph and network models for reversal-networks in south-anterior configuration and with $\beta = 30°$. **a)** The head-direction graph shows the bimodality effect; the plot is the same for both the counter-clockwise and clockwise senses. **b)** reversal-network with the particles arranged in a counter-clockwise sense and **c)** in a clockwise sense.

Regardless of the head direction, the bird will sense the field in one of two directions in a right-left axis perpendicular to the current head direction. The behavior of the bird can be described with the assistance of the decision-window method. The bird will align its head with the true north and make a decision regarding the geomagnetic field direction. The direction chosen, right or left, will vary from bird to bird. This depends on the noise in the neural circuit. Although, the two half circles, in Fig. 4.9b&c, are competing, the noise will unbalance the competition in favor of one of the two half circles and thus leading to single sensed geomagnetic field direction.

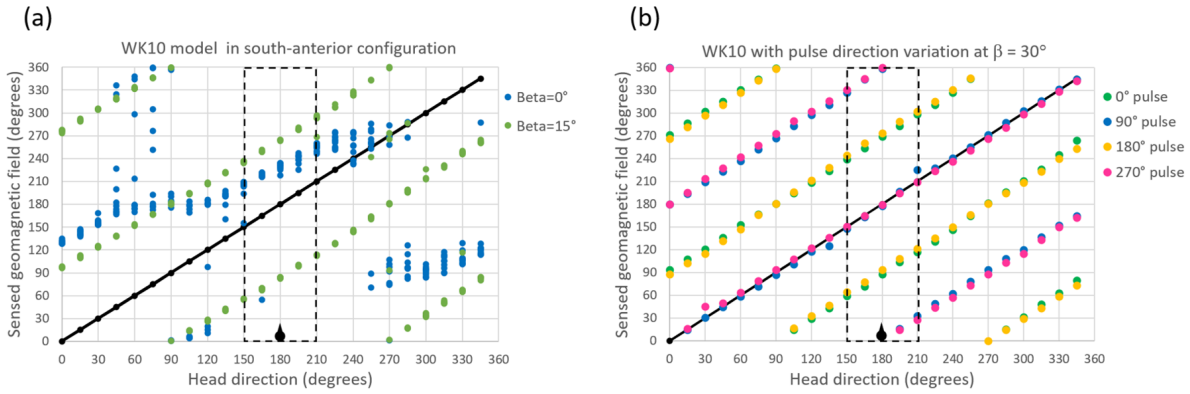

Fig. 4.10: Head-direction graphs for reversal-networks. **a)** Varying β for the south-anterior (0° pulse) configuration **b)** Varying the pulse direction with $\beta = 30°$. The dashed box is the decision-window; in this window, the bird perceives the geomagnetic field direction. The back head is the true north (or south) which is coincident with the bird's head direction during the pulsing experiments.

Some properties of the reversal-networks can be inferred by the study of Fig. 4.10. In contrast to the impaired-networks, varying the parameter β (Fig. 4.10a) has a drastic effect on the sensed geomagnetic field. This can be understood by the study of the two network cases in Fig. 4.4 with $\beta = 0°$ and $\beta = 30°$. The $\beta = 0°$ network does not have two similar competing half circles (13 nodes vs 11 nodes), a requirement for bimodality. This result is due to a simulation assumption; when the pulse is perpendicular to the magnetic moment the particles are not affected. This is also the case when the pulse do effect perpendicular magnetic moments. Thus, and in comparison to the case of $\beta = 30°$, the way to produce bimodality is to introduce similarity between the two competing half circles, which is a condition satisfied by the a $\beta > 0°$. In addition to varying β, varying the magnetic pulse direction (Fig. 4.10b) in 90° steps, leads to a similar 90° shift in the sensed geomagnetic field. The 90° and 270° pulses lead to north-south(forward-backward) bimodality.

Maximum-intensity model

Bimodality can arise in maximum-intensity models as shown in Fig. 4.11. However, this result is based on the assumption that the pulse does not reverse or impair the magnetite particle; this leads to preserved-networks as shown. This assumption leads to different discussions regarding the nature of the magnetite particles: are they a cluster of single domains not single-stranded chains? Again, this question cannot be readily answered and a better treatment of this assumption can be discussed with further insights into the nature of these particles.

Like in the head-direction model, east-west bimodality arises irrespective of the pulse direction (south-anterior or north-anterior). Also, bimodality is independent of the particles arrangement (counter-clockwise or clockwise). However, and unlike the head-direction model, the model inherently does not include noise. Hence, the bird will sense two maximum values of the integrated network activity. In this regard, the decision (or the unbalance) can happen from noise in the higher layers in the cognitive hierarchy.

So far, the discussion has excluded the effect of the biasing field, and yet, it seems that in literature the separator between east/west unimodal and bimodal orientations is the direction of the biasing field. In this regard, there seem to be few possible ways where the biasing field can lead to these results: i) for both the head-direction and maximum-intensity models the biasing field somehow shifts the network architecture from impaired-networks to reversal-networks or preserved-networks. ii) for only the head-direction model, the biasing field perturbs the symmetry of the reversal-networks leading to asymmetrical distributions which lead to east/west deflections. However, and regardless of the method, until further insights are provided regarding the nature of the magnetite particles, adding

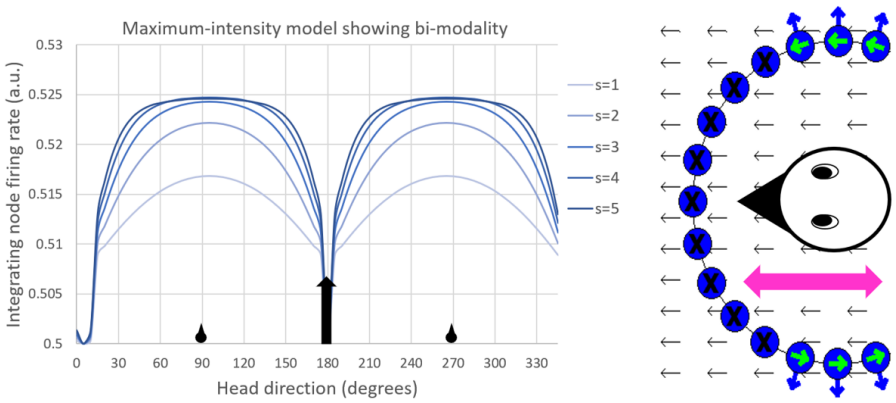

Fig. 4.11: Maximum-intensity graph and preserved-network illustration showing bimodality; this was done for various values of the field intensity parameter s. The short black arrow is the true field direction. The black heads are the oppositely-sensed field directions. These simulations were done with 39 nodes in a 85° to 275° angular distribution and with $\beta = 80°$.

the biasing field effect to the simulations requires extra degrees of freedom in the model that may hamper its predictive powers.

4.3.3 The map sense interpretation

So far, the discussion has treated the results as change in the compass orientation. However, the results can be also interpreted as a virtual displacement as there is a wealth of literature supporting the hypothesis of an inclination compass based on radical pair mechanisms [Mouritsen et al., 2004; Mouritsen and Ritz, 2005; Hiscock et al., 2016; Hore and Mouritsen, 2016]. Subsequently, the pulse might have an effect on the map sense. This conclusion can be supported by the observation that under the application of the same pulse, the departure direction of juvenile european robins is unaffected, while the adults failed to show significant orientation and their heading was compromised [Holland and Helm, 2013]. This was also the case for silvereyes in captivity [Munro et al., 1997a].

A map sense requires two linearly independent coordinates to function. Such two coordinates can be found in the intensity, inclination and the declination angles (or their derivatives, for example, the horizontal field strength). By definition, the inclination and declination angles need a reference frame. For inclination, this can be the gravitation pull or the horizon view, while for declination the true north is need. Technically, any 2 of these parameters can be used in a map sense, but which ones does the bird use or does it use other metrics is not fully known. Subsequently, the rest of the discussion in this section will focus on arguments about each of these navigation parameters.

Intensity

There exists no systematic map-behavioral studies regarding the effect of the magnetic field intensity (or its derivatives) on the orientation of birds. However, the anomaly studies [Mora et al., 2004; Freire et al., 2012] show a non-vision mediated conditioning to the magnetic anomalies. Although these studies served their cause, they did not pin down which component of the magnetic field is the cause for the anomaly detection (for example, both the inclination and intensity are changed). In the study by Freire et al., 2012, it was mentioned that lignocaine-treated ducks did more head scanning than saline-treated ones. In this regard, why would the duck change its head direction (probably in the horizontal) to sense the anomaly. It would be expected that the sense of the field intensity is independent of the head direction.

There are very few non-behavioral studies. The electrophysiological studies by [Beason and Semm, 1987 and Semm and Beason, 1990] and the ZENK study by Heyers et al., 2010. These categories of studies showed a response to the magnetic field and that the trigeminal nerve mediates this information, but there was no separation between the various field parameters (intensity, vertical and horizontal field components).

Aside from the experimental studies, one of the arguments in literature is that; since the magnetic compass detects direction, then the magnetite sensor has to detect intensity. However, this argument is based solely on logical exclusion without a wealth of supportive experimental observations. It is possible that two systems detect the same quantity but on different spatial scales (precision), or that the information from one system can be more easily integrated in a map system.

Finally, there are two extra points to be made regarding the intensity sense: i) it is not clear how a change in the sensed intensity values would lead to a universal (position independent) east/west unimodal and bimodal orientations. Since the field intensity mainly changes across the latitude it would be expected to get a north-south bimodal orientations, which is not the case. ii) it is technically possible to construct a model that senses the horizontal field direction by sensing the maximum intensity in the horizontal. Hence, the change in intensity is the means by which the bird senses direction. In that case, a direct neuronal response to a change in intensity cannot argue for or against the utilization of this parameter in a map sense. In this regard, it can deducted that, the crucial experimental evidence for a map sense based on intensity is a systematic study of the effect of intensity variation on the perceived geographical location in adult birds.

Inclination

There are parallels between the arguments presented here and the ones made for intensity; i) there are no systematic behavioral studies regarding the effect of the inclination angle variation on the sensed geographical location. ii) the non-behavioral studies are nonspecific. iii) it is not conceivable how a change in the sensed inclination angle can lead to a global east-west bimodality instead of a north-south one.

The bimodality observed in literature due to an inclination angle change is tied to the compass system. For example, the bimodality observed from pied flycatchers at high inclinations with no access to celestial cues[Weindler et al., 1995] and this bimodality is along the migratory direction.

Declination

The non-behavior studies are nonspecific. However, in the case of behavioral studies, it was found that adult reed warblers can correct for longitudinal displacements [Chernetsov et al., 2008]. Also, it was found that adult birds compensate for a declination change while other cues are left intact [Chernetsov et al., 2017]. This compensation was performed by adult birds which is in agreement that adult, not juveniles, possess the map sense. Also, it is possible to interpret the pulse experiments as a change in the observed declination; this is because the declination changes mainly across the longitude. Hence, it would be expected that a change in the observed declination would lead to east/west unimodal and bimodal deflections, which is the results from these experiments. Finally, it should be noted that the declination angle needs the true north; this is mentioned by Pakhomov et al., 2018. In this study, it was mentioned that both the trigeminally mediated and visual inputs are required for a functional magnetic.

Declination followup

The neural circuit presented in this study cannot alone determine the declination angle, as the angle requires also the true north as the sun or stars. Also, several studies were performed indoors [Wiltschko et al., 1994; Beason et al., 1995; Wiltschko et al., 1998a] with no access to clear sky. In this regard, it is not readily available how can the bird sense the declination angle and with no decisive experimental support, any attempts to explain this would be speculation. However, there is the possibility that the bird can make associations between the true north and the indoor environment structure. If juvenile birds can make an association between the center of rotation of light dots and the true north [Wiltschko et al., 1987; Able and Able, 1990; Weindler et al., 1997], then maybe adults can make association between an indoor object and the true north. A study of

the visual acuity of birds found that they are superior to most other animals and have the same values as primates [Donner, 1951]. Then, it might be possible for adult to make associations between the known true north in a familiar environment and other new fine details. Also, the experiments were done on adult birds which should have familiarity with the available cues in the experimental grounds.

Finally, it is fruitful to emphasize the difference between the compass and map interpretations in terms of the network architecture; this is done for the head-direction model. The main culprit (for the WK10 model) is the sense of the arrangement of the magnetite particles. This feature separates between the different interpretations and the behavior of the different bird groups and is summarized in Table 4.2. The same argument can be applied the maximum-intensity model but with the reversal of the sense of arrangement.

	Counter-clockwise	Clockwise
Compass	Silvereyes	Bobolinks, european robins and reed warblers
Map	Bobolinks, european robins and reed warblers	Silvereyes

Table 4.2: The effect of the arrangement of the magnetite particles on the different interpretations (compass or map) and on the behavior of the different bird groups. This is done for the head-direction model.

The reinterpretation of the simulation results in terms of a change in the map cues can be elaborated with a model, a case and a behavioral hypothesis. The model is the head-direction based on the WK10 input model, the case is the bobolinks and the behavior hypothesis is the decision-window. After a pulse, in a south-anterior setup, the bird will detect a field shifted to the left relative to the true north. This implies that the bird will sense that it was displaced to negative declination conditions and thus will compensate by a north-east/east-ward orientation. The opposite is true for the north-anterior case, which is also in agreement with the WK10 input model. The decision-window hypothesis means that the bird makes a decision about its location when its head direction is within a small angular window of the true north, where a sense for the declination angle is formed. After making that decision, the bird uses the compass mechanism to orient with the decided upon heading. The same analysis can be made for the read warblers and european robins, but not for silvereyes. The silvereyes behave in an opposite trend relative to the rest of the birds in this study. Again, it would be rather speculative to explain such a difference in behavior. However, silvereyes migrate around the southern hemisphere only, and with reference to a declination map, in positive declination conditions. Though, it is not clear how these two factors would affect the behavior of silvereyes to warrant a different trend

in pulsing experiments. However, epigenetic reasons that could lead to opposite polarities of the magnetite particles cannot be fully ruled out.

4.4 Predictions

Predictions are offered in three categories according to the sensing model: i) predictions shared between the head-direction and maximum-intensity models, ii) head-direction only predictions and iii) maximum-intensity only predictions. The predictions are provided with the compass sense interpretation of the model in context. Also, it is recommended to utilize the birds mentioned in this study, namely, the bobolinks, european robins and reed warblers.

4.4.1 Shared predictions

Bimodality in null-bias environments

With reversal-networks and preserved-networks, applying a pulse, in null-bias conditions, would lead to east-west bimodality. This bimodality should exist for both the south-anterior and north-anterior configurations. In literature bimodality was observed under south-anterior conditions. Therefore, observing bimodality in a north-anterior setup with null-bias conditions, or with the same experimental conditions as done in south-anterior experiments, would test for the symmetry of the magnetic field sensing network.

Pulse direction change

According to the present study, pulsing european robins and reed warblers under north-anterior conditions should lead to west/north westerly deflections. Also, for all birds mentioned in this study a the 270° pulse should lead to no change in orientation; the birds will sense the true direction of the field.

Double pulse experiments

Two magnetic pulses applied in a rapid sequence (within minutes) can be a diagnostic for the predictive power of the model provided in this study. In this case, Table 4.3 provides predictions for various combination of double pulses.

Bias direction	Network type	First pulse	First result	Second pulse	Second result
Null/local	Impaired-network	South-anterior	eastward deflection	South-anterior	eastward deflection
Null/local	Impaired-network	South-anterior	eastward deflection	North-anterior	Total impairment / Disorientation
Null/local	Impaired-network	270°	no change	270°	no change
Null/local	Impaired-network	270°	no change	90°	Total impairment / Disorientation
Null/local	*Rev/pre networks	South-anterior	east-west bimodality	North-anterior	east-west bimodality
Null/local	*Rev/pre networks	South-anterior	east-west bimodality	South-anterior	east-west bimodality

Table 4.3: Double pulse experiments. This is done with the WK10 input model and the compass sense interpretation in context. *Reversal and preserved networks.

4.4.2 Head-direction model

Pulse direction change

A 90° pulse would induce a 180° shift in the sensed field. In this case, it is not clear how the bird would behave; it might reverse its orientation or ignore the new field information completely.

4.4.3 Maximum-intensity model

Pulse direction change

A 90° pulse would induce a total impairment of the network. Hence, it is expected that the result would be a huge scatter in the chosen migratory direction by the birds as a group.

Acknowledgments

This work was supported by the Deutsche Forschungsgemeinschaft (DFG). Also, we thank the Molecular Sensory Biology (MSB) research training group of the University of Oldenburg for their support, discussions and insights.

Chapter 5

Manuscript two: navigation simulations

Learning Navigation by Compass in Migratory Birds: a Deep Reinforcement Learning Approach

Karim Habashy [1] and Michael Winklhofer [1,2]

[1] Institut für Biologie und Umweltwissenschaften, Carl von Ossietzky Universität Oldenburg, Oldenburg, Germany

[2] Research Centre for Neurosensory Sciences, Oldenburg, Germany

April 26, 2024

Abstract

There is a common consensus that for migratory birds to perform long distance migration two mechanisms are required; a compass mechanism and a map mechanism. Compared to the compass mechanism, the map mechanism (navigation) is poorly understood and is under heavy study. Some of these studies aim at a better understanding of the utilized navigational cues, their priority systems and relative impact on the navigational performance. For navigational cues, the most regarded ones are the olfactory and magnetic cues. For the magnetic cues, it thought that the bird utilizes some combination of the fields inclination, declination and intensity. Here, a theory is put forward that tackles the navigational problem as a whole. This theory explores the visual system as the navigational system with the utilized cues being the magnetic inclination and declination. This visual-based navigation theory is tested through a model. This model is not hard-coded what to do, but learns the correct way to navigate based on the available cues. After learning, this model can navigate and shows other common navigational properties like alignment after displacement and extrapolation. Also, the model shows novel solutions to unfamiliar and artificial magnetic field environments. Finally, predictions are put forward that can aid in testing this model and a better understanding of the navigational system.

Keywords: Magnetic map , Reinforcement learning, Orientation and navigation, Visual compass, Magnetic field sensor, Navigation simulation

5.1 Introduction

For decades, the biological processes through which birds perform long distance migrations have been under intense study. Subsequently, it is widely accepted that for birds to perform these migrations, two mechanisms are needed; a compass mechanism and a location-finding (map) mechanism. For the compass mechanism, it is thought to be redundant, where the bird can find the orientation direction from different categories of environmental cues; these being, the sun, the stars and the magnetic field. The sun compass relies on the perceived motion of the sun in the sky [Schmidt-Koenig, 1990], the stellar (star) compass is based on the constellation pattern and/or the center of rotation of the celestial view [Wiltschko et al., 1986; Weindler et al., 1997; Chernetsov, 2016; Pakhomov et al., 2017a] and the magnetic field compass is based on the axial orientation of the field lines.

In literature, the most widely used parameters to describe the magnetic field are the declination angle, the inclination angle and the total field intensity. The declination angle is the angle formed between the field and the true north. The inclination angle is the angle formed between the field and horizontal plane. Using this parametrization, the magnetic compass is attributed to an inclination compass as it ignores the field polarity and depends on the inclination of the field lines in space [Wiltschko and Wiltschko, 1996, 2005]. Physiologically, the compass system is based on a chemical transduction mechanism. Specifically, the magnetic field affects the biochemical reactions of radical-pair intermediates generated by light absorption [Schulten et al., 1978; Ritz et al., 2000]. Proof for this light-dependent magnetoreception comes from the investigation of Cluster N in the forebrain [Mouritsen et al., 2005; Zapka et al., 2009].

Relative to the compass mechanism, the map mechanism is not fully understood. In literature, two main hypotheses exist regarding the nature of the environmental cues used as a basis for the map. The olfactory map hypothesis [Papi et al., 1971; Gagliardo et al., 2013] and the magnetic map hypothesis [Walker et al., 2002; Kishkinev, 2015; Heyers et al., 2017]. A wealth of evidence for the map hypothesis comes from physical and virtual displacement experiments, where the bird is physically (or virtually) displaced to a new location and tested for corrective behavior tendencies [Thorup et al., 2007; Chernetsov et al., 2008]. In those experiments, it was found that adult birds can compensate for longitudinal displacements but not juvenile ones. However, it was shown that young common cuckoos (Cuculus canorus) can also compensate; this was shown using long distance satellite tracking [Thorup et al., 2020]. Although, the necessity of sensing the magnetic field in a map mechanism is not disputed, its sufficiency is shown to be lacking [Thorup and Rabøl, 2007]. Celestial cues are also needed, which leads to the hy-

pothesis that perceiving declination is a part of the map sense [Chernetsov et al., 2017]. Physiologically, the map sense is thought to be mediated by the ophthalmic branch of the trigeminal nerve (V1) [Kishkinev et al., 2013]. This branch is the only non-olfactory nerve innervating the upper peak where iron rich structures, involving magnetite particles, are found [Wiltschko and Wiltschko, 2013].

Bird navigation studies incorporate experiments where migratory birds are tagged and tracked to study their trajectories. Although experimental studies are powerful and necessary, they often incur high temporal and physical costs. These costs can be averted by using various simulation tools at the expense of a great abstraction of the experimental environment and conditions. However, a carefully designed model with the relevant assumptions can guide experimental procedures through testable predictions. In this regard, models have been employed to study the navigation in various taxa. Specifically, the navigation of the marine green turtles in a dynamic fluid environment has been studied by Lagrangian-based particle models [Painter and Hillen, 2015b]. Another turtle-inspired study [Taylor, 2017] showed that bicoordinate navigation is possible when the agent(turtle) follows the gradient of one ordinate at a time. Aside from turtle studies, long-distance animal navigation has been simulated using the the extended Kalman filter; in this modeling approach, the animal navigates by perceiving the spatial angle included between the geographic direction and the magnetic field vector [Qi et al., 2017]. In another approach, animal navigation was modeled by a signature-based navigation strategy, where the animal measures the local field intensity and inclination and compares them with the goal values. The difference between these two values produces a vector which assists the animal in orienting towards the desired goal location [Taylor, 2018; Pizzuti et al., 2021]. In addition, the Long-distance trans-equatorial navigation was modeled by an agent performing sequential measurements of the inclination angle [Taylor et al., 2021].

As an alternative of directly specifying and coding the desired behavior of a navigating agent (animal), the correct behavior that is required for navigation can be gained by learning. A field that deals with learning efficient behavior through interactions with an environment is Reinforcement Learning (hereafter RL). RL has been compared with Stochastic Dynamic programming in behavioral ecology [Frankenhuis et al., 2019]; it is shown that RL can decrease the severity of both the curse of dimensionality and the curse of modeling. The curse of dimensionality is a synonym for an environment with a huge number of variables; this means that the state space is large. The curse of modeling is a synonym for the incomplete knowledge of the environment dynamics. Due its advantages, RL has been employed to show that the combined influence of asocial and social learning can facilitate the learning of task-related action sequences; this was shown for the case of nettle processing by mountain gorillas [Whalen et al., 2015]. Also,

it was shown that RL coupled with genetic predispositions can explain the ontogeny of efficient behavior in non-human animals [Enquist et al., 2016], deep RL was used to study predator-prey ecosystems [Park et al., 2021], and inverse RL has been used to extract the behavioral strategy of animals from the time series of their interaction with the environment [Yamaguchi et al., 2018]. For a review about the usage of RL in modeling biological and artificial agents see Neftci and Averbeck, 2019, and for a discussion about RL and it possible brain implementations see Gershman and Ölveczky, 2020.

In this work, a theory is provided that explains how migratory birds can navigate using the visual system. Technically, a visual compass system can be used to measure, roughly, both the magnetic declination and inclination. This theory is tested through a learning model. This model learns the correct way to navigate through interactions with an artificial environment, where the available cues are the true north and the magnetic field. After learning, the model showed true navigation behavior from any location on the learned area to the target goal. The effects of the various model parameters are tested; namely, the impact of the available cues on the navigational performance, the impact of the visual acuity and the impact of the magnetic field gradient. Also, the model showed highly regarded navigational properties like alignment after displacement and extrapolation. The model showed novel behavior in unfamiliar and complex environments. Finally, predictions are presented to shine light on this enigmatic system.

5.2 Methods

The general approach is to study the performance and behavior of a bird model that learns the ability to navigate by utilizing local environmental cues. As outlined, this learning is presented through the framework of RL, and in this regard, a brief introduction to the methodology is presented here. Then, an overview of the learning environment is shown accompanied by a brief outline of the input representation of the magnetic field, which is based on the model by Wang et al., 2006. Finally, a brief description is provided for the technique by which the RL problem is solved. This technique is called Proximal Policy Optimization.

5.2.1 The reinforcement learning problem

RL is a sub-field of machine learning that deals with understanding goal-directed learning and behavior [Sutton and Barto, 2018; Lapan, 2018]. It is different from supervised learning where the correct actions(labels) are explicitly presented by an external supervisor, and different from unsupervised learning where the goal is to find underlying structure

in the data. In RL, the correct actions are learned through interactions with the environment. These actions are reinforced, hence the name, by feedback signals from the environment. These signals can be positive or negative, but they are formally called rewards in literature. The goal of these interactions is to learn actions that maximize the expected total rewards in the long run. In this regard, the actions learned should not only seek the highest immediate reward but the highest accumulative total rewards.

The RL problem is formally defined through the Markov Decision Process (MDP hereafter) framework, which is a mathematical realization of the general RL problem. A visual framing of this framework is shown in Fig. 5.1. In this figure, the agent is

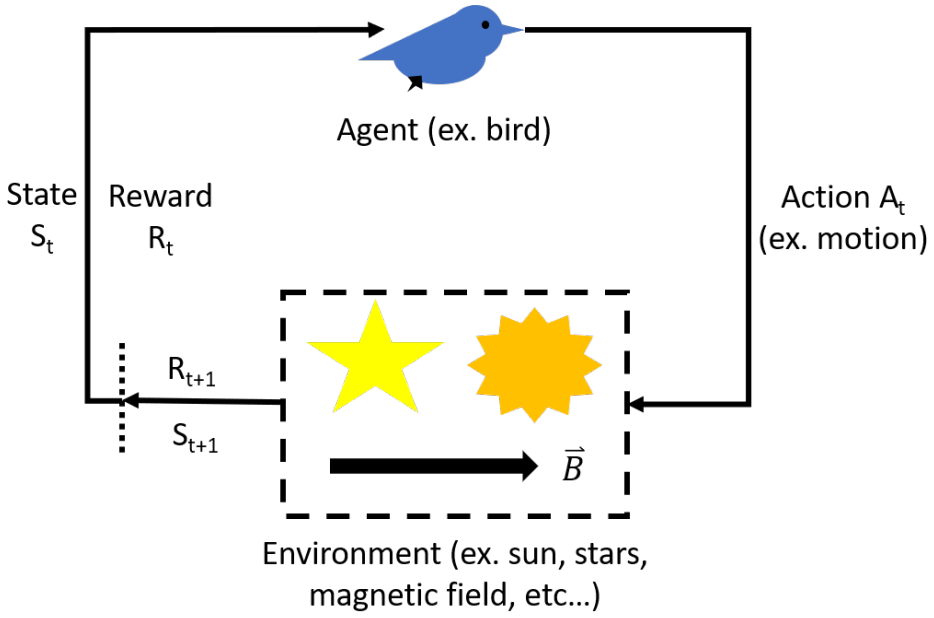

Fig. 5.1: Visual representation of the general RL problem as framed by the MDP. An agent(bird) interacts with the environment by actions A_t. The consequence of this action is the acquisition of a new observation S_{t+1} and reward R_{t+1}.

the entity that tries to learn the correct behavior by interactions with an environment. Here, it is assumed that the interactions happen at discrete time steps t. At each time step, the agent perceives the current state of the environment S_t, while also acquiring a reward R_t due to its previous action. Having acquired these two variables, the agent interact with the environment through an action A_t. Then, due to its action, the agent perceives a new state S_{t+1} and acquires a new reward R_{t+1}. In general, the reward acquired is conditional on both the perceived state and the action taken. Symbolically, the trajectory resulting from the agent-environment interaction and feedback is shown in (5.1). In this trajectory, the transitions between subsequent states in the environment are governed by the dynamics equation (5.2).

$$S_0, A_0, R_1, S_1, A_1, R_2, S_2, A_2, R_3, S_3, A_3, R_4, ... \tag{5.1}$$

$$p(s', r|s, a) = Pr(S_t = s', R_t = r|S_{t-1} = s, A_{t-1} = a) \tag{5.2}$$

This equation states that the probability distribution of the newly encountered states and available rewards is conditionally dependent on the observed state and action taken in the previous time step. Regarding the observed state, it is assumed that it contains all the relevant information in the environment for the agent to maximize its reward acquisition. Hence, only the last observed state is needed to solve the RL problem and not the history of the state transitions. When this is the case, the RL is said to have the Markov property.

5.2.2 The environment and magnetic field sensory models

The environment is a plane area where the bird learns navigation to a goal marked by the green box as shown in Fig. 5.2a. The red frame is the boundary within which the bird learns to utilize the available cues to reach the desired goal.

These cues include the inclination angle and the declination angle. The declination angle is formed between the magnetic field in the horizontal and the true north, which is provided by visual image of a star (Fig. 5.2b). The star is a symbol for true north and not a realistic representation of how the bird perceives the true north from celestial cues. The magnetic field, which contains information about the inclination and declination angles, is provided as a visual input (Fig. 5.2c). The field visual input is provided according to the analysis by the Wang et al., 2006. It should be noted that the true north view is invariant under agent translations and is only changed by rotation.

Together, the two images in, Fig. 5.2b & 2c, form the input state to the learning model. In this case, the bird model is said to have a memory length of one with the current input being the state. However, most of the simulations are using a memory length of three with the current input and two historical inputs. In this case, the state is composed of six images, 3 visual and 3 magnetic. For both cases, it is assumed that the RL problem has the Markov property, although the one memory case is oblivious to the magnetic gradient information. The actions taken by the agents in this environment are discrete and divided into three actions: move forward by 6 units, turn left and turn right by 15°. All the states in the environment have a reward of zero except the states within the green/goal box, which have a reward of five.

The magnetic field environment presented in this study is both simple and symbolic. The aim is to study the influence of certain properties of the field topography on the learned navigational behavior. In this regard, the field is reduced to be a static field with constant gradients. In the 400x400 field area, the horizontal field direction spans a 90° change, while the vertical field a 180° one. The inclination changes in a way that the

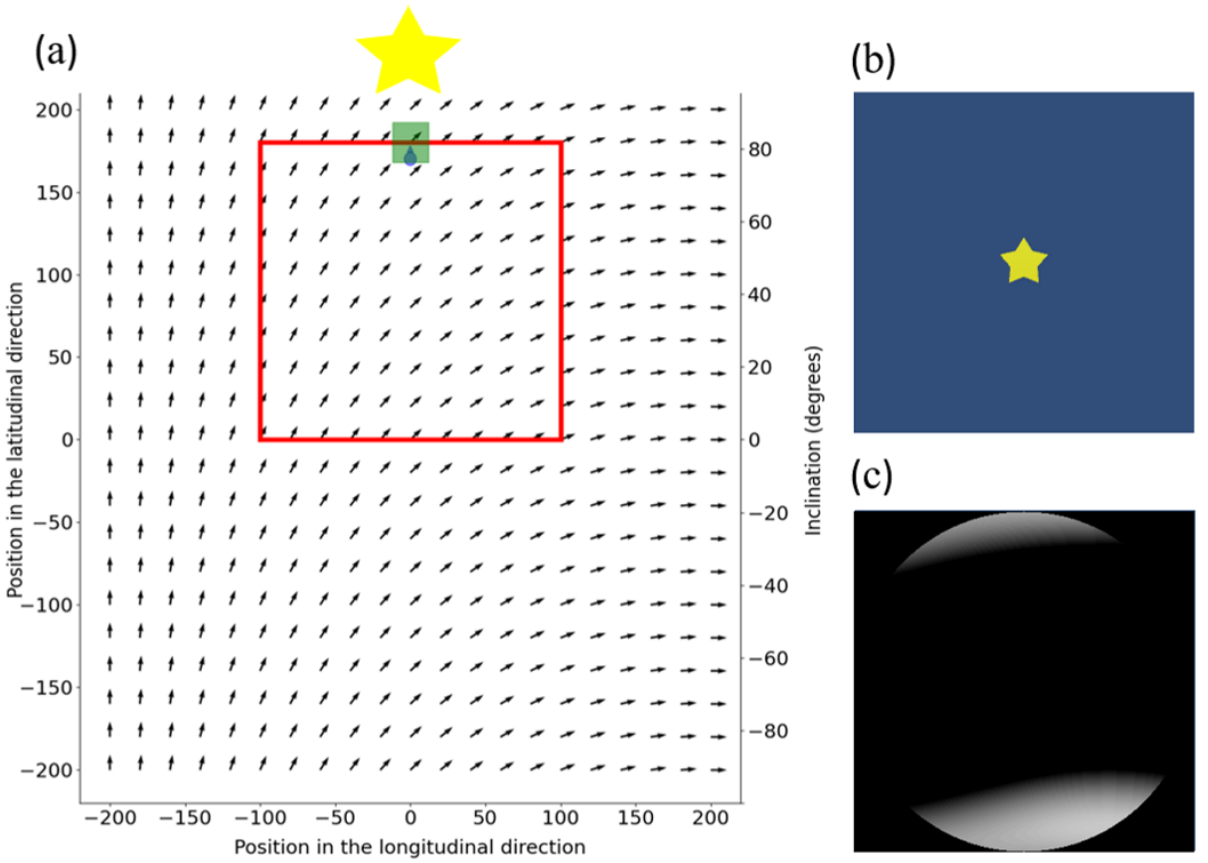

Fig. 5.2: The interactive environment. a) top view of the environment showing the agent as the blue head, the training training as the red box and the true north by a star symbol. Shown is the gradient of the horizontal field which when coupled with the true north provides declination information. The inclination can be inferred from the vertical field axis on the right. b) view of the true north as provided by the unity environment. c) view of the magnetic field as described by the Wang et al., 2006 model. Both of these views are obtained by the birds current position as shown in the top view.

equator is at the center of the field area.

To form a perspective of this field area, the migratory step of Pied Flycatchers is about 100-149 km [Mouritsen and Mouritsen, 2000]. Assuming a 100 km migratory step and with the training step being 6 units, the field area can be thought of as approx. 6670x6670 km^2. This estimate changes with different training step sizes, which span the range 6-8. From this analysis, both the declination and inclination would have a 0.0135 and 0.027°s/km rate of change respectively. Compared to the 0.004°/km change in central Europe, the declination change utilized is approx. four times larger than the real one. However, this is of little relevance, as real migratory birds would expectedly have higher visual acuity than the current model. Thus, they are able to detect smaller change in the horizontal field direction.

5.2.3 Solving the RL problem with Proximal Policy Optimization

To solve the RL problem, few extra concepts and variables that are widely used in literature are to be defined. i) the policy $\pi(a, s)$, is the set of rules by which the agent executes actions. Mathematically, it is defined as a probability distribution over actions in a given state. In this work, it is parameterized by a neural network. ii) the value of the state (hereafter VoS) $\nu_\pi(s)$, is a measure of how good is it to be in a given state or the expected total reward gained from being in a specific state. It is mainly a function of the state and also the policy, because different policies (rules) lead to different rewards in the long run. It is also parameterized by a neural network. iii) the quality of the action Q(a,s), is defined as the expected total rewards after taking a specific action in a given state. iv) the advantage of the action A(a,s), is a measure of how good is it to take an action in a given state compared to the other actions. It is this given by (5.3).

$$A(a, s) = Q(a, s) - \nu(s) \tag{5.3}$$

The techniques used to solve the RL problem are based on the Proximal Policy Optimization method Schulman et al., 2017. As mentioned above, the policy and the VoS are both parameterized by a neural network as shown in Fig. 5.3, which encapsulates the agent. This neural network is trained by the combination of two loss functions. One for the policy-head and the other for the VoS-head. The policy-objective is given by equations (5.4)&(5.5).

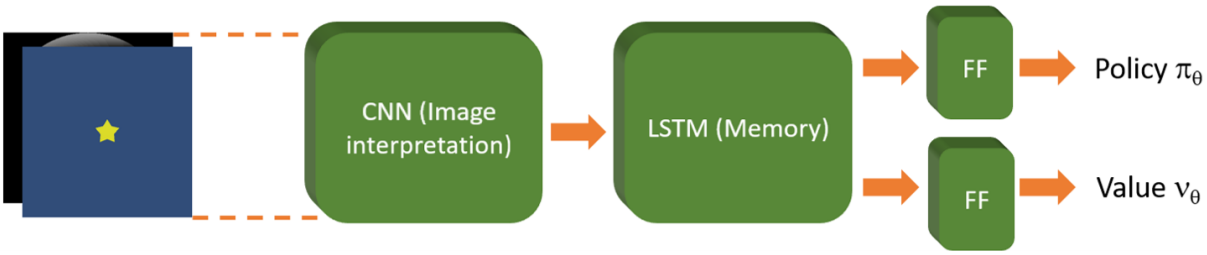

Fig. 5.3: Architecture of the neural network representing the agent. CNN is the convolution network. LSTM is the long short term memory network. FF is the feed forward network.

$$L(\theta) = \frac{\pi_\theta(a, s)}{\pi_{\theta old}(a, s)} \tag{5.4}$$

$$J^{clip}(\theta) = \hat{E}[min(A(a, s) * L(\theta), A(a, s) * clip(L(\theta), 1 - \epsilon, 1 + \epsilon))] \tag{5.5}$$

In these equations, $L(\theta)$ is the ratio between the probability distributions of the actions from the current policy $\pi_\theta(a, s)$ over the old policy $\pi_{\theta old}(a, s)$. $J^{clip}(\theta)$ is the clipped objective. Clipping limits the size of the update which depends on the ratio

between policies. The parameter ϵ controls the allowed update size. Regarding the value loss, it is given by the mean square error (MSE) loss between $\nu(\theta)$, the output of the value head, and the discounted total reward calculated from the trajectories undertaken by the agent.

5.3 Results and discussion

In this section, the results from simulating the bird navigation are presented in the form of the training performance and trajectory graphs. This performance is the average of three learning birds/agents. The performance metric used is the averaged trajectory rewards which takes a maximum value of five. A trajectory is the path taken by the bird from the random spawning point, with a random orientation, to the end of its path. The end can be either the desired goal or the boundaries of the training area.

Shown here is the effect of cue availability, the change in the magnetic field gradient and the visual acuity on the navigational performance. In addition, we demonstrate the effect of periodic environments and magnetic anomalies on navigation. Also, shown are emergent navigational strategies which arises under novel and stringent magnetic field conditions. Finally, a discussion is presented aimed at a better understanding of the results and relating the findings with what is known in literature.

5.3.1 Effect of cue availability

The available cues during navigation is the true north (via the stars) and the magnetic field. From these cues, four cue subsets are formed and tested for navigational performance: i) all cues available. ii) absence of vertical field sense (null vertical). iii) absence of horizontal field sense (null horizontal). iv) absence of a true north cue. The results of these simulations are shown in (Fig. 5.4a).

As inferred from the simulations, the true north is necessary for successful navigation using the visual compass. While, albeit with decreased performance, a navigational strategy can be achieved in the absence of a vertical field sense (inclination sense). Subsequently, it can be seen that a declination sense is more important for reliable navigation than the inclination. The argument is that, with a declination sense the bird can determine its position in the longitudinal axis and follows the true north (in our case) until it reaches the desired goal. While, in the absence of a declination sense, the true north and the inclination sense provide overlapping information and the position on the longitudinal axis is not determined.

Two other variables are tested and compared in Fig. 5.4; the chromatic nature of the

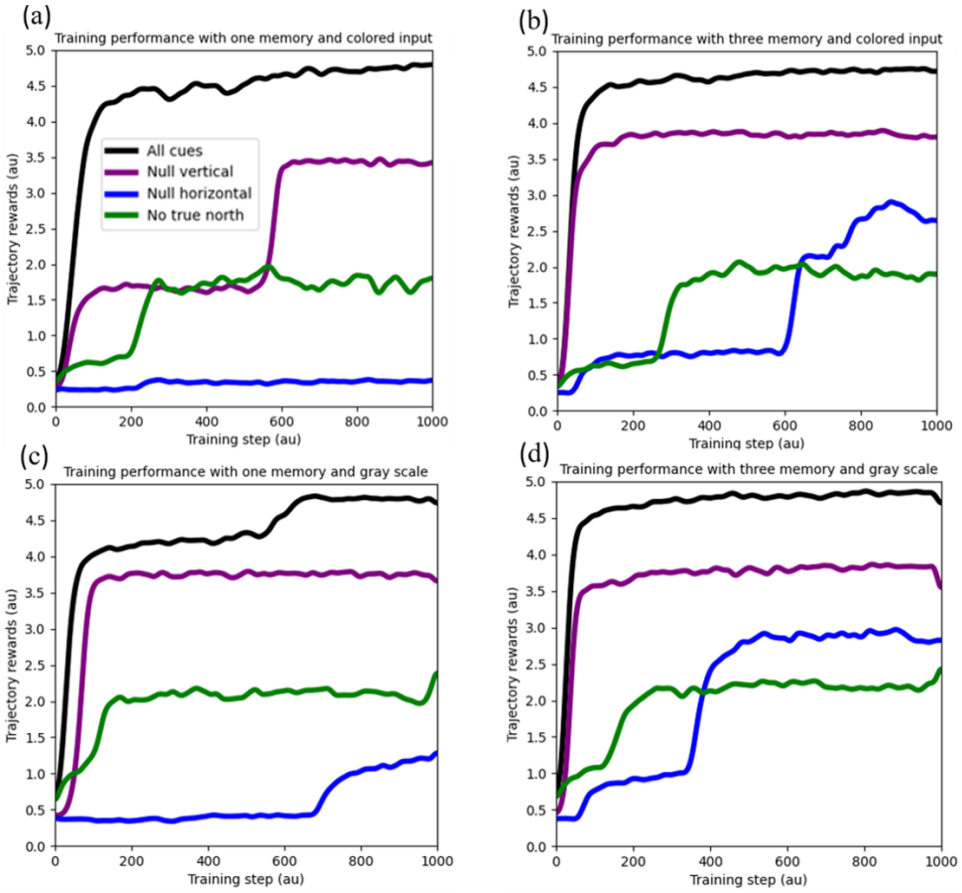

Fig. 5.4: Effect of the cue availability on the navigational performance; this is done for different memory sizes and input format. In all graphs, the black plot is the performance with all cues available, the purple is in the absence of vertical field sense, the green plot is in the absence of horizontal field sense and the blue plot is in the absence of a true north. Also, the graphs show the performance achieved with **(a)** memory length of one and chromatic input. **(b)** memory length of three and chromatic input. **(c)** memory length of one and gray scale input. **(d)** memory length of 3 and gray scale input. All plots are achieved by smoothing scatter plots with a Gaussian filter having a standard deviation of ten.

input and the memory length of the observation. For the chromatic content, it is seen that the RGB and gray-scale inputs show qualitatively similar results. This emphasizes the invariance of the model to irrelevant features. While for the memory length, it was employed to test for the effect of the magnetic field gradient on navigation. It was thought that, more than one observation is needed to measure the direction and magnitude of the change in the magnetic field. Comparing the left and right graphs, the effect of having a memory length of three is comparable to the one case. There is a slight increase is performance, and initially, this questions the significance of the magnetic field gradient in learning navigation. However, as seen below, magnetic field gradients have an effect under a different context.

5.3.2 Effect of magnetic field gradient and the magnetic field sensor sensitivity

In this subsection, some of the parameters that affect the learning performance are discussed. These include the visual acuity and the magnetic field gradient in the horizontal. For the visual acuity, the model parameter used is the observation/input image size in pixels. The lower the input size, the lower the resolution, and this artificially mimics lower visual acuity. The effect of these two parameters on the navigation performance is show in Fig. 5.5.

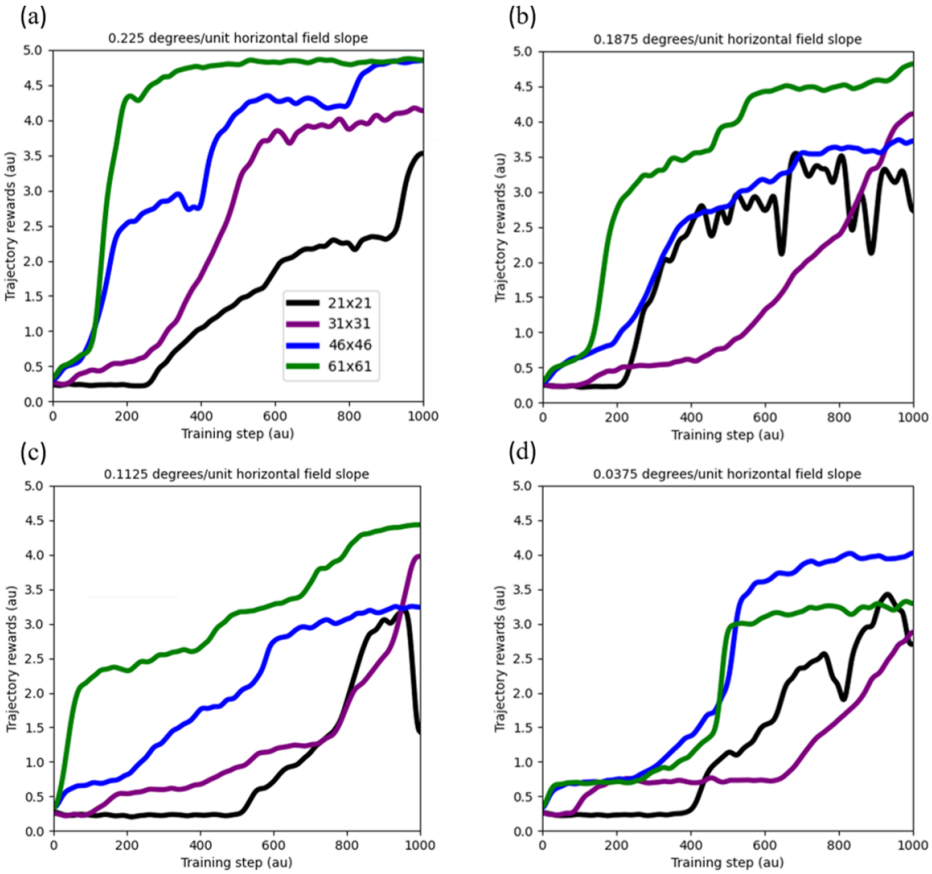

Fig. 5.5: Effect of the field gradients and visual acuity on the navigational performance. This is performed with gray scale input and a memory size of three. In all graphs, the black plot is the navigational performance with input size 21x21 pixels, the purple is 31x31 pixels, the blue is 46x46 pixels and the green is 61x61 pixels. Also, the graphs show the performance achieved with a horizontal field slope of **(a)** 0.225 degrees/unit. **(b)** 0.1875 degrees/unit. **(c)** 0.1125 degrees/unit. **(d)** 0.0375 degrees/unit. All plots are achieved by smoothing scatter plots with a Gaussian filter having a standard deviation of ten.

It can be seen that the performance decreases with decreasing the visual acuity. For visual navigation, the visual acuity puts a fundamental lower limit on learning. Visual acuity depends on several parameters; these include the head size and the photoreceptors

density. According to this, it is expected that migratory birds with larger head sizes and dense photoreceptors to perform better in navigational strategies. Also, as can be seen from the figures, the navigational performance decreases with smaller magnetic field gradients. The shallower the gradients the harder it is to discern the changes in field direction. There is an interdependence between the visual acuity and the magnetic field gradient. This stems from the fact that higher visual acuity is needed to resolve smaller changes in the declination angle as the bird moves in the longitudinal direction.

It should be noted that, the gradients affect the learning phase or the training performance. However, once trained the bird model can navigate in shallower gradients, this was seen by decreasing the migratory step size, which mimics a decrease in the gradient value. The decrease in the step size had negligible effect on the homing performance.

5.3.3 Periodic environments

Real magnetic fields have areas where is the field is not unique. This increases the difficulty of navigation due to the ambiguity of the extracted information from these areas. Here, we went to the extreme and modeled non-uniqueness by periodic environments, where no location is unique. The results are shown in Fig. 5.6. These environments were constructed by independent cosine functions for both the inclination and declination. The inclination varies between -45° and 45°, while the declination between 0° and 90°. The spatial frequency values used for the simulations range between $2.5e^{-3}$ to $2.0e^{-2}$. The larger the spatial frequency the more periodicity an environment can possess.

Generally speaking, the higher the spatial frequency the lower the performance. This is due to the ambiguity in the observed states. Since the states are redundant and the actions are the same in every state, assigning a value to the state-action pair is a difficult task. For example, if the bird is in the left half of the training area, the action right should have higher value than left. However, this same state can be also found the on right half but there, the action values are swapped. One of the ways that the bird utilizes to overcome such a hurdle is reaching a zone with unique declination states; this is marked by the dashed black box in Fig. 5.6c. Once in this zone, the bird follows the unique migratory corridor to the goal. A question still exists about how the bird model can reach the corridor in the first place. Analyzing this is not a trivial task and one solution is the bird counts the number of steps (time) to change a particular state and rotates if the desired outcome is not reached. This can be seen from the curved paths at the beginning of a trajectory.

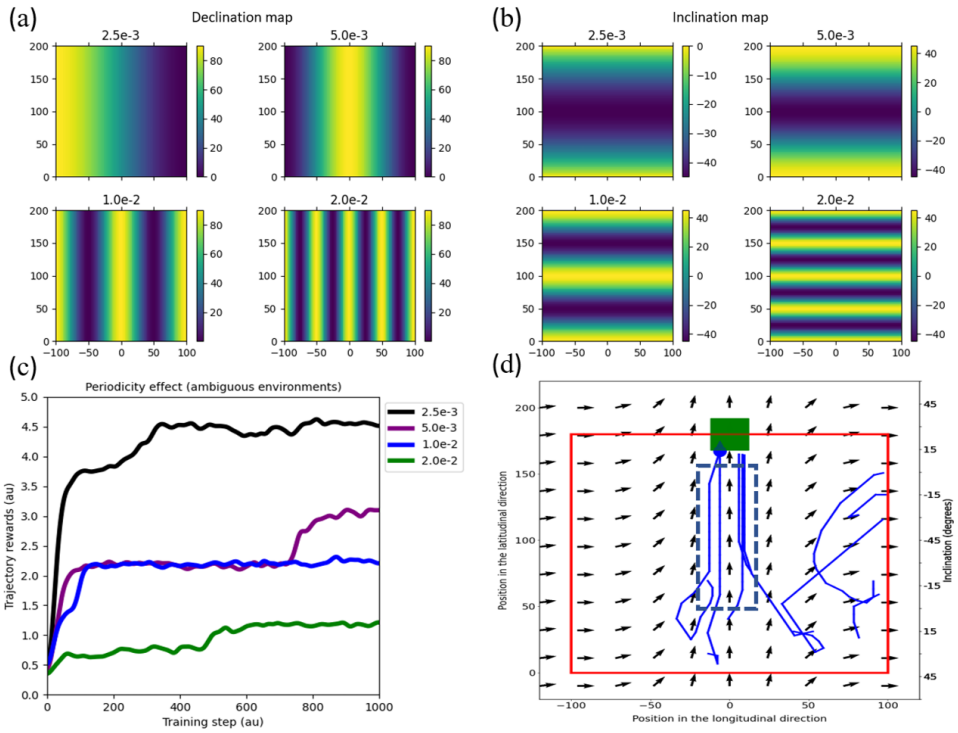

Fig. 5.6: Effect of the spatial periodicity on the navigational performance. This is achieved by independent sinusoidal functions for the inclination and declination. **(a)** & **(b)** density maps with the employed spatial frequencies for the declination and inclination respectively. **(c)** the effect of the spatial frequency on performance. **(d)** trajectories of the bird post training in the 5.0e-3 environment. This study uses the best performing model (61x61 pixels gray scale inputs and a memory size of 3). All performance plots are achieved by smoothing scatter plots with a Gaussian filter having a standard deviation of ten.

5.3.4 Magnetic anomalies

A related but less abstract study compared to the periodic environments is the effect of magnetic anomalies (MA) on the navigational capabilities. MA are called as such because they break the predictable and smooth variation in the magnetic field isolines and their related gradients. They arise because of the magnetic properties of the Earth's crust, where areas rich in magnetized minerals would produce stronger anomalies than less mineral-rich areas. A demonstration of the MA effects on the navigational trajectories are shown in Fig. 5.7.

In this figure, it is shown the trajectories of birds/agents trained then tested in different environments. A bird trained in a no-anomaly environment then tested in an environment with positive anomalies, would perceive the goal location as shifted to the right as shown in Fig. 5.7a. The bird stays in this slanted trajectory until it is out of the anomaly field. However, as demonstrated in Fig. 5.7b to 7d, this slanted trajectory is not observed when the bird is pre-trained in an anomaly environment before testing it in different anomaly environments. In these cases, the bird learns to accommodate for the

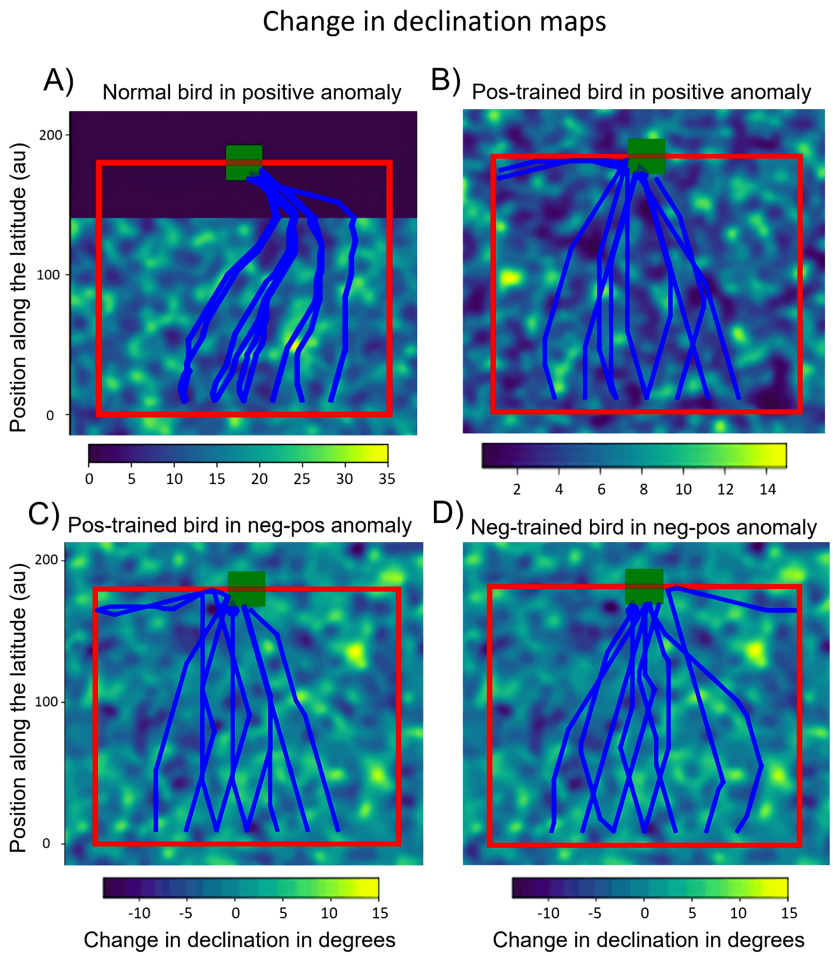

Fig. 5.7: The effect of declination anomalies on trajectories. **(a)** a bird trained in a normal (no anomalies) environment then tested in a positive anomaly field. A bird trained in a positive anomaly field then tested in another **(b)** positive and **(c)** negative anomaly fields. **(d)** a bird trained in a negative anomaly field then tested in a negative one. Here positive and negative symbolize the change in declination in degrees relative to the local field.

variations in the magnetic field leading to converging, albeit a little ragged, trajectories to the goal.

It is observed that there are few outliers in the trajectories. Regardless, the divergence of these trajectory happen too near to the goal, where in real scenarios this wouldn't happen as birds would have more profound local shot-range cues for guidance like landmarks. Also, the approach to the goal in these outliers are from the side which is a rare case in north-south migrants, where the approach is along the north-south axis. Finally, it should be noted that one part of the reasons for this study was the claim made by Hagstrum, 2023; that the total geomagnetic field (GMF) is not suitable for bi-coordinate navigation due to the anomalies. However, this claim was based on an inclination-intensity map and not inclination-declination map. It is also stated that the international geomagnetic reference field (IGRF) is a good representation for the GMF vector field direction. Hence,

our model for navigation (based on inclination-declination) should be least affected by anomalies, which is the case.

5.3.5 Novel and emergent properties

Novel routes

In this work, novel routes refer to the new behavioral strategies undertaken by the model animal to solve a particular task in the learning phase. These is achieved within artificial environments which are not normally or commonly encountered in real scenarios, but can be constructed in a simulation or by an experiment. In this regard and as shown in Fig. 5.8, a bird learning navigation in an artificial environment will produce the shown trajectories. This environment is achieved by the removal of the horizontal component of the magnetic field and hence no declination sense.

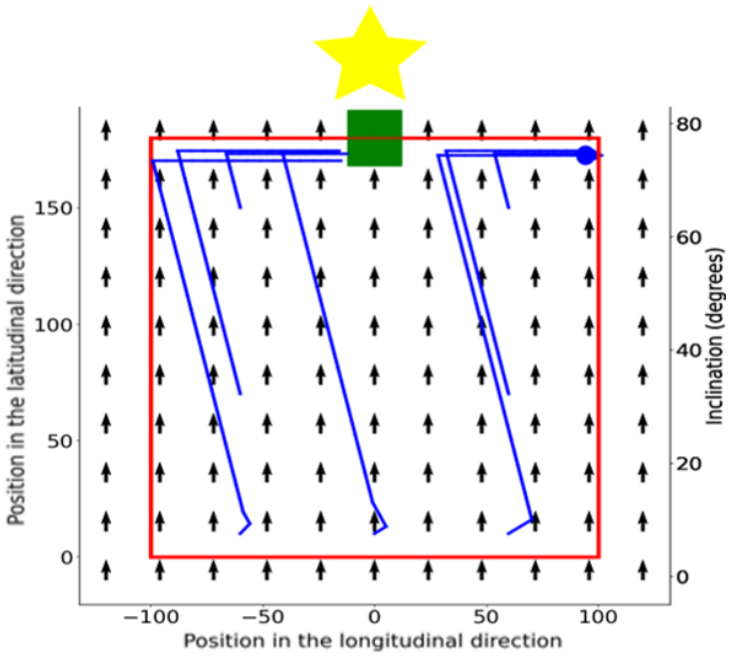

Fig. 5.8: The trajectories of a bird which learns to solve the navigational problem in the absence of a horizontal field (no declination sense). The training and test environments are the same.

The birds learned a novel strategy of navigation; it moves in an inclined straight line followed by a rightward horizontal movement. Why this happens, can be illuminated by two observations: i) since there is no declination sense, one strategy to solve this problem is for the bird to move straight upward till the target inclination and move left or right. This strategy has a 50% chance of success. ii) a slopped trajectory can increase those chances. Thus, through learning, the bird model increases this chance by moving in inclined paths compared to the vertical. Hence, even if the bird is spawned on the right,

it can still reach its target. This demonstrates the power of studying behavior through learning algorithms. Here, the model bird solves the navigation problem in a way that might not be immediately available to a human observer. Both the environment and bird models are simple, but with more complex models, the probability of different novel behavior increases.

Curved trajectories

In the novel routes subsection, it was shown that a bird model trained in a new and unfamiliar environment can solve the navigational problem given that the environment has sufficient information for the task. This was one case of the effect of the environment on the emergent behavior. Another case is when the bird is trained in one environment then tested in another. In this regard, it would be expected that, from an observer point of view, birds would behave differently in the new environment; that being, they take different trajectories. Although, from the birds point of view, they are behaving as they learned. The results of these observations are shown in Fig. 5.9. Where training a bird in one environment, then testing in another can lead to curved trajectories which are proponent to the straight paths one can expect in true navigational behavior.

Curved trajectories are an emergent property that arises when birds are trained then tested in different magnetic field environments. The cases shown demonstrates the effect of the horizontal field gradients on the navigational path. A bird trained in a constant gradient environment and tested on the same environment will take straight goal-directed trajectories as shown in Fig. 5.9a. While, shown in Fig. 5.9b is the same bird tested in a nonlinear gradient environment. The opposite is done for the bottom figures. Fig. 5.9c shows a bird trained in a nonlinear environment and tested in constant one, while Fig. 5.9d shows the same bird tested in the nonlinear environment. This nonlinear gradient is achieved by a simple power low dependence between the angle of the horizontal field and the location on the longitudinal axis and is described by equation (5.6).

$$\varphi(x, y) = \frac{-90(200 + x)^{z(y)}}{400^{z(y)}} + 270 \tag{5.6}$$

In this equation, $\varphi(x, y)$ is the angle of the magnetic field in the horizontal, x is the position in the longitudinal axis, y is the position in the latitudinal axis and z is the applied power. However, the change in z with y is not continuous but discrete and has its values in the range $[0.5, 1]$ with a step size of 0.03 for every ten units in the range $[0, 180]$.

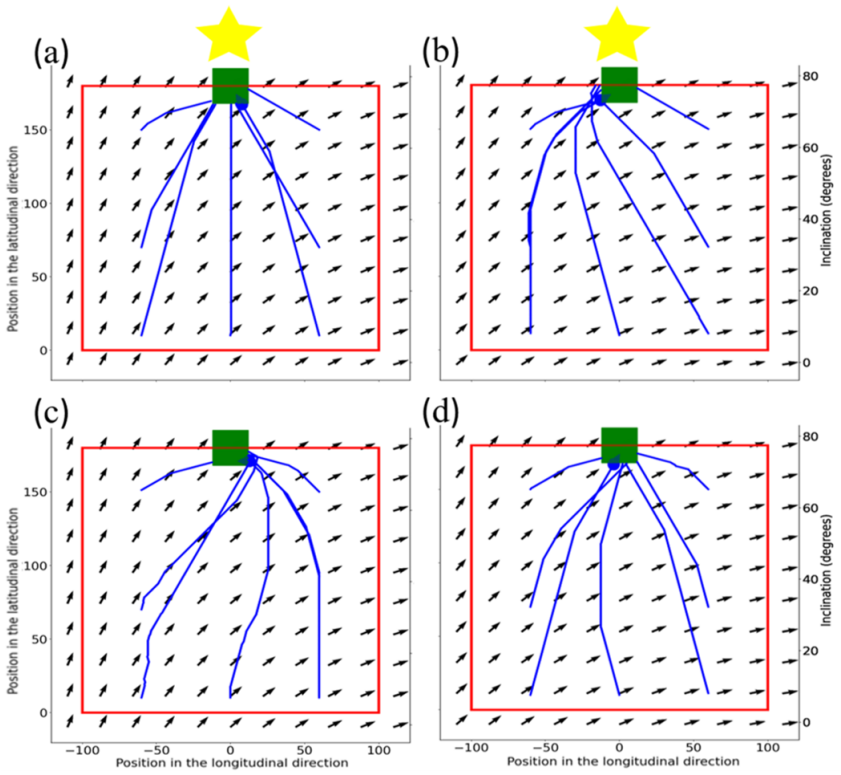

Fig. 5.9: Effect of the horizontal field gradients on the navigational trajectories. The figure shows a bird trained in a constant gradient environment then tested in **(a)** constant gradient (the same environment as the training one) and **(b)** changing gradient environments. Also shown, another bird trained in a changing gradient environment then tested in **(c)** constant gradient and **(d)** changing gradient environments (the same environment as the training one).

Extrapolation

The bird model shows extrapolation behavior outside the training area as shown in Fig. 5.10. The training for this model was performed in a noisy environment, where the visual field input is noisy and not complete. This can mimic the field observation at night, since the stars form a point-like light sources. These sources excite a small subset of the photoreceptors, which lead to the noisy input. Also, in the training of this input, there was uncertainty in the observed magnetic field angle in the horizontal. Namely, at each time step the magnetic field angle is sampled from a normal distribution having the mean equating to the true angle and a standard deviation of two degrees. For comparison, testing a normally trained model (the black curve in Fig. 5.4a) leads to states where the agent gets stuck and hence doesn't move. Also, when not stuck, the normally trained model performs worse than the noisy model. This emphasizes the important role of uncertainty in improving generalization.

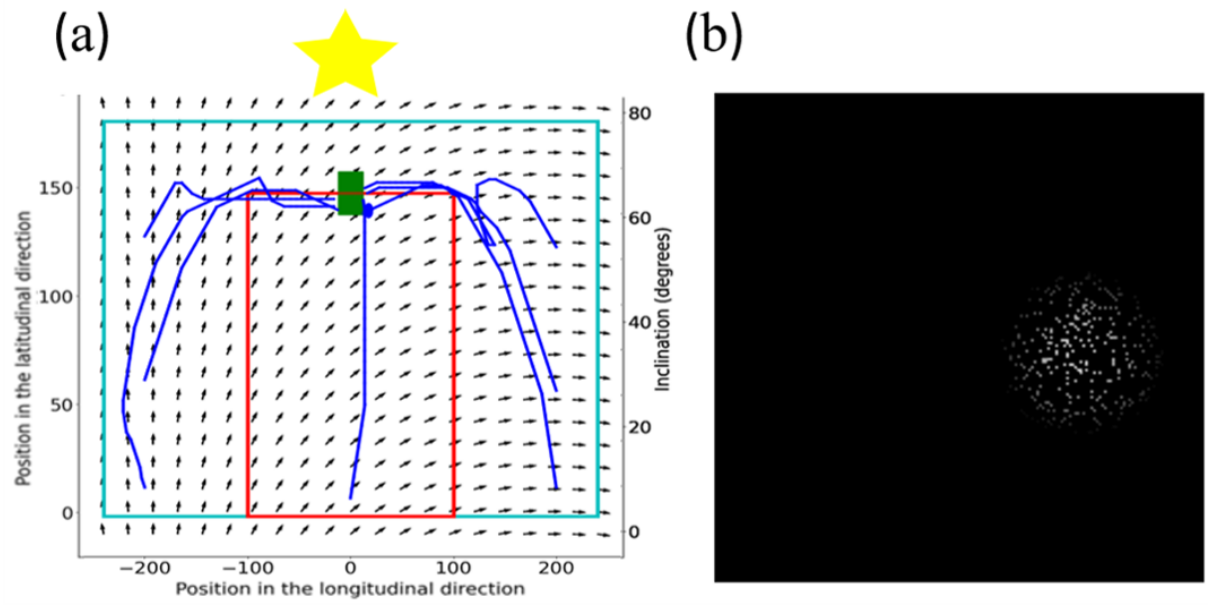

Fig. 5.10: Extrapolation with noisy observations. **(a)** the bird model shows extrapolation capabilities in between the training area (red box) and the test area (cyan box). **(b)** a high resolution version of the noisy magnetic field observation when the bird is at position (0, 10) and looking north.

5.3.6 General discussion

The discussion so far have not touched the observation that the ophthalmic nerve of trigeminal nerve, which innervates the upper beak, mediates magnetic field information [Heyers et al., 2010]. The encoded information is thought to be intensity and might form a component of the multi-factorial map [Wiltschko and Wiltschko, 2013]. Regardless, as seen in the simulations, it is evident that one cue/coordinate is not sufficient for reliable navigation. Two gradient fields are needed for navigation and one can be the inclination angle gradient. Recent studies have shown that birds use inclination as a sign/stop post [Wynn et al., 2022]. Besides, inclination information is readily available from the magnetic compass, so there is supporting evidence that inclination is one of the coordinates. The other coordinate can include declination, intensity or a combination of magnetic cues. Regarding declination, studies have shown that birds can correct for declination [Chernetsov et al., 2017] and it is an ingredient in true navigation [Kishkinev et al., 2021]. Also, birds don't correct for displacements when there is no access to celestial cues[Pakhomov et al., 2018].

Thus, we have two systems (eye and upper peak) and three cues, how can this all be connected? Here, we propose two scenarios. One, the visual navigation system and the upper beak system work at various spatial scales, with the upper beak system taking priority. Hence, when it is impaired, it inhibits the map sense. Two, all magnetic information is needed for true navigation, with the declination and inclination provided

by the visual system and the intensity by the beak system. There is evidence that all cues are needed [Kishkinev et al., 2021]. Although, the current study showed that the visual compass is sufficient for navigation, it is not clear what modulatory effect intensity (assuming it is the information encoded by the ophthalmic branch) might have on the navigational performance. However, it is clear that this information is necessary for navigation. Also, the information from the visual system is necessary for magnetic navigation. This assertion can be supported by the fixed direction response of migratory birds under certain light conditions [Wiltschko et al., 2010].

There is a philosophical argument for a visual navigation theory based on declination and inclination. Evolution is an optimization algorithm. Hence, it is expected that minimizing energy consumption is a major goal that is necessary for survival. A neural network with many layers and parameters would consume more energy than a smaller network. In this regard, a map system that uses two or more sensory inputs to determine location would consume more energy than a system that uses one sensory mechanism. With this observation, sensing the declination and inclination with the same sensory system is advantageous computationally and energy wise. If the map coordinates are sensed by multiple sensory systems, then multiple representational transformations are needed to reach a common scaffold representation upon which decisions can be made. These representational transformations are computationally and energy demanding. Hence, it is preferable to have unified system for the map sense. This argument can be summed up by the Occam's Razor principal.

Finally, although the Wang et al., 2006 is utilized because it is a classic study, any modulation pattern can be used given that it doesn't have a rotational symmetry in the declination and inclination axis. For example, a modulation pattern that is a ribbon spanning the east-west axis in the whole retinal view would provide no declination information. Also, aside from declination and inclination, pairs of cues that are linearly independent can be used for bi-coordinate navigation. These cues need to have large enough gradients to allow navigation and the bird needs to be able to sense them with the required accuracy for a navigational task.

5.4 Summary and predictions

5.4.1 Summary

Given the high visual acuity of migratory birds, the visual system can act as a map system. For reliable bi-coordinate navigation using this system, the declination angle and the true north are the most important parameters for navigation. There is interde-

pendence between the visual acuity and the magnetic field gradients, where very shallow gradients need high visual acuity for learning. Decreasing the visual acuity leads to worse navigational performance. In a similar manner to shallow gradients, ambiguous magnetic field information leads to degrading navigational performance. Taken together, unique and large gradients are needed for reliable learning. In addition, the simulations with RL showed that the bird model can find solutions in periodic environments and perform reliable navigation in an anomaly-ridden one.

The learning model also showed interesting behavior when trained and/or tested in unfamiliar environments. In a uni-coordinate environment the bird model solved the navigational problem with a unique strategy where it used the inclination value as a stop sign. Training and testing in different environments lead to different initial orientations and trajectories. This is very pronounced when training is performed in a linear gradient environment then tested in a nonlinear one. Finally, uncertainty can dramatically improve the generalization performance by extrapolating outside the training area.

5.4.2 Prediction one: minimum learning area

Based on the visual navigation hypothesis and the presented simulations, one can qualitatively deduce the existence of a minimum learning area. Within this learning area, the change in the magnetic field parameters and birds biological capabilities are not sufficient for learning navigation. These capabilities include the memory, visual acuity and the nature of the modulation pattern.

Since navigation is a behavior learned though experience, the minimum learning area hypothesis can test for the relevant cues for navigation. For example, the minimum learning area can test for whether the birds use an inclination/declination gird or an inclination/intensity grid.

5.4.3 Prediction two: departure direction

Two birds trained in two environments with different magnetic field gradients will show different initial orientations when tested in a new environment with a different gradient. Also, if the gradients are nonlinear, these birds will have different trajectories with different curvatures when pursing a migratory path.

Acknowledgments

This work was supported by the Deutsche Forschungsgemeinschaft (DFG). Also, we thank the Molecular Sensory Biology (MSB) research training group of the University of Old-

enburg for their support, discussions and insights.

Chapter 6

Synthesis and conclusion

The magnetic pulse pre-treatment of animals is the single most important manipulation technique used in magnetic orientation experiments testing for the involvement of magnetic particles. However no satisfying theory exists yet to predict pulse effects systematically. Therefore, a key aim of this thesis was to develop a theoretical framework to model a magnetic pulse at the neuronal level. The objective of that approach was to first find out what model assumptions are critical for obtaining pulse effects on the neuronal output and then to make new predictions to be tested in a refined behavioral experiment. In brief, the magnetosensory cortex was assumed to be topographically organized, where the preferential magnetic field angle for firing varies systematically over adjacent neurons and thus covers all possible magnetic field directions. At the level of the receptor cells in the periphery, the preferential directional excitability is assumed to be due to a given orientation of the magnetic dipole moment of the magnetic sensory organelle. The latter in turn is the physical substrate on which the magnetic field and the pulse act, and which is described by a physical equation for the transduction mechanism. Here, two possibilities were considered: torque detection or variance detection, each one translating the field input into a different sensory output. The interaction of the cortical cells was described with the neuronal field model. The output of this network was fed in a head-direction network to relate the perceived magnetic field direction to the head orientation of the bird, telling the bird where magnetic North is in terms of its head direction. Then a pulse is applied simultaneously to each cell in silico, which results in differential effects, integrated at the level of the network to output the perceived magnetic field direction.

It turns out that the simulated pulse has an effect on the network output only when the underlying magnetic field detection is based on magnetic torque, but not on variance detection. This provides an important constraint on the detection mechanism and shows the benefit of the modeling approach. The modeled pulse effects include: eastward deflection, westward deflection, bimodality, and even no effect. This broad range of effects

is in agreement with what has been observed experimentally. Apart from the directional network, a network that is based on translating the sensed magnetic field intensity to direction is introduced. This model is called the 'Maximum-intensity' model, because the true field direction is in alignment with the maximum magnetic field intensity. Like the directional model, the maximum-intensity model was also able to reproduce, within its assumptions, the pulse effects seen experimentally. In addition, this model also uses the torque model, which demonstrates the generalizing power of that mechano-transduction model. Aside from the similarity between the presented results and experimental literature, some predictions are offered that might aid in unearthing the nature of the elusive magnetite-based receptor. A key prediction is that a 270° pulse would lead to no change in orientation, provided that the topographic organization of the receptive fields at the cortex level is counterclockwise in terms of preferential magnetic directions. Similarly, for a clockwise organization, 90° pulse would be neutral in terms of network output. Further, to find out if the pulse has a damaging effect or just a remagnetizing effect, a new type of pulse pre-treatment is suggested, where a pulse is administered first in one direction and subsequently in the opposite direction, before the actual orientation tests are conducted. The outcomes of simulated double pulse experiments are summarized in a table together with the type of networks that would produce such results.

Regarding the affected navigational system, the results can be interpreted in terms of a perturbation of a compass sense or a map sense. This is the case because, in essence, the networks measure direction, which can be used not only in a compass, but also in a map when coupled with true North as geographic reference for declination. Although the most popular interpretation of pulse effects is in terms of the magnetic map, there is still the puzzling phenomenon of altered orientations in birds when pulsed and tested indoors. But how can a bird determine location indoors from magnetic field readings only? There is no satisfying answer yet to this problem, which has led some to argue that the behavior after pulsing is more akin to a perturbation of a compass mechanism, which in an indoor setting cannot be disambiguated from a perturbation of a map. Therefore, to test the predictions made here, birds should be tested in orientation funnels placed outdoors with a view to the sky, in order to have the appropriate setting for a map experiment.

While the inclination compass is innate, the map is acquired by experience. This begs the question if inclination compass readings, connected with geographic information during the map acquisition phase, could act as the basis of a cognitive magnetic map. This has led to the second study, focusing on the navigation problem, asking specifically if the detection of declination and inclination angles is sufficient for goal based navigation. Without loss of generality, the magnetic field perception process here is modeled as visual modulation pattern, as has been suggested for the radical-pair based inclination compass

sense earlier. That pattern, which is concentric about the axial direction of the magnetic field in space, has all the information necessary to detect both inclination and declination when combined with visual information about the horizon and true North. To test the potential of the inclination compass for navigation, we modeled an in silico bird equipped with inclination compass and star compass, and trained and tested this "navigational agent" in a simulated environment with systematically varying magnetic gradients. The approach utilized here is relatively novel as it bypasses the need to hard code the agent's actions, but rather allows the agent to learn the correct behavior through the framework of reinforcement learning. Put differently, the correct behavior was not encoded in the model birds, who instead learned the correct behavior from interactions with the environment. During training, the only cues available are the true North and the magnetic field, ie., the declination and inclination. The agent (bird model) was a neural network that extracted from visual input (position of "North star" and magnetic-field modulation pattern) the necessary information about true North and the orientation of the magnetic field axis in space, from which it produced actions that would lead it to the desired destination.

After training, the bird model showed real navigation capabilities, like reorientation after displacements. We also demonstrated that certain cues are more important than others for navigation. True north is the most important cue, while the inclination angle is the least important. Then, we showed that navigation is affected by the visual acuity and the magnetic field gradients, with lower acuity and shallower gradients leading to a decrease in the navigational performance. Thus learning of map-like navigation requires a sufficiently large region, the size of which depends inversely on the steepness of the local gradients and the visual acuity. In addition to these systematic studies, we demonstrated an effect of spatial ambiguity in the magnetic field distribution on the performance. The higher the spatial periodicity (ambiguity), the lower the performance. As a follow up, we studied of navigation in presence of local magnetic anomalies superimposed on the smooth regional gradient. It was shown that birds trained in smooth gradient only would follow slanted trajectories when tested in an anomaly-ridden environment. Conversely, birds trained in environments with varying degrees of anomaly sizes would be less susceptible to misorientation and follow directed, albeit ragged, trajectories to the goal, which again demonstrates that the environment shapes the behavior. Lastly, we ended these studies with a series of simulations showing the power of RL, starting with i) novel routes, where the bird model, unexpectedly, solved a difficult navigational problem. Ii) curved trajectories, where we showed that the nature of the training environments affects the observed behavior in new environments. Iii) extrapolation, where we demonstrated the ability of the model to reach the target area even if placed outside the training area, and the placement can be far away (half the width of the training area). Besides the study

findings, predictions were offered to aid future experimentation, such as behavioral studies to investigate the minimum learning area. This invites studies where new hatchings are raised and trained within certain geographic limits and tested for navigational capabilities at adulthood, while systematically varying the limits to test for the critical learning area as a function of the local gradients. Another, albeit specific prediction is that two birds raised and trained in two different magnetic field gradients will demonstrate different navigational orientation when tested in a third gradient.

Finally, it should be stressed again that a compass sense can act as a map sense given the nature of the visual modulation pattern, as shown in this work. There is no denying that a magnetite receptor, most likely to be mediated by the trigeminal nerve, has an important function in the map sense, and that the visual system encapsulates a magnetic compass sense. However, we argue that the two receptor pathways should not be considered as two systems independent of each other. Under varying conditions, both can influence and get influenced by the other. As shown in this study, the retina-based inclination compass system, when coupled to other sources of spatial and directional information provided by the visual system, appears to be an excellent basis for a navigational system. Moreover, the magnetite system can work as both map and compass in theory. With these two observations, it is reasonable to assume that the inclination compass and magnetite system can complement or even augment each other so that there is the possibility that disturbing one disturbs both, which ultimately depends on the neural wiring, i.e. on synaptic connections between the two pathways in high-level integration centers. For example, the two systems would complement each other when working at different spatial scales or when detecting different quantities of the local magnetic field vector, which would help to disambiguate the magnetic field polarity to which the inclination compass is blind, and similarly for the equator. Also, it is known that the inclination compass needs to be calibrated at sunset before departure. If the sun is not available, then the magnetite system could provide the direction for calibration of the inclination compass. Since navigation is essential for survival, it make good biological sense to have a backup from a redundant system. Summing up the above points, there might be some ambiguity regarding the precise role of the trigeminally-mediated system and the visual compass. All of this discussion and work questions the following prevailing notion that both systems are isolated from each other, each with a singular function. Finally, it should be noted that birds are opportunistic (and have to be so to survive!) so they use every cue they can, with all senses wide open. Provided they have the neuronal wiring, they will integrate it all and then weigh the different pieces of evidence in the process of decision-making before resuming their journey.

The work in this thesis can be followed up in various ways. Regarding the first study, a

network model could be designed that unifies the deflection and bimodality behaviors. Till now, both these behaviors arise in different networks under different assumptions. This unification can be achieved with different network models and/or input functions. For the second study, a possible upgrade would consist in a more sophisticated environment with more cues available, which would invite studies of conflict-of-cue situations. Also, a second sensor mimicking the magnetite system could be included in the model to test if there is a performance gain due to mutual augmentation of the two.

Chapter 7

Bibliography

Able, K. P. and Able, M. A. Calibration of the magnetic compass of a migratory bird by celestial rotation. *Nature*, 347:378–80, 1990. doi:https://doi.org/10.1038/347378a0.

Able, K. P. and Able, M. A. Daytime calibration of magnetic orientation in a migratory bird requires a view of skylight polarization. *Nature*, 364:523–5, 1993. doi:https://doi.org/10.1038/364523a0.

Banino, A., Barry, C., Uria, B., Blundell, C., Lillicrap, T., Mirowski, P., Pritzel, A., Chadwick, M. J., Degris, T., Modayil, J., and others. Vector-based navigation using grid-like representations in artificial agents. *Nature*, 557:429–33, 2018. doi:https://doi.org/10.1038/s41586-018-0102-6.

Beason, R., Dussourd, N., and Deutschlander, M. Behavioural evidence for the use of magnetic material in magnetoreception by a migratory bird. *J. Exp. Biol.*, 198:141–46, 1995. doi:https://doi.org/10.1242/jeb.198.1.141.

Beason, R., Wiltschko, R., and Wiltschko, W. Pigeon homing: Effects of magnetic pulses on initial orientation. *The Auk*, 114:405–15, 1997. doi:https://doi.org/10.2307/4089242.

Beason, R. C. and Semm, P. Magnetic responses of the trigeminal nerve system of the bobolink (dolichonyx oryzivorus). *Neurosci. Lett.*, 80:229–34, 1987. doi:https://doi.org/10.1016/0304-3940(87)90659-8.

Beason, R. C. and Semm, P. Does the avian ophthalmic nerve carry magnetic navigational information? *J. Exp. Biol.*, 199:1241–4, 1996. doi:https://doi.org/10.1242/jeb.199.5.1241.

Ben-Yishai, R., Bar-Or, R., and Sompolinsky, H. Theory of orientation tuning in visual cortex. *Proc. Natl. Acad. Sci. USA*, 92:3844–48, 1995. doi:https://doi.org/10.1016/0042-6989(94)90308-5.

Ben-Yishay, E., Krivoruchko, K., Ron, S., Ulanovsky, N., Derdikman, D., and Gutfreund, Y. Head-direction coding in the hippocampal formation of birds. *BioRxiv*, 2020. doi:https://doi.org/10.1101/2020.08.31.274928.

Benhamou, S. Bicoordinate navigation based on non-orthogonal gradient fields. *J. Theor. Biol.*, 225:235–39, 2003. doi:https://doi.org/10.1016/S0022-5193(03)00242-X.

Berlemont, K., Martin, J.-R., Sackur, J., and Nadal, J.-P. Nonlinear neural network dynamics accounts for human confidence in a sequence of perceptual decisions. *Sci. Rep.*, 10:7940, 2020. doi:https://doi.org/10.1038/s41598-020-63582-8.

Berthold, P. Evolutionary aspects of migratory behavior in european warblers. *J. Evol. Biol.*, 1:195–209, 1988. doi:https://doi.org/10.1046/j.1420-9101.1998.1030195.x.

Best, E. N. Null space in the hodgkin-huxley equations. a critical test. *Biophys. J.*, 27: 87–104, 1979. doi:https://doi.org/10.1016/S0006-3495(79)85204-2.

Bingman, V. P. Magnetic field orientation of migratory savannah sparrows with different first summer experience. *Behaviour*, 87:43–51, 1983. doi:https://doi.org/10.1163/156853983X00110.

Blakemore, R. Magnetotactic bacteria. *Science*, 190:377–79, 1975. doi:https://doi.org/10.1126/science.170679.

Blaser, N., Guskov, S. I., Meskenaite, V., Kanevskyi, V. A., and Lipp, H.-P. Altered orientation and flight paths of pigeons reared on gravity anomalies: A gps tracking study. *PLOS one*, 8:e77102, 2013. doi:https://doi.org/10.1371/journal.pone.0077102.

Blaser, N., Guskov, S. I., Entin, V. A., Wolfer, D. P., Kanevskyi, V. A., and Lipp, H.-P. Gravity anomalies without geomagnetic disturbances interfere with pigeon homing – a gps tracking study. *J. Exp. Biol.*, 217:4057–67, 2014. doi:https://doi.org/10.1242/jeb.108670.

Cadieu, C. F., Hong, H., Yamins, D. L. K., Pinto, N., Ardila, D., Solomon, E. A., Majaj, N. J., and DiCarlo, J. J. Deep neural networks rival the representation of primate it cortex for core visual object recognition. *PLoS Comput. Biol.*, 10:e1003963, 2014. doi:https://doi.org/10.1371/journal.pcbi.1003963.

Chernetsov, N. Orientation and navigation of migrating birds. *Biol. Bull.*, 43:788–803, 2016. doi:https://doi.org/10.1134/S1062359016080069.

Chernetsov, N., Kishkinev, D., and Mouritsen, H. A long-distance avian migrant compensates for longitudinal displacement during spring migration. *Curr. Biol.*, 18:188–90, 2008. doi:https://doi.org/10.1016/j.cub.2008.01.018Get.

Chernetsov, N., Pakhomov, A., Kobylkov, D., Kishkinev, D., Holland, R. A., and Mouritsen, H. Migratory eurasian reed warblers can use magnetic declination to solve the longitude problem. *Curr. Biol.*, 27:2647–51, 2017. doi:https://doi.org/10.1016/j.cub.2017.07.024.

Cichy, R. M., Khosla, A., Pantazis, D., Torralba, A., and Oliva, A. Comparison of deep neural networks to spatio-temporal cortical dynamics of human visual object recognition reveals hierarchical correspondence. *Sci. Rep.*, 10:27755, 2016. doi:https://doi.org/10.1038/srep27755.

Colombo, M. and Broadbent, N. Is the avian hippocampus a functional homologue of the mammalian hippocampus? *Neurosci. Biobehav. Rev.*, 24:465–84, 2000. doi:https://doi.org/10.1016/S0149-7634(00)00016-6.

Curdt, F., Haase, K., Ziegenbalg, L., Greb, H., Heyers, D., and Winklhofer, M. Prussian blue technique is prone to yield false negative results in magnetoreception research. *Sci. Rep.*, 12(8803), 2022. doi:https://doi.org/10.1038/s41598-022-12398-9.

Davila, A. F., Fleissner, G., .Winklhofer, M., and Petersen, N. A new model for a magnetoreceptor in homing pigeons based on interacting clusters of superparamagnetic magnetite. *Phys. Chem. Earth*, 28:647–52, 2003. doi:https://doi.org/10.1016/S1474-7065(03)00118-9.

Donner, K. O. The visual acuity of some passerine birds. *Societas pro fauna et flora Fennica*, 1951.

Engels, S., Schneider, N.-L., Lefeldt, N., Hein, C. M., Zapka, M., Michalik, A., Elbers, D., Kittel, A., Hore, P. J., and Mouritsen, H. Anthropogenic electromagnetic noise disrupts magnetic compass orientation in a migratory bird. *Nature*, 509:353–56, 2014. doi:https://doi.org/10.1038/nature13290.

Engels, S., Treiber, C. D., Salzer, M. C., Michalik, A., Ushakova, L., Keays, D. A., Mouritsen, H., and Heyers, D. Lidocaine is a nocebo treatment for trigeminally mediated magnetic orientation in birds. *J. R. Soc. Interface.*, 15:20180124, 2018. doi:https://doi.org/10.1038/nature11046.

Enquist, M., Lind, J., and Ghirlanda, S. The power of associative learning and the ontogeny of optimal behaviour. *R. Soc. Open Sci.*, 3:160734, 2016. doi:https://doi.org/10.1098/rsos.160734.

Ernst, D. A. and Lohmann, K. J. Effect of magnetic pulses on caribbean spiny lobsters: implications for magnetoreception. *J. Exp. Biol.*, 219:1827–32, 2016. doi:https://doi.org/10.1242/jeb.136036.

Fitak, R. R., Wheeler, B. R., and Johnsen, S. Effect of a magnetic pulse on orientation behavior in rainbow trout (*Oncorhynchus mykiss*). *Behav. Processes*, 172:104058, 2020. doi:https://doi.org/10.1016/j.beproc.2020.104058.

Fleissner, G., Holtkamp-Rötzler, E., Hanzlik, M., Winklhofer, M., Fleissner, G., Petersen, N., and Wiltschko, W. Ultrastructural analysis of a putative magnetoreceptor in the beak of homing pigeons. *J. Comp. Neurol.*, 458:350–60, 2003. doi:https://doi.org/10.1002/cne.10579.

Foster, J. J., Smolka, J., Nilsson, D.-E., and Dacke, M. How animals follow the stars. *Proc. R. Soc. B*, 285:20172322, 2017. doi:http://dx.doi.org/10.1098/rspb.2017.2322.

Frankel, R. B., Blakmore, R. P., and Wolfe, R. S. Magnetite in freshwater magnetotactic bacteria. *Science*, 203:1355–6, 1979. doi:https://doi.org/10.1126/science.203.4387.1355.

Frankenhuis, W. E., Panchanathan, K., and Barto, A. G. Enriching behavioral ecology with reinforcement learning methods. *Behav. Process.*, 161:94–100, 2019. doi:https://doi.org/10.1016/j.beproc.2018.01.008.

Freire, R., Dunston, E., Fowler, E. M., McKenzie, G. L., Quinn, C. T., and Michelsen, J. Conditioned response to a magnetic anomaly in the pekin duck (anas platyrhynchos domestica) involves the trigeminal nerve. *J. Exp. Biol.*, 215:2399–404, 2012. doi:https://doi.org/10.1242/jeb.068312.

Gagliardo, A., Bried, J., Lambardi, P., Luschi, P., Wikelski, M., and Bonadonna, F. Oceanic navigation in cory's shearwaters: evidence for a crucial role of olfactory cues for homing after displacement. *J. Exp. Biol.*, 216:2798–805, 2013. doi:https://doi.org/10.1242/jeb.085738.

Gershman, S. J. and Ölveczky, B. P. The neurobiology of deep reinforcement learning. *Curr. Biol.*, 30:R617–34, 2020. doi:https://doi.org/10.1016/j.cub.2020.04.021.

Greener, J. G., Kandathil, S. M., Moffat, L., and Jones, D. T. A guide to machine learning for biologists. *Nat. Rev. Mol. Cell. Biol.*, 23:40–55, 2022. doi:https://doi.org/10.1038/s41580-021-00407-0.

Guttman, R., Lewis, S., and Rinzel, J. Control of repetitive firing in squid axon membrane as a model for a neuroneoscillator. *J. Physiol.*, 305:377–95, 1980. doi:https://doi.org/10.1113/jphysiol.1980.sp013370.

Günther, A., Einwich, A., Sjulstok, E., Feederle, R., Bolte, P., Karl-WilhelmKoch, Solov'yov, I. A., and Mouritsen, H. Double-cone localization and seasonal expression pattern suggest a role in magnetoreception for european robin cryptochrome 4. *Curr. Biol.*, 28:211–23, 2018. doi:https://doi.org/10.1016/j.cub.2017.12.003.

Hagstrum, J. T. Infrasound and the avian navigational map. *J. Exp. Biol.*, 203:1103–11, 2000. doi:https://doi.org/10.1242/jeb.203.7.1103.

Hagstrum, J. T. Avian navigation: the geomagnetic field provides compass cues but not a bicoordinate "map" plus a brief discussion of the alternative infrasound direction-finding hypothesis. *J. Comp. Physiol.*, 2023. doi:https://doi.org/10.1007/s00359-023-01627-9.

Hanzlik, M., Heunemann, C., Holtkamp-Rötzler, E., Winklhofer, M., Petersen, N., and Fleissner, G. Superparamagnetic magnetite in the upper beak tissue of homing pigeons. *Biometals*, 13:325–31, 2000. doi:https://doi.org/10.1023/A:1009214526685.

Hein, C. M., Zapka, M., Heyers, D., Kutzschbauch, S., Schneider, N.-L., and Mouritsen, H. Night-migratory garden warblers can orient with their magnetic compass using the left, the right or both eyes. *J. R. Soc. Interface*, 7:S227–33, 2010. doi:https://doi.org/10.1098/rsif.2009.0376.focus.

Helbig, A. J. Inheritance of migratory direction in a bird species: a cross-breeding experiment with se- and sw-migrating blackcaps (sylvia atricapilla). *Behav. Ecol. Sociobiol.*, 28:9–12, 1991. doi:https://doi.org/10.1007/BF00172133.

Heyers, D., Elbers, D., Bulte, M., Bairlein, F., and Mouritsen, H. The magnetic map sense and its use in fine-tuning the migration programme of birds. *J. Comp. Physiol. A*, 203:491–97, 2017. doi:https://doi.org/10.1007/s00359-017-1164-x.

Heyers, D., Manns, M., Luksch, H., Güntürkün, O., and Mouritsen, H. A visual pathway links brain structures active during magnetic compass orientation in migratory birds. *PLoS One*, 2007. doi:https://doi.org/10.1371/journal.pone.0000937.

Heyers, D., Zapka, M., Hoffmeister, M., Wild, J. M., and Mouritsena, H. Magnetic field changes activate the trigeminal brainstem complex in a migratory bird. *PNAS*, 107: 9394–399, 2010. doi:https://doi.org/10.1073/pnas.0907068107.

Hiscock, H. G., Worster, S., Kattnig, D. R., Steers, C., Jin, Y., Manolopoulos, D. E., Mouritsen, H., and Hore, P. J. The quantum needle of the avian magnetic compass. *PNAS*, 113:4634–39, 2016. doi:https://doi.org/10.1073/pnas.1600341113.

Hodgkin, A. and Huxley, A. A quantitative description of membrane current and its application to conduction and excitation in nerve. *J. Physiol.*, 117:500–44, 1952. doi:https://doi.org/10.1113/jphysiol.1952.sp004764.

Holland, R. A., Thorup, K., Gagliardo, A., Bisson, I. A., Knecht, E., Mizrahi, D., and Wikelski, M. Testing the role of sensory systems in the migratory heading of a songbird. *J. Exp. Biol.*, 212:20180124, 2009. doi:https://doi.org/10.1038/nature11046.

Holland, R., Filannino, C., and Gagliardo, A. A magnetic pulse does not affect homing pigeon navigation: a gps tracking experiment. *J. Exp. Biol.*, 216:2192–200, 2013. doi:https://doi.org/10.1242/jeb.083543.

Holland, R. A. Differential effects of magnetic pulses on the orientation of naturally migrating birds. *J. R. Soc. Interface*, 7:1617–25, 2010. doi:https://doi.org/10.1098/rsif.2010.0159.

Holland, R. A. and Helm, B. A strong magnetic pulse affects the precision of departure direction of naturally migrating adult but not juvenile birds. *J. R. Soc. Interface*, 10: 20121047, 2013. doi:https://doi.org/10.1098/rsif.2012.1047.

Holland, R. A., Kirschvink, J. L., Doak, T. G., and Wikelski, M. Bats use magnetite to detect the earth's magnetic field. *PLOS one*, 3:e1676, 2008. doi:https://doi.org/10.1371/journal.pone.0001676.

Hore, P. J. and Mouritsen, H. The radical-pair mechanism of magnetoreception. *Annu. Rev. Biophys.*, 45:299–344, 2016. doi:https://doi.org/10.1146/annurev-biophys-032116-094545.

Irwin, W. P. and Lohmann, K. J. Disruption of magnetic orientation in hatchling loggerhead sea turtles by pulsed magnetic fields. *J. Comp. Physiol.*, 191:475–80, 2005. doi:https://doi.org/10.1007/s00359-005-0609-9.

Johnsen, S. and Lohmann, K. J. The physics and neurobiology of magnetoreception. *Nat. Rev.*, 6:703–12, 2005. doi:http://doi.org/10.1038/nrn1745.

Jungerman, R. L. and Rosenblum, B. Magnetic induction for the sensing of magnetic fields by animals—an analysis. *J. Theor. Biol.*, 87:25–32, 1980. doi:https://doi.org/10.1016/0022-5193(80)90217-9.

Kalmijn, A. J. and Blakemore, R. P. "the magnetic behavior of mud bacteria" in animal migration, navigation, and homing, k. schmidt-koenig and w. t. keeton, eds. *Springer, N.Y, 1978*, pages 354–55, 1978. doi:https://doi.org/10.1007/978-3-662-11147-5_35.

Karwinkel, T., Winklhofer, M., Christoph, P., Allenstein, D., Hüppop, O., Brust, V., Bairlein, F., and Schmaljohann, H. No apparent effect of a magnetic pulse on free-flight behaviour in northern wheatears (oenanthe oenanthe) at a stopover site. *J. R. Soc. Interface*, 19:20210805, 2022a. doi:https://doi.org/10.1098/rsif.2021.0805.

Karwinkel, T., Winklhofer, M., Janner, L. E., Brust, V., Hüppop, O., Bairlein, F., and Schmaljohann, H. A magnetic pulse does not affect free-flight navigation behaviour of a medium-distance songbird migrant in spring. *J. Exp. Biol.*, 225:jeb244473, 2022b. doi:https://doi.org/10.1242/jeb.244473.

Kavokin, K., Chernetsov, N., Pakhomov, A., Bojarinova, J., Kobylkov, D., and Namozov, B. Magnetic orientation of garden warblers (sylvia borin) under 1.4 mhz radiofrequency magnetic field. *J. R. Soc. Interface*, 11:20140451, 2014. doi:https://doi.org/10.1098/rsif.2014.0451.

Kirschvink, J. L. and Gould, J. L. Biogenic magnetite as a basis for magnetic field detection in animals. *Biosystems*, 13:181–201, 1981. doi:https://doi.org/10.1016/0303-2647(81)90060-5.

Kishkinev, D. Sensory mechanisms of long-distance navigation in birds: a recent advance in the context of previous studies. *J. Ornithol.*, 156:S145–61, 2015. doi:https://doi.org/10.1007/s10336-015-1215-4.

Kishkinev, D., Chernetsov, N., Heyers, D., and Mouritsen, H. Migratory reed warblers need intact trigeminal nerves to correct for a 1,000 km eastward displacement. *PLOS one*, 8:e65847, 2013. doi:https://doi.org/10.1371/journal.pone.0065847.

Kishkinev, D., Packmor, F., Zechmeister, T., Winkler, H.-C., Chernetsov, N., Mouritsen, H., and Holland, R. A. Navigation by extrapolation of geomagnetic cues in a migratory songbird. *Curr. Biol.*, 31:1563–69.e4, 2021. doi:https://doi.org/10.1016/j.cub.2021.01.051.

Klimley, A. Highly directional swimming by scalloped hammerhead sharks, sphyrna lewini, and subsurface irradiance, temperature, bathymetry, and geomagnetic field. *Marine Biology*, 117:1–22, 1993. doi:https://doi.org/10.1007/BF00346421.

Kobylkov, D., Wynn, J., Winklhofer, M., Chetverikova, R., Xu, J., Hiscock, H., Hore, P. J., and Mouritsen, H. Electromagnetic 0.1–100 khz noise does not disrupt orientation in a night-migrating songbird implying a spin coherence lifetime of less than 10 µs. *J. R. Soc. Interface.*, 16:20190716, 2019. doi:https://doi.org/10.1098/rsif.2019.0716.

Kobylkov, D., Schwarze, S., Michalik, B., Winklhofer, M., Mouritsen, H., and Heyer, D. A newly identified trigeminal brain pathway in a night-migratory bird could be dedicated to transmitting magnetic map information. *Proc. R. Soc. B*, 287:20192788, 2020. doi:https://doi.org/10.1098/rspb.2019.2788.

Lapan, M. *Deep Reinforcement Learning Hands-on*. Packet Publishing Ltd., Birmingham B3 2PB, UK, 2018.

Laurens, J. and Angelaki, D. E. The brain compass: A perspective on how self-motion updates the head direction cell attractor. *Neuron*, 97:275–89, 2018. doi:https://doi.org/10.1016/j.neuron.2017.12.020.

Leberecht, B., Kobylkov, D., Karwinkel, T., Döge, S., Burnus, L., Wong, S. Y., Apte, S., Haase, K., Musielak, I., Chetverikova, R., Dautaj, G., Bassetto, M., Winklhofer, M., Hore, P. J., and Mouritsen, H. Broadband 75–85 mhz radiofrequency fields disrupt magnetic compass orientation in night-migratory songbirds consistent with a flavin-based radical pair magnetoreceptor. *J. Comp. Physiol. A*, 208:97–106, 2022. doi:https://doi.org/10.1007/s00359-021-01537-8.

Lohmann, K. J., Lohmann, C. M. F., and Putman, N. F. Magnetic maps in animals: nature's gps. *J. Exp. Biol.*, 210:3697–705, 2007. doi:https://doi.org/10.1242/jeb.001313.

McNaughton, B. L., Battaglia, F. P., Jensen, O., Moser, E. I., and Moser, M.-B. Path integration and the neural basis of the 'cognitive map'. *Nat. Rev. Neurosci.*, 7:663–78, 2006. doi:https://doi.org/10.1038/nrn1932.

Meyer, C. G., Holland, K. N., and Papastamatiou, Y. P. Sharks can detect changes in the geomagnetic field. *J. R. Soc.*, 2:129–30, 2005. doi:https://doi.org/10.1098/rsif.2004.0021.

Miranda, B., Malalasekera, W. M. N., Behrens, T. E., Dayan, P., and Kennerley, S. W. Combined model-free and model-sensitive reinforcement

learning in non-human primates. *PLoS Comput. Biol.*, 16:e1007944, 2020. doi:https://doi.org/10.1371/journal.pcbi.1007944.

Mora, C. V., Davison, M., Wild, J. M., and Walker, M. M. Magnetoreception and its trigeminal mediation in the homing pigeon. *Nature*, 432:508–11, 2004. doi:https://doi.org/10.1038/nature03077.

Mouritsen, H. Long-distance navigation and magnetoreception in migratory animals. *Nature*, 558:50–9, 2018. doi:https://doi.org/10.1038/s41586-018-0176-1.

Mouritsen, H. and Mouritsen, O. A mathematical expectation model for bird navigation based on the clock-and-compass strategy. *J. theor. Biol.*, 207:283–291, 2000. doi:https://doi.org/10.1006/jtbi.2000.2171.

Mouritsen, H. and Ritz, T. Magnetoreception and its use in bird navigation. *Curr. Biol.*, 15:406–14, 2005. doi:https://doi.org/10.1016/j.conb.2005.06.003.

Mouritsen, H., Janssen-Bienhold, U., Liedvogel, M., Feenders, G., Stalleicken, J., Dirks, P., and Weiler, R. Cryptochromes and neuronal-activity markers colocalize in the retina of migratory birds during magnetic orientation. *PNAS*, 101:14294–99, 2004. doi:https://doi.org/10.1073/pnas.0405968101https://doi.org/10.1073/pnas.0405968101.

Mouritsen, H., Feenders, G., Liedvogel, M., Wada, K., and Jarvis, E. D. Night-vision brain area in migratory songbirds. *PNAS*, 102:8339–44, 2005. doi:https://doi.org/10.1073/pnas.0409575102.

Muheim, R., Moore, F. R., and Phillips, J. B. Calibration of magnetic and celestial compass cues in migratory birds - a review of cue-conflict experiments. *J. Exp. Biol.*, 209:2–17, 2006. doi:https://doi.org/10.1242/jeb.01960.

Munro, U., Munro, J. A., Phillips, J. B., Wiltschko, R., and Wiltschko, W. Evidence for a magnetite-based navigational "map" in birds. *Naturwiss.*, 84:26–28, 1997a.

Munro, U., Munro, J. A., Phillips, J. B., and Wiltschko, W. Effect of wavelength of light and pulse magnetisation on different magnetoreception systems in a migratory bird. *Aust. J. Zool.*, 45:189–98, 1997b. doi:https://doi.org/10.1071/ZO96066.

Müller, U. and Stieglitz, R. Can the earth's magnetic field be simulated in the laboratory? *Naturwissenschaften*, 87:381–90, 2000. doi:https://doi.org/10.1007/s001140050746.

Naisbett-Jones, L. C., Putman, N. F., Scanlan, M. M., Noakes, D. L. G., and Lohmann, K. J. Magnetoreception in fishes: the effect of magnetic pulses

on orientation of juvenile pacific salmon. *J. Exp. Biol.*, 223:jeb222091, 2020. doi:https://doi.org/10.1242/jeb.222091.

Neftci, E. O. and Averbeck, B. B. Reinforcement learning in artificial and biological systems. *Nat. Mach. Intell.*, 1:133–43, 2019. doi:https://doi.org/10.1038/s42256-019-0025-4.

Nimpf, S., Nordmann, G. C., Kagerbauer, D., Malkemper, E. P., Landler, L., Papadaki-Anastasopoulou, A., Ushakova, L., Wenninger-Weinzierl, A., Novatchkova, M., Vincent, P., et al. A putative mechanism for magnetoreception by electromagnetic induction in the pigeon inner ear. *Curr. Biol.*, 29:4052–59, 2019. doi:https://doi.org/10.1016/j.cub.2019.09.048.

O'Keefe, J. Place units in the hippocampus of the freely moving rat. *Exp. Neurol.*, 51: 78–109, 1976. doi:https://doi.org/10.1016/0014-4886(76)90055-8.

Painter, K. J. and Hillen, T. Navigating the flow: individual and continuum models for homing in flowing environments. *J. R. Soc. Interface*, 12:20150647, 2015a. doi:https://doi.org/10.1098/rsif.2015.0647.

Painter, K. J. and Hillen, T. Navigating the flow: individual and continuum models for homing in flowing environments. *J. R. Soc. Interface*, 12:20150647, 2015b. doi:http://dx.doi.org/10.1098/rsif.2015.0647.

Pakhomov, A., Anashina, A., and Chernetsov, N. Further evidence of a time-independent stellar compass in a night-migrating songbird. *Behav. Ecol. Sociobiol.*, 71:48(2017), 2017a. doi:https://doi.org/10.1007/s00265-017-2279-3.

Pakhomov, A., Bojarinova, J., Cherbunin, R., Chetverikova, R., Grigoryev, P. S., Kavokin, K., Kobylkov, D., Lubkovskaja, R., and Chernetsov, N. Very weak oscillating magnetic field disrupts the magnetic compass of songbird migrants. *J. R. Soc. Interface*, 14:20170364, 2017b. doi:https://doi.org/10.1098/rsif.2017.0364.

Pakhomov, A., Anashina, A., Heyers, D., Kobylkov, D., Mouritsen, H., and Chernetsov, N. Magnetic map navigation in a migratory songbird requires trigeminal input. *Sci. Rep.*, 8:11975, 2018. doi:https://doi.org/10.1038/s41598-018-30477-8.

Papi, F., Fiore, L., Fiaschi, V., and Benvenuti, S. The influence of olfactory nerve section on the homing capacity of carrier pigeons. *Monitore Zoologico Italiano*, 5:265–67, 1971. doi:https://doi.org/10.1080/00269786.1971.10736180.

Park, J., Lee, J., Kim, T., Ahn, I., and Park, J. Co-evolution of predator-prey ecosystems by reinforcement learning agents. *Entropy*, 23:461, 2021. doi:https://doi.org/10.3390/e23040461.

Perdeck, A. C. Two types of orientation in migrating starlings, sturnus yulgaris l., and chaffinches, fringilla coelebs l., as revealed by displacement experiments. *Ardea*, 55: 1–2, 1958. doi:https://doi.org/10.5253/arde.v1i2.p1.

Phillips, J. B. and Borland, S. C. Behavioural evidence for use of a light-dependent magnetoreception mechanism by a vertebrate. *Nature*, 359:142–44, 1992. doi:https://doi.org/10.1038/359142a0.

Pizzuti, S., Bernish, M., Harvey, A., Tourangeau, L., Shriver, C., Kehl, C., and Taylor, B. Uncovering how animals use combinations of magnetic field properties to navigate: a computational approach. *J. Comp. Physiol. A*, 2021. doi:https://doi.org/10.1007/s00359-021-01523-0.

Postlethwaite, C. M. and Walker, M. M. A geometric model for initial orientation errors in pigeon navigation. *J. Theor. Biol.*, 269:273–9, 2011. doi:https://doi.org/10.1016/j.jtbi.2010.10.036.

Prinz, K. and Wiltschko, W. Migratory orientation of pied flycatchers: interaction of stellar and magnetic information during ontogeny. *Animal Behaviour*, 44:539–45, 1992. doi:https://doi.org/10.1016/0003-3472(92)90063-F.

Putman, N. F., Verley, P., Shay, T. J., and Lohmann, K. J. Simulating transoceanic migrations of young loggerhead sea turtles: merging magnetic navigation behavior with an ocean circulation model. *J. Exp. Biol.*, 215:1863–70, 2012. doi:https://doi.org/10.1242/jeb.067587.

Qi, X., Ye, D., Sun, Y., Li, C., and Ran, L. Simulations to true animals' long-distance geomagnetic navigation. *IEEE Trans. Magn.*, 53:1–8, 2017. doi:http://dx.doi.org/10.1109/TMAG.2016.2600540.

Rigoli, L. M., Patil, G., Stening, H. F., Kallen, R. W., , and Richardson, M. J. Navigational behavior of humans and deep reinforcement learning agents. *Front. Psychol.*, 12:725932, 2021. doi:https://doi.org/10.3389/fpsyg.2021.725932.

Rinzel, J. On repetitive activity in nerve. *Federation Proceedings*, 37:2793–802, 1978.

Ritz, T., Adem, S., and Schulten, K. A model for photoreceptor-based magnetoreception in birds. *Biophys. J.*, 78:707–18, 2000. doi:https://doi.org/10.1016/S0006-3495(00)76629-X.

Ritz, T., Thalau, P., Phillips, J. B., Wiltschko, R., and Wiltschko, W. Resonance effects indicate a radical-pair mechanism for avian magnetic compass. *Nature*, 429:177–80, 2004. doi:https://doi.org/10.1038/nature02534.

Riveros, A. J. and Srygley, R. B. Do leafcutter ants, atta colombica, orient their path-integrated home vector with a magnetic compass? *Anim. Behav.*, 75:1273–81, 2008. doi:https://doi.org/10.1016/j.anbehav.2007.09.030.

Rolls, E. T. An attractor network in the hippocampus: theory and neurophysiology. *Learn Mem.*, 14:714–31, 2007. doi:https://doi.org/10.1101/lm.631207.

Sandberg, R., Bäckman, J., R.Moore, F., and Lõhmus, M. Magnetic information calibrates celestial cues during migration. *Animal Behaviour*, 60:453–62, 2000. doi:https://doi.org/10.1006/anbe.2000.1582.

Schmidt-Koenig, K. The sun compass. *Experientia*, 46:336–42, 1990. doi:https://doi.org/10.1007/BF01952166.

Schulman, J., Wolski, F., Dhariwal, P., Radford, A., and Klimov, O. Proximal policy optimization algorithms, 2017.

Schulten, K., Swenberg, C. E., and Weller, A. A biomagnetic sensory mechanism based on magnetic field modulated coherent electron spin motion. *Z. Phys. Chem*, 111:1–5, 1978.

Schwarze, S., Schneider, N.-L., Reichl, T., Dreyer, D., Lefeldt, N., Engels, S., Baker, N., Hore, P. J., and Mouritsen, H. Weak broadband electromagnetic fields are more disruptive to magnetic compass orientation in a night-migratory songbird (erithacus rubecula) than strong narrow-band fields. *Front. Behav. Neurosci.*, 10:55, 2016. doi:https://doi.org/10.3389/fnbeh.2016.00055.

Semm, P. and Beason, R. C. Responses to small magnetic variations by the trigeminal system of the bobolink. *Brain Res. Bull.*, 25:735–40, 1990. doi:https://doi.org/10.1016/0361-9230(90)90051-Z.

Shcherbakov, V. P. and Winklhofer, M. The osmotic magnetometer: a new model for magnetite-based magnetoreceptors in animals. *Eur. Biophys. J.*, 28:380–92, 1999. doi:https://doi.org/10.1007/s002490050222.

Sherry, D., Grella, S., Guigueno, M., White, D., and Marrone, D. Are there place cells in the avian hippocampus? *Brain Behav. Evol.*, 90:73–80, 2017. doi:https://doi.org/10.1159/000477085.

Shipston-Sharman, O., Solanka, L., and Nolan, M. F. Continuous attractor network models of grid cell firing based on excitatory–inhibitory interactions. *J. Physiol.*, 594: 6547–57, 2016. doi:https://doi.org/10.1113/JP270630.

Si, B., Romani, S., and Tsodyks, M. Continuous attractor network model for conjunctive position-by-velocity tuning of grid cells. *PLOS Comput. Biol.*, 10:e1003558, 2014. doi:https://doi.org/10.1371/journal.pcbi.1003558.

Steiner, U. E. and Ulrich, T. Magnetic field effects in chemical kinetics and related phenomena. *Chem. Rev.*, 89:51–147, 1989. doi:https://doi.org/10.1021/cr00091a003.

Sutton, R. S. and Barto, A. G. *Reinforcement Learning an Introduction, second edition.* The MIT Press., London, England, 2018.

Taube, J. S., Muller, R. U., and Jr., J. B. R. Head-direction cells recorded from the postsubiculum in freely moving rats. i. description and quantitative analysis. *J. Neurosci.*, 10:420–35, 1990. doi:https://doi.org/10.1523/JNEUROSCI.10-02-00420.1990.

Taylor, B. K. Validating a model for detecting magnetic field intensity using dynamic neural fields. *J. Theor. Biol.*, 408:53–65, 2016. doi:https://doi.org/10.1016/j.jtbi.2016.08.010.

Taylor, B. K. Bioinspired magnetic reception and multimodal sensing. *Biol. Cybern.*, 111:287–308, 2017. doi:https://doi.org/10.1007/s00422-017-0720-3.

Taylor, B. K. Bioinspired magnetoreception and navigation using magnetic signatures as waypoints. *Bioinspir. Biomim*, 13:046003, 2018. doi:https://doi.org/10.1088/1748-3190/aabbec.

Taylor, B. K., Lohmann, K. J., Havens, L. T., Lohmann, C. M. F., and Granger, J. Long-distance transequatorial navigation using sequential measurements of magnetic inclination angle. *J. R. Soc. Interface*, 18:20200887, 2021. doi:https://doi.org/10.1098/rsif.2020.0887.

Thorup, K. and Rabøl, J. Compensatory behaviour after displacement in migratory birds. *Behav. Ecol. Sociobiol.*, 61:825–41, 2007. doi:https://doi.org/10.1007/s00265-006-0306-x.

Thorup, K., Bisson, I.-A., Bowlin, M. S., Holland, R. A., Wingfield, J. C., Ramenofsky, M., and Wikelski, M. Evidence for a navigational map stretching across the continental u.s. in a migratory songbird. *PNAS*, 104:18115–19, 2007. doi:https://doi.org/10.1073/pnas.0704734104.

Thorup, K., Ortvad, T. E., Rabøl, J., Holland, R. A., Tøttrup, A. P., and Wikelski, M. Juvenile songbirds compensate for displacement to oceanic islands during autumn migration. *PLoS One*, 6:e17903, 2011. doi:https://doi.org/10.1371/journal.pone.0017903.

Thorup, K., Vega, M. L., Snell, K. R. S., Lubkovskaia, R., Willemoes, M., Sjöberg, S., Sokolov, L. V., and Bulyuk, V. Flying on their own wings: young and adult cuckoos respond similarly to long-distance displacement during migration. *Sci. Rep.*, 10:7698, 2020. doi:https://doi.org/10.1038/s41598-020-64230-x.

Tian, L., Xiao, B., Lin, W., Zhang, S., Zhu, R., and Pan, Y. Testing for the presence of magnetite in the upper-beak skin of homing pigeons. *Biometals*, 20:197–203, 2007. doi:https://doi.org/10.1007/s10534-006-9027-x.

Trappenberg, T. P. *Fundamentals of Computational Neuroscience, second edition.* Oxford University Press, New York, 2010.

Treiber, C. D., Marion Claudia Salzer, J. R., Edelman, N., Sugar, C., Breuss, M., Pichler, P., Cadiou, H., Saunders, M., Lythgoe, M., Shaw, J., and Keays, D. A. Clusters of iron-rich cells in the upper beak of pigeons are macrophages not magnetosensitive neurons. *Nature*, 484:367–70, 2012. doi:https://doi.org/10.1038/nature11046.

Treloar, N. J., Fedorec, A. J. H., Ingalls, B., and Barnes, C. P. Deep reinforcement learning for the control of microbial co-cultures in bioreactors. *PLoS Comput. Biol.*, 16:e1007783, 2020. doi:https://doi.org/10.1371/journal.pcbi.1007783.

Walker, M. M. A model for encoding of magnetic field intensity by magnetite-based magnetoreceptor cells. *J. Theor. Biol.*, 250:85–91, 2008. doi:https://doi.org/10.1016/j.jtbi.2007.09.030.

Walker, M. M., Diebel, C. E., Haugh, C. V., Pankhurst, P. M., Montgomery, J. C., and Green, C. R. Structure and function of the vertebrate magnetic sense. *Nature*, 390: 371–76, 1997. doi:https://doi.org/10.1038/37057.

Walker, M. M., Dennisa, T. E., and Kirschvink, J. L. The magnetic sense and its use in long-distance navigation by animals. *Curr. Opin. Neurobiol.*, 12:735–44, 2002. doi:https://doi.org/10.1016/S0959-4388(02)00389-6.

Wang, C. X., Hilburn, I. A., Wu, D.-A., Mizuhara, Y., Cousté, C. P., Abrahams, J. N. H., Bernstein, S. E., Matani, A., Shimojo, S., and Kirschvink, J. L. Transduction of the geomagnetic field as evidenced from alpha-band activity in the human brain. *eNeuro*, pages 0483–18, 2019. doi:https://doi.org/10.1523/ENEURO.0483-18.2019.

Wang, K., Mattern, E., and Ritz, T. On the use of magnets to disrupt the physiological compass of birds. *Phys. Biol.*, 3(3):220–31, 2006. doi:https://doi.org/10.1088/1478-3975/3/3/007.

Weindler, P., Baumetz, M., and Wiltschko, W. The direction of celestial rotation influences the development of stellar orientation in young garden warblers (sylvia borin). *J. Exp. Biol.*, 200:2107–13, 1997. doi:https://doi.org/10.1242/jeb.200.15.2107.

Weindler, P., Beck, W., Liepa, V., and Wiltschko, W. Development of migratory orientation in pied flycatchers in different magnetic inclinations. *Anim. Behav.*, 49:227–34, 1995. doi:https://doi.org/10.1016/0003-3472(95)80171-5.

Whalen, A., Cownden, D., and Laland, K. The learning of action sequences through social transmission. *Anim. Cogn.*, 18:1093–103, 2015. doi:https://doi.org/10.1007/s10071-015-0877-x.

Wilson, H. R. *Spikes, Decisions, and Actions: The dynamical foundations of neuroscience*. Oxford University Press, New York, 1999.

Wilson, H. R. and Kim, J. Perceived motion in the vector sum direction. *Vision Research*, 34:1835–42, 1994. doi:https://doi.org/10.1016/0042-6989(94)90308-5.

Wiltschko, R. and Wiltschko, W. The magnetite-based receptors in the beak of birds and their role in avian navigation. *J. Comp. Physiol. A Neuroethol. Sens. Neural Behav. Physiol.*, 199:89–98, 2013. doi:https://doi.org/10.1007/s00359-012-0769-3.

Wiltschko, R. and Nehmzow, U. Simulating pigeon navigation. *Anim. Behav.*, 69:813–26, 2005. doi:https://doi.org/10.1016/j.anbehav.2004.07.007.

Wiltschko, R., Munro, U., Ford, H., and Wiltschko, W. After-effects of exposure to conflicting celestial and magnetic cues at sunset in migratory silvereyes zosterops l. lateralis. *J. Avian Biol.*, 30:56–62, 1999. doi:https://doi.org/10.2307/3677243.

Wiltschko, R., Stapput, K., Thalau, P., and Wiltschko, W. Directional orientation of birds by the magnetic field under different light conditions. *J. R. Soc. Interface*, 7: S163–77, 2010. doi:https://doi.org/10.1098/rsif.2009.0367.focus.

Wiltschko, W., Munro, U., Ford, H., and Wiltschko, R. Magnetic inclination compass: A basis for the migratory orientation of birds in the northern and southern hemisphere. *Experientia*, 49:167–70, 1993. doi:https://doi.org/10.1007/BF01989423.

Wiltschko, W., Munro, U., Beason, R. C., Ford, H., and Wiltschko, R. A magnetic pulse leads to a temporary deflection in the orientation of migratory birds. *Experientia*, 50: 697–700, 1994. doi:https://doi.org/10.1007/BF01952877.

Wiltschko, W., Munro, U., Ford, H., and Wiltschko, R. Effect of a magnetic pulse on the orientation of silvereyes, zosterops l. lateralis, during spring migration. *J. Exp. Biol.*, 201:3257–61, 1998a. doi:https://doi.org/10.1242/jeb.201.23.3257.

Wiltschko, W. and Wiltschko, R. Magnetic compass of european robins. *Science*, 176: 62–64, 1972. doi:https://doi.org/10.1126/science.176.4030.62.

Wiltschko, W. and Wiltschko, R. Migratory orientation of european robins is affected by the wavelength of light as well as by a magnetic pulse. *J. Comp. Physiol. A*, 177: 363–69, 1995. doi:https://doi.org/10.1007/BF00192425.

Wiltschko, W. and Wiltschko, R. Magnetic orientation in birds. *J. Exp. Biol.*, 199:29–38, 1996. doi:https://doi.org/10.1242/jeb.199.1.29.

Wiltschko, W. and Wiltschko, R. Magnetic orientation and magnetoreception in birds and other animals. *J. Comp. Physiol.*, 191:675–93, 2005. doi:https://doi.org/10.1007/s00359-005-0627-7.

Wiltschko, W., Daum, P., Fergenbauer-Kimmel, A., and Wiltschko, R. The development of the star compass in garden warblers. *Sylvia Borin. Ethology*, 74:285–89, 1986.

Wiltschko, W., Daum, P., Fergenbauer-Kimmel, A., and Wiltschko, R. The development of the star compass in garden warblers, sylvia borin. *Ethology*, 74:285–92, 1987.

Wiltschko, W., Weindler, P., and Wiltschko, R. Interaction of magnetic and celestial cues in the migratory orientation of passerines. *J. Avian Biol.*, 29:606–17, 1998b. doi:https://doi.org/10.2307/3677181.

Wiltschko, W., Munro, U., Wiltschko, R., and Kirschvink, J. L. Magnetite-based magnetoreception in birds: the effect of a biasing field and a pulse on migratory behavior. *J. Exp. Biol.*, 205:3031–37, 2002. doi:https://doi.org/10.1242/jeb.205.19.3031.

Wiltschko, W., Ford, H., Munro, U., Winklhofer, M., and Wiltschko, R. Magnetite-based magnetoreception: the effect of repeated pulsing on the orientation of migratory birds. *J. Comp. Physiol. A*, 193:515–22, 2007. doi:https://doi.org/10.1007/s00359-006-0207-5.

Wiltschko, W., Munro, U., Ford, H., and Wiltschko, R. Avian orientation: the pulse effect is mediated by the magnetite receptors in the upper beak. *Proc. R. Soc. B.*, 276: 2227–32, 2009. doi:https://doi.org/10.1098/rspb.2009.0050.

Winklhofer, M. Magnetoreception: A dynamo in the inner ear of pigeons. *Curr. Biol.*, 29:R1224–26, 2019. doi:https://doi.org/10.1016/j.cub.2019.10.022.

Winklhofer, M. and Kirschvink, J. L. A quantitative assessment of torque-transducer models for magnetoreception. *J. R. Soc. Interface*, 7:S273–89, 2010. doi:https://doi.org/10.1098/rsif.2009.0435.focus.

Winklhofer, M., Holtkamp-Rötzler, Hanzlik, M., Fleissner, G., and Petersen, N. Clusters of superparamagnetic magnetite particles in the upper-beak skin of homing pigeons : evidence of a magnetoreceptor? *European Journal of Mineralogy*, 13:659–69, 2001. doi:https://doi.org/10.1127/0935-1221/2001/0013-0659.

Wispinski, N. J., Butcher, A., Mathewson, K. W., Chapman, C. S., Botvinick, M. M., and Pilarski, P. M. Adaptive patch foraging in deep reinforcement learning agents. *arXiv*, page 2210.08085, 2022. doi:https://doi.org/10.48550/arXiv.2210.08085.

Wu, H., Scholten, A., Einwich, A., Mouritsen, H., and Koch, K.-W. Protein-protein interaction of the putative magnetoreceptor cryptochrome 4 expressed in the avian retina. *Sci. Rep.*, 10:7364, 2020. doi:https://doi.org/10.1038/s41598-020-64429-y.

Wynn, J., Padget, O., Mouritsen, H., Morford, J., MORFORD, J., and Guilford, T. Magnetic stop signs signal a european songbird's arrival at the breeding site after migration. *Science*, 375:446–9, 2022. doi:https://doi.org/10.1126/science.abj4210.

Xiaohui, X., Hahnloser, R. H. R., and Seung, H. S. Double-ring network model of the head-direction system. *Phys. Rev.*, E66:041902, 2002. doi:https://doi.org/10.1103/PhysRevE.66.041902.

Xu, J., Jarocha, L. E., Zollitsch, T., Konowalczyk, M., Henbest, K. B., Richert, S., Golesworthy, M. J., Schmidt, J., Déjean, V., Sowood, D. J. C., Bassetto, M., Luo, J., Walton, J. R., Fleming, J., Wei, Y., Pitcher, T. L., Moise, G., Herrmann, M., Yin, H., Wu, H., Bartölke, R., Käsehagen, S. J., Horst, S., Dautaj, G., Murton, P. D. F., Gehrckens, A. S., Chelliah, Y., Takahashi, J. S., Koch, K.-W., Weber, S., Solov'yov, I. A., Xie, C., Mackenzie, S. R., Timmel, C. R., Mouritsen, H., and Hore, P. J. Magnetic sensitivity of cryptochrome 4 from a migratory songbird. *Nature*, 594:535–40, 2021. doi:https://doi.org/10.1038/s41586-021-03618-9.

Yamaguchi, S., Naoki, H., Ikeda, M., Tsukada, Y., Nakano, S., Mori, I., and Ishii, S. Identification of animal behavioral strategies by inverse reinforcement learning. *PLoS Comput. Biol.*, 14:e1006122, 2018. doi:https://doi.org/10.1371/journal.pcbi.1006122.

Yo, C. and Wilson, H. R. Perceived direction of moving two-dimensional patterns depends on duration, contrast and eccentricity. *Vision Research*, 32:135–47, 1992. doi:https://doi.org/10.1016/0042-6989(92)90121-X.

Yu, X., Wu, W., Feng, P., and Tian, Y. Swarm inverse reinforcement learning for biological systems. *IEEE International Conference on Bioinformatics and Biomedicine (BIBM)*, pages 274–9, 2021. doi:https://doi.org/10.1109/BIBM52615.2021.9669656.

Zapka, M., Heyers, D., Hein, C. M., Engels, S., Schneider, N.-L., Hans, J., Weiler, S., Dreyer, D., Kishkinev, D., Wild, J. M., et al. Visual but not trigeminal mediation of magnetic compass information in a migratory bird. *Nature*, 461:1274–77, 2009. doi:https://doi.org/10.1038/nature08528.

Zhao, Z., Hu, T., Cui, W., Huangfu, J., Li, C., and Ran, L. Long-distance geomagnetic navigation: Imitations of animal migration based on a new assumption. *IEEE Transactions on Geoscience and Remote Sensing*, 52:6715–23, 2014. doi:https://doi.org/10.1109/TGRS.2014.2301441.

Eigenständigkeitserklärung

Hiermit erkläre ich, dass ich die vorliegende Dissertation selbst verfasst und nur die angegebenen Quellen und Hilfsmittel verwendet habe. Außerdem versichere ich, dass ich die allgemeinen Prinzipien wissenschaftlicher Arbeit und Veröffentlichung, wie sie in den Leitlinien guter wissenschaftlicher Praxis der Carl von Ossietzky Universität Oldenburg festgelegt sind, befolgt habe.

Hereby I confirm that I completed the work independently and used only the indicated resources. Also, The dissertation has, neither as a whole, nor in part, been submitted for assessment in a doctoral procedure at another university

_____ _____

Date Karim Mohsen Ghatas Habashy

"The brain is the last and grandest biological frontier, the most complex thing we have yet discovered in our universe. It contains hundreds of billions of cells interlinked through trillions of connections. The brain boggles the mind." —James D. Watson, Nobel Laureate and co-discoverer of the structure of DNA.